NASA CR-143838

RIDE QUALITIES CRITERIA VALIDATION/PILOT PERFORMANCE STUDY - FLIGHT SIMULATOR RESULTS

Louis U. Nardi, Harry Y. Kawana,
Christopher J. Borland, and Norman M. Lefritz

Rockwell International Corporation
Los Angeles Aircraft Division
Los Angeles, California 90009

March 1976

Prepared for

NATIONAL AERONAUTICS AND SPACE ADMINISTRATION
Dryden Flight Research Center
Edwards, Calif. 93523

(NASA-CR-143838) RIDE QUALITIES CRITERIA VALIDATION/PILOT PERFORMANCE STUDY: FLIGHT SIMULATOR RESULTS Final Report (Rockwell International Corp., Los Angeles) 101 p HC $5.50 CSCL 05E G3/54

N76-20825

Unclas
23689

1. Report No.	2. Government Accession No.	3. Recipient's Catalog No.
NASA CR-143838		

4. Title and Subtitle	5. Report Date
RIDE QUALITIES CRITERIA VALIDATION/PILOT PERFORMANCE STUDY - FLIGHT SIMULATOR RESULTS	March 1976
	6. Performing Organization Code: H-936
7. Author(s): Louis U. Nardi, Harry Y. Kawana, Christopher J. Borland, and Norman M. Lefritz	8. Performing Organization Report No.
	10. Work Unit No.
9. Performing Organization Name and Address: Rockwell International Corporation, Los Angeles Aircraft Division, Los Angeles, California 90009	11. Contract or Grant No.: NAS4-2236
	13. Type of Report and Period Covered: Contractor Report - Final
12. Sponsoring Agency Name and Address: National Aeronautics and Space Administration, Washington, D. C. 20546	14. Sponsoring Agency Code

15. Supplementary Notes

NASA Technical Monitor: Melvin Sadoff, NASA Ames Research Center
NASA Program Manager: Jack Nugent, NASA Dryden Flight Research Center

16. Abstract

A research program was conducted to study pilot performance during simulated manual terrain following flight for ride quality criteria validation. An existing B-1 simulation program provided the data for these investigations.

The B-1 simulation program included terrain following flights under varying controlled conditions of turbulence, terrain, mission length, and system dynamics. The flight simulator consisted of a moving base cockpit which reproduced motions due to turbulence and control inputs. The B-1 aircraft dynamics were programmed with six-degrees-of-freedom equations of motion with three symmetric and two antisymmetric structural degrees of freedom.

The results of this study provided preliminary validation of existing ride quality criteria and identified several ride quality/handling quality parameters which may be of value in future ride quality/criteria development.

17. Key Words (Suggested by Author(s))	18. Distribution Statement
Ride qualities criteria Pilot performance Manual terrain following Flight simulation	Unclassified - Unlimited

19. Security Classif. (of this report)	20. Security Classif. (of this page)	21. No. of Pages	22. Price*
Unclassified	Unclassified	101	

For sale by the National Technical Information Service, Springfield, Virginia 22151

TABLE OF CONTENTS

LIST OF ILLUSTRATIONS

LIST OF TABLES

RIDE QUALITIES CRITERIA VALIDATION/PILOT PERFORMANCE STUDY - FLIGHT SIMULATOR RESULTS

Louis U. Nardi, Harry Y. Kawana,
Christopher J. Borland, and Norman M. Lefritz
Rockwell International Corporation
Los Angeles, California

SUMMARY

This report presents the results of a research contract to study pilot performance during simulated manual terrain-following (MTF) flight for ride quality criteria validation. An existing B-1 simulation program provided the data for these investigations.

The ride quality design criteria for the B-1 include both aircraft response to gusts and flexible mode response to control excitation requirements to provide satisfactory ride qualities for long-duration missions. Accomplishment of MTF during B-1 simulations to date has provided preliminary validation of these B-1 ride quality criteria, in that design to the existing criteria is satisfactory. The simulations conducted to date have not included conditions in excess of the criteria, to permit assessment of the criteria as limits (an aircraft outside of the limits is unsatisfactory).

The B-1 simulation program included terrain-following (TF) flights under varying controlled conditions of turbulence, terrain, mission length, and system dynamics. The B-1 flight simulator consisted of a moving base cockpit which reproduced motions due to turbulence and control inputs. The B-1 aircraft dynamics were programmed with six-degrees-of-freedom equations of motion with three symmetric and two antisymmetric structural degrees of freedom. The simulation also included the B-1 TF system, display system, and flight control system. Experienced test pilots participated in the simulated flights.

The performance measures considered in this study included TF performance parameters, pilot/aircraft performance parameters, and subjective assessments by the pilot. The environmental and system parameters included the motion or vibration level, maneuver spectrum, display and control system dynamics, and task loading.

The results of this study show general concurrence with the results of previous studies. In addition to preliminary validation of the ride quality criteria, several new ride quality/handling quality parameters were identified which may be useful in future ride quality criteria development.

INTRODUCTION

The low-altitude, high-speed (LAHS) flight environment poses potentially serious ride quality problems for accomplishment of long-duration missions. The persistent threat in flying LAHS demands intense concentration by the pilot. Associated cockpit duties compound the task loading. The aircraft is subjected to motions caused by turbulence and to maneuver loads imposed by TF. These motions can cause problems of inadvertent stick inputs, pilot-induced oscillations, difficulty in reading instruments, pilot fatigue, and body discomfort. These factors tend to reduce the pilot's ability to fly the mission with precision.

Aircraft handling and ride qualities in LAHS flight have been extensively studied and reported in the literature. However, there are very little data available for prediction of acceptability or performance capability during exposure to multiaxis vibration conditions in the LAHS environment. Ride quality criteria have been developed based upon available data, and these criteria are being used for current aircraft, including the B-1. The development of these criteria is presented in reference 1, but the criteria have not been validated in any current application.

The B-1 program provides a contemporary application of ride quality design for potential validation of the criteria. Both simulation and actual flight tests are being accomplished in the B-1 program to demonstrate performance.

This study is the initial effort by Rockwell and NASA to utilize B-1 data to validate ride qualities criteria.

SYMBOLS

Airframe

cg	Center of gravity
CSSL	Continuous system simulation language
FS	Fuselage station
Fs	Pilot-applied stick force

g	Acceleration of gravity
Δh	Clearance altitude (aircraft minus terrain)
Δh_e	Clearance altitude (aircraft minus desired set clearance altitude)
$L_{\delta H'}(\delta_{H'})_{max}$	Maximum lateral control power
Mn	Mach number
$n_{x_{cg}}, n_{y_{cg}}, n_{z_{cg}}$	Accelerations at aircraft cg along X,Y,Z body axes in g's
$n_{x_{ps}}, n_{y_{ps}}, n_{z_{ps}}$	Accelerations at pilot station along X,Y,Z body axes in g's
T_R	Roll-subsidence time constant
T_{θ_2}	Time constant in pitch transfer function
w_g, v_g	Vertical and lateral gust velocity components
X,Y,Z	Vehicle body axes
X_θ, X_ϕ	Pitch and roll stick displacements
p, q, r	Roll, pitch, and yaw rates about X, Y, and Z body axes
α, β	Angles of attack and sideslip
γ	Flight path angle
ψ, θ, ϕ	Euler azimuth, pitch, and roll angles
Λ	Wing leading edge sweep angle
ζ	Longitudinal short-period damping ratio
ζ_L	Dutch roll damping ratio
ω_n	Undamped longitudinal short-period frequency
ω_d	Undamped Dutch roll natural frequency
$(\omega_\phi/\omega_d)^2$	Dutch roll coupling parameter
σ_{turb}	Turbulence level $= \sqrt{\sigma_{w_g}^2 + \sigma_{v_g}^2}$
η_i	Deflection of the ith normalized structural mode
δ_H	Horizontal tail control surface deflection
$\delta_{H'}$	Rolling tail control surface deflection
δ_{R_U}	Upper rudder control surface deflection
δ_{R_L}	Lower rudder control surface deflection
$\delta_{CV_{(S)}}$	Symmetric SMCS vane deflection

$\delta_{CV_{(A)}}$	Antisymmetric SMCS vane deflection

TF System

R	Radar range
β	Radar scan angle
Ho	Set clearance altitude
V	Aircraft velocity
γ_{FL}	Flight path angle command from radar return signal
γ_H	Flight path angle command from altimeter return signal

Motion System

$\Delta x, \Delta y, \Delta z$	Motion system displacement
V_x, V_y, V_z	Motion system velocity
$S_1, S_2, S_3, S_4, S_5, S_6$	Motion system leg displacement command signals

Display System

g_c	TF normal acceleration (g) command
$g_{feedback}$	Display feedback (g)
Horiz Bar	Pitch display error into VSD proportional to $(g_c - g)$
Vert Bar	Roll display error into VSD proportional to $(\phi_c - \phi)$
ϕ_c	Roll angle command

Miscellaneous

$\bar{H}$	Crew sensitivity index
rms	Root mean square
s	Laplace variable
t	Time
T_D	Human frequency response function
K	System gain

Δ	Incremental value
ω	Frequency (= $2\pi f$)
Φ	Power spectral density
Σ	Summation
σ	Standard deviation
σ_D	RMS discomfort index
$\sigma_{D_{\delta_H}}$	RMS discomfort index due to control surface excitation
τ	Time constant

B-1 FLIGHT SIMULATION PROGRAM

The flight simulation program described in this section was planned and conducted as part of the B-1 development program to evaluate B-1 handling qualities, ride qualities, and manual TF performance in the low-altitude, high-speed mission environment.

The B-1 basic flight simulator (six-degrees-of-freedom, moving base simulator) (figure 1) was used to evaluate pilot performance in the LAHS mission. The cockpit motions were provided by six servo-controlled, fast-response hydraulic actuators. This system operates under computer control to produce motion (accelerations, velocities, and positions) to simulate the responses of the aircraft in flight.

The elastic effects of the structure on the aerodynamics and the motion of key structural modes were simulated. In addition to total aircraft response, pilot station response to combined vertical and lateral turbulence was represented. The flight control system (FCS), stability and control augmentation system (SCAS), structural mode control system (SMCS), TF system (TF), and displays are included in the mechanization. A block diagram showing the interrelationships of all systems is presented in figure 2. Expansion on these topics as well as discussions of subjects (pilots), terrain, data recording, and data test conditions are included in this section.

Aircraft Dynamics

The mathematical model of the B-1 represents the aircraft at medium weight with wings swept aft to 65 degrees. A high-subsonic, low-altitude flight condition is represented. All six degrees of freedom were programmed; the

aerodynamics were incorporated for a single mach number. Three symmetric structural degrees of freedom and two antisymmetric structural degrees of freedom were simulated. Aeroelastic effects of other structural modes were reflected in flexible-to-rigid corrections to the aerodynamic coefficients. The structural modes selected for simulation were those most likely to be excited by the pilot in flying the aircraft.

Simulator Motion System

The regular algorithm converting the equations of motion output into simulator motion would not faithfully reproduce high-frequency structural motion. Other means had to be found to drive the motion system to represent structural dynamics. Thus, it was necessary to separate the motion system input due to "rigid body" response from that generated by structural deflection in response to control input, as shown in figure 3.

Because of the possibility of control surface motion exciting certain structural motion and adversely affecting ride quality or pilot performance, the following scheme was developed to enable a correct mechanization of the cockpit response and to maintain the closed-loop nature of control system-structural motion interaction:

(1) The cockpit translations and rotations due to rigid body motions and those due to structural vibrations were calculated separately.

(2) The rigid body motions were fed to the standard digital computation system for conversion to motion system inputs. Washout circuits were used to eliminate sustained steady-state accelerations.

(3) Structural motions were fed to a separate analog computation system for calculation of additional simulator motion system inputs via a linear approximation of the motion system algorithm. This approximation was acceptable because the additional angles and deflections due to structural motion were small.

In addition to the simulator inputs which represent pilot and SCAS induced motions, inputs that represent the rigid body and structural response of the aircraft to random atmospheric turbulence also drive the motion system. Because of the desire to evaluate ride quality and pilot performance in the most realistic environment possible and determine the effect of the SMCS on these aircraft characteristics, a separate digital simulation program was developed to calculate aircraft response in turbulence. A schematic of the conversion from aircraft rigid body and modal generalized coordinates to motion system inputs is shown in figure 4. This program was used to provide time histories of motion

system leg deflections on punched cards. These cards, in turn, were used to produce an FM tape to drive the motion system, as shown in figure 3. Data were provided for the cases of SMCS on and off. The turbulence level was approximately $\sigma_{w_g} = \sigma_{v_g} = 1.5$ m/sec (5 ft/sec) rms in both the vertical and lateral directions. The effect was therefore equivalent to a combined level of approximately $\sigma_{turb} = 2.15$ m/sec (7 ft/sec) rms. The capability of varying this level, correlated with terrain and as a function of time in extended mission simulations, was implemented.

Flight Control Systems

Flight controls consisted of a center-stick controller functional in lateral and longitudinal axes, rudder pedals, and throttles. The control stick had a trim switch to provide pitch and roll trim. Detailed descriptions of control stick force and displacement characteristics are given in reference 2.

The B-1 has an SCAS in each of the three airplane axes, as shown in figure 5. The pitch axis SCAS includes a pitch gyro and vertical accelerometer near the center of gravity (cg) whose signals are combined and processed through compensation networks to drive the horizontal tail. The yaw SCAS includes a yaw gyro and a lateral accelerometer near the cg whose combined signals, processed through compensation, drive the lower rudder panel. The roll SCAS includes roll gyros and compensation to drive the left and right horizontal tail panels differentially.

Handling quality parameters are tabulated in appendix A for the basic and augmented (SCAS) configuration.

Structural Mode Control System

The SMCS block diagrams for both the vertical and lateral system are shown in figure 6. The vertical system consists of a vertical accelerometer at the control vane, slightly forward of the cockpit, a washout to separate structural motion from total aircraft motion, compensation, and a set of control vanes which deflect symmetrically to produce a vertical force.

The lateral system has one accelerometer at the control vane and one near the cg. The net signal, composed of the difference of these two signals, is processed through a washout and compensation to drive the control vanes differentially. Since the control vanes are canted down 30 degrees from the horizontal, differential deflection produces a net lateral force.

Terrain-Following System

The TF system provides vertical acceleration error signals to the vertical situation display (VSD) and automatic flight control system (AFCS) so that the clearance between the trajectory and the terrain profile along the ground track is held to a specification value within the constraints of climb, dive and acceleration limits, aircraft response, and speed. The B-1 TF avionics system utilizes a modified version of the AN/APQ-146 radar and guidance control laws. A functional block diagram of the TF system is presented in figure 2 to show the interface between the avionics system and pitch flight control system.

The vertical acceleration error to VSD was computed from the commanded vertical acceleration minus a feedback signal. In this study, three different feedback signals were used. The first was a function of stick displacement, the second was from a normal accelerometer, and the third was a combination of stick and normal accelerometer feedbacks.

Run Conditions

Two types of runs were used in the simulation: (1) short runs of 7 to 30 minutes duration, and (2) long runs of 4 hours duration. One of the short-run routes, known as CAL 6201, is representative of low mountainous terrain. The other short-run route, known as Air Force 8, is a standard training route over high, rugged mountainous terrain. The long route has been constructed of repeated elements of both of these two short routes plus elements of routes Air Force 2 and Air Force 10, as well as simulated overwater flight. The profiles of each of these route segments and the percentage of representation in the long route are presented in figure 7.

The turbulence levels used were correlated with the terrain for the long-duration route. Figure 8 shows the probability of finding a given turbulence level, $P(\sigma)$, over several types of terrain. These probability distributions were obtained from the B-66 low-level gust study (reference 3). The levels used during the 4-hour flight vary from 0.30 to 2.1 m/sec (1 to 7 ft/sec rms) combined turbulence.

Displays and Cockpit Instrumentation

The B-1 instrument panel layout is illustrated in figure 9. The information displayed to the pilot utilized a vertical situation display, vertical scale flight instruments, and a radar altimeter.

The VSD indicates two command errors through movements of a cross-like symbol. A symbol represented by ⌐ was the aircraft reference and was stationary; the other line representing the horizon was movable and indicated pitch and roll attitudes. The steering cross-vertical displacement is driven by the error signal required to fly the oncoming terrain. The steering cross-lateral displacement is driven by the roll attitude error. As long as the cross is centered, the aircraft is flying the desired TF trajectory and ground track. A displacement of 2.5 cm (1 inch) in the vertical axis is equivalent to 0.875 g error, and a displacement of 2.5 cm (1 inch) in the lateral bar is equivalent to 68 degrees in roll error.

Test Subjects

Five experienced test pilots were used as subjects in the short-run study. Two of these pilots were used in the long-duration runs. Their ages ranged from 33 to 49. Jet flying experience ranged from 6,000 to 10,000 hours, and all had prior LAHS flying experience.

Test Conditions

Table I contains the test conditions studied in this report. Run sets 1 and 4 are short-duration runs (7 to 30 minutes), and run sets 2 and 3 are long-duration runs (4 hours). Run set 1 data were taken with SMCS on and off, two different VSD feedback signals, prefilter in and out, and turbulence at three constant levels over the CAL 6201 terrain route. The significance of the prefilter will be discussed later. The turbulence levels for the 4-hour run were varied as a function of the terrain. Since the 4-hour simulation runs were repeated with the same terrain routes (table IV), the turbulence levels varied were the same between runs.

The purpose of run set 2 was to evaluate the pilot's ability to follow terrain for long periods of time in the expected variable turbulent environment with the SMCS off. The purpose of run set 3 was to determine the pilot's ability to perform the same TF task of run set 2 with the SMCS on. Run set 4 is the ATF baseline data taken with the SMCS on, over terrain routes CAL 6201 and AP 8, to provide a comparison with MTF performance. The data used in the analysis were recorded on FM tape and strip charts, as indicated in tables II and III.

DATA ANALYSIS

The performance measures considered in this study included TF performance parameters, pilot/aircraft performance parameters, and qualitative assessments by the flight crew. The environmental parameters included the motions, vibrations, system dynamics, and task loading associated with the MTF mission. The performance and environment parameters were those measured in the study. The system dynamics and task loading parameters were designed into the simulation study and were not measured. In general, the following statistical values of the available data were generated

(1) Mean value

$$\overline{X} = \frac{1}{N}\sum_{i=o}^{N} X_i$$

where X = parameter of interest

N = number of data samples

(2) Standard deviation

$$\sigma_X = \sqrt{\frac{1}{N}\sum_{i=o}^{N} (X_i - \overline{X})^2}$$

(3) Power spectral density (selected test runs)

$$\Phi_{X_k} = \frac{2\Delta t}{N}\left|\sum_{m=o}^{N-1} X(m\Delta t)\cos\left(2\pi\frac{km}{N}\right)\right|^2 \qquad k = 1,2,\ldots N/2$$

This is one of many possible representations of spectral density computations. The actual data analyses shown in this report were performed using the Fast Fourier Transform method.

Identification of Performance Parameters

TF performance.- The statistical measure of the clearance altitude of the aircraft above terrain, Δh, was used for a TF performance parameter. In addition, specific measurements of Δhe and γ over the several prominent terrain peaks were made from recorded strip chart data to further evaluate TF performance.

Pilot performance. - The following pilot performance measures were processed for data analysis:

(1) Horizontal bar $(g_c - g_{feedback})$

(2) Vertical bar $(\phi_c - \phi)$

(3) ΔMn $(Mn_{ref} - Mn)$

(4) Control stick displacements (X_θ and X_ϕ) for long mission runs

(5) Throttle displacement for long mission runs

Pilot comments on handling quality and ride quality. - Pilot comments included assessment in the form of Cooper-Harper handling quality and ride quality ratings (appendix B) which can be related to pilot performance. A sample of the pilot questionnaires used in this study is presented in appendix C.

System and Environmental Conditions

Statistical values of the following environmental parameters or ride quality indicators were used:

(1) Pilot seat accelerations $\left(\sigma_{n_{x_{ps}}}, \sigma_{n_{y_{ps}}}, \text{and } \sigma_{n_{z_{ps}}}\right)$

(2) Crew sensitivity index $(\bar{H})$ or σ_D

(3) Discomfort index $\left(\sigma_{D_{\delta_H}}\right)$ due to control exitation

Motion levels simulated. - As discussed previously, crew station motion due to turbulence was provided by direct inputs to the motion system leg servos from the FM tape, with appropriate scaling (attenuation) to provide specified turbulence levels. Motions due to control inputs were superimposed upon the turbulence induced motions, within the simulator response limits. The standard deviations of the measured accelerations at the pilot seat versus the turbulence magnitude are shown in figures 10 and 11 for SMCS on and off for the conditions tested. The measured pilot seat accelerations and turbulence inputs have a linear relationship, as seen in the figures. The offset g observed in the figures when there is no turbulence is the residual motion due to the washed-out maneuver load and some structural motion due to control input. The measured $\sigma_{n_{x_{ps}}}$ results from the pitching motion of the cockpit about a point aft of the crew station, due to bending in the structural modes.

Crew sensitivity index ($\overline{H}$). - Ride quality specifications for the B-1 are defined in terms of the crew sensitivity indexes for vertical and lateral motion, $\overline{H}_z$ and $\overline{H}_y$. The crew sensitivity index is determined by considering the effect of the aircraft response on the discomfort sensed by the crew, through the use of a human frequency response function. This frequency response function provides a means for "weighting" the effects of the various frequency components of the crew compartment response on the crew. The crew sensitivity index is determined as follows:

$$\overline{H} = \frac{\sigma_D}{\sigma_u} = \left[\int_0^\infty \left|T_D(\omega)\right|^2 \left|T_{A/P}(\omega)\right|^2 \frac{\Phi(\omega)}{\sigma_g^2}\, d\omega\right]^{1/2}$$

σ_D = rms discomfort

σ_u = rms gust velocity

$\overline{H}$ = crew sensitivity index

$\left|T_D(\omega)\right|$ = human frequency response function

$\left|T_{A/P}(\omega)\right|$ = crew compartment acceleration frequency response function

$\frac{\Phi(\omega)}{\sigma_g^2}$ = turbulence spectrum for unit rms gust velocity, as defined by the von Karman power spectral density function

For vertical accelerations ($\bar{H}_z$)

$$\left|T_{A/P}(\omega)\right| = \left|n_z(\omega)^{F.S.\ 294}_{W_g}\right|$$

and for lateral accelerations ($\bar{H}_y$)

$$\left|T_{A/P}(\omega)\right| = \left|n_y(\omega)^{F.S.\ 294}_{V_g}\right|$$

where the acceleration frequency response functions are defined for a unit sinusoidal gust velocity input.

Because of the mechanization of the turbulence motion using FM tape inputs, an alternate definition is used for the simulation program:

$$\bar{H}_z = \left[\int_0^{\omega_c} \left|T_{D_z}(\omega)\right|^2 \frac{\Phi_{n_z}^{ps}(\omega)}{\sigma_g^2}\, d\omega\right]^{1/2}$$

and

$$\bar{H}_y = \left[\int_0^{\omega_c} \left|T_{D_y}(\omega)\right|^2 \frac{\Phi_{n_y}^{ps}(\omega)}{\sigma_g^2}\, d\omega\right]^{1/2}$$

where

T_{D_z}, T_{D_y} are the human frequency response functions of figure 12.

$\frac{\Phi_{n_z}^{ps}(\omega)}{\sigma_g^2}, \frac{\Phi_{n_y}^{ps}(\omega)}{\sigma_g^2}$ are the measured power spectral densities for vertical and lateral acceleration at the pilot station, normalized to a unit rms gust velocity

and

ω_c is a cutoff frequency, beyond which there is no significant power

Linear and angular accelerations on the platform near the pilot's seat were measured, and these values were used to compute the accelerations at the pilot seat location. The following relationships were used.

$$n_{z_{ps}} = n_{z_{PLATFORM}} + \frac{70\ddot{\theta}}{12g} + \frac{20\ddot{\phi}}{12g}$$

$$n_{y_{ps}} = n_{y_{PLATFORM}} + \frac{70\ddot{\psi}}{12g} + \frac{55\ddot{\phi}}{12g}$$

The process for measuring the $\bar{H}$ levels achieved in the simulator was as follows:

(1) The $n_{z_{ps}}$ and $n_{y_{ps}}$ transformed output signals on FM tape were recorded while the simulator cab was driven with the FM input tape at full level (2.1 m/sec) rms.

(2) A power spectral density (PSD) analysis of the recorded signals was performed.

(3) The PSD's were normalized to a 0.30 m/sec (1 ft/sec) rms gust level and scaled for accelerometer calibrations (volts/g).

(4) The PSD's were multiplied by the appropriate human frequency response functions (figure 12).

(5) The resulting functions were numerically integrated, and the square root taken to produce $\bar{H}$.

This process was performed for the vertical and lateral accelerations for the SMCS-off and SMCS-on cases. Table IV shows a comparison of the $\bar{H}$ levels from the simulator and from two separate analytical representations. The first is the model used in the CSSL digital simulation program, which has a quasi-steady representation of the response and gust aerodynamics with scaling factors. The second is a fully unsteady response and gust aerodynamic model. It may be seen that the simulator more closely duplicated the unsteady aerodynamic

representation than the CSSL representation. This is due to the frequency response characteristics of the simulator motion system, which has additional high-frequency attenuation added to the output signals to eliminate extraneous noise in the direct motion input channels. A set of first-order filters with a corner frequency of 33 rad/sec was used for this purpose.

Power spectral density of pilot seat acceleration due to turbulence.- It was desirable to simulate the actual B-1 motion environment as accurately as possible, rather than just duplicate the spectral characteristics of the vertical and lateral accelerations. To this end, power spectral densities of the three angular accelerations $\ddot{\theta}$, $\ddot{\psi}$, and $\ddot{\phi}$ were also measured for the SMCS-off and SMCS-on cases. Comparisons of the measured PSD's for the two linear and one angular accelerations, SMCS off and on, with the PSD's calculated by the digital simulation program system from time histories are given in figures 13 through 18. It may be seen that the agreement between measured and calculated PSD's of the n_z, n_y, and $\ddot{\theta}$ is quite good, especially at the important structural frequencies for both SMCS-off and SMCS-on cases. Pitch acceleration was a very noticeable and important component of motion in this study. This pitching motion at the crew station results from bending of the airframe in the structural modes.

RMS discomfort due to control excitation ($\sigma_{D\delta_H}$).- In addition to $\overline{H}$, another index used to define ride quality criteria is the discomfort index, $\sigma_{D\delta_H}$. This discomfort index is a measure of pilot discomfort caused by the horizontal tail control surface excitation of the flexible aircraft structure. The discomfort index for the vertical axis is determined by the following expression:

$$\sigma_{D_{\delta_H}} = \left[\int_0^\infty \left| T_D(\omega) \right|^2 \left| T_{A/P}(\omega) \right|^2 \Phi_{\delta_H}(\omega) \, d\omega \right]^{1/2}$$

$\sigma_{D\delta_H}$ = rms discomfort due to control excitation

$T_{A/P}(\omega) = \frac{n_{z_{ps}}}{\delta_H}(\omega)$ = crew compartment acceleration frequency response function due to control surface excitation (acceleration due to structural mode motion only)

$\Phi_{\delta_H}(\omega)$ = power spectral density of surface deflection

It was necessary to assure that the cockpit motions in response to control inputs were adequately simulated. To this end, calculated frequency responses of the accelerations at various locations (including the pilot's station), in response to sinusoidal control surface inputs, were compared to measured values. Figure 19 shows the comparison between the measured and calculated frequency response of control vane station n_z acceleration due to horizontal tail input. Figure 20 shows a similar comparison for n_y acceleration at control vane station due to lower rudder input. It may be seen that cockpit motions due to control surface inputs were adequately represented in this study.

Although the frequency data of $T_{A/P}(\omega)$ and $\Phi_{\delta_H}(\omega)$ were not available for calculation of $\sigma_{D\delta_H}$ in all control configurations of interest, the analytical transfer function of $n_{z_{ps}}/\delta_H$ data and the power spectral density data of the control surface motion (figure 54) were available from the program checkout conditions. These data were used to estimate the $\sigma_{D\delta_H}$ used in this simulation program. When flying the AF 8 terrain route, the values are as follows:

$$\sigma_{D_{\delta_H}} = 0.0171 \quad \text{with SCAS}$$

$$\sigma_{D_{\delta_H}} = 0.0056 \quad \text{with SCAS and SMCS}$$

These simulated values are within the B-1 design requirement during ATF of $\sigma_{D\delta_H}$ less than or equal to 0.021. In this expression for $\sigma_{D\delta_H}$, aircraft and structural characteristics are reflected in the term $T_{A/P}(\omega)$, and control system characteristics are reflected in the resultant power spectral density Φ_{δ_H}. A similar parameter which contains all of the aircraft, structure, and control characteristics was identified and used in this study to indicate sensitivity to pilot control excitation of structural modes in the TF task. This parameter is the frequency response amplitude of the acceleration at the pilot's station per unit of control stick input at the first structural mode frequency. This parameter is proposed as a possible sensitivity indicator for configurations where one predominant structural mode exists in the pilot's control bandwidth. The peak amplitude of the frequency response for various control system combinations is as follows.

SMCS	Prefilter	$n_{z_{ps}}/X_\theta$ at 2.07 Hz
Off	Out	3.6 g/cm (9.2 g/in.)
On	Out	1.8 g/cm (4.6 g/in.)
Off	In	1.44 g/cm (3.67 g/in.)
On	In	0.72 g/cm (1.83 g/in.)

Aircraft/Control/Display Dynamics

Three different types of VSD feedback signals (figure 2) were tested, as previously mentioned. These three configurations modify the dynamics of the resultant control task, and the pilot's performance is sensitive to this variation in response dynamics. The phase shift of the display feedback was selected as a possible parameter to indicate the aircraft/control/display dynamics. The phase shifts of $n_{z_{FB}}/X_\theta$ at 0.25 Hz (typical pilot control frequency) for the three feedbacks were computed, as follows:

VSD feedback	Phase lag of $n_{z_{FB}}/X_\theta$ at 0.25 Hz
X_θ + lag	38°
n_z + lag	63°
Combination of X_θ and n_z	44°

Terrain Roughness

Terrain roughness has been defined in reference 4 as a function of terrain slope, terrain amplitude and frequency components, aircraft velocity, and aircraft acceleration maneuver limits. The product of terrain frequency (cycles per foot) and aircraft velocity (feet per second) yields an apparent terrain frequency (cycles per second) which has been valuable in previous descriptions of terrain roughness.

The terrain altitude profiles were not recorded on FM tape; therefore, the terrain shape in terms of the aforementioned quantities was not defined in this report. Apparent terrain roughness, as defined in reference 4, is the level of rms vertical acceleration attained when performing the TF mission. In this study, maneuver load factors required for B-1 flight over the various terrain types were used to define the terrain roughness. The values computed in the simulation are:

Terrain	Maneuver load factor (g)
Water	$\sigma_{\Delta n_{z_{cg}}} = 0.1$
Flat (AF10)	= 0.2
CAL 6201	= 0.33
AF 8	= 0.4

Pilot Physiological and Biomedical Parameters

Two physiological variables were measured during each of the simulated long-duration TF missions. These were breath temperature (to obtain respiration rate) and heart rate, using an electrocardiogram (ECG). Triaxial linear accelerations at the head were also measured. Respiration and heart rate gave a real-time indication of pilot stress and, thereby, served as a medical safety backup to verbal communications. Head and seat accelerations were collected for later correlation with pilot performance, flight control mechanization, and SMCS mode.

Breath temperature was measured by three small chromel-alumel thermocouples attached to the pilot's boom microphone. A thermocouple was below each nostril and one just in front of the mouth. The highs and lows of the thermocouple output correspond to the exhalations and inhalations of the pilot. Respiration rate was derived from this signal by manually counting the number of exhalations per minute.

The pilot's ECG was recorded with commercially available medical-type disposable ECG electrodes. The primary signal was picked up by two electrodes. One was on the sternum, just below the throat; the other was on a lower rib on the left side of the chest. A ground reference electrode was placed on a middle rib on the right side of the chest. The two primary electrodes provided

input to a commercially available biomedical-type differential amplifier which provided a clear ECG signal. Heart rate was obtained by manually counting the number of spikes per minute in the ECG signal on the oscillograph record.

Triaxial accelerations of the pilot's head were measured with a triaxial arrangement of three piezo-resistive linear accelerometers mounted on a lightweight, but rigid, plastic bump hat worn by the pilot. To assure good coupling between the hat and the pilot's head, the hat liner was adjusted to each pilot's head size and the pilot was requested to keep the under-the-chin hat strap tight. Each accelerometer was zero-biased at zero g while the hat was manually held at an attitude which kept the gravity component on the accelerometer axis at near zero.

Blood pressure readings (systolic and diastolic) were taken preflight and postflight using standard clinical equipment (sphygmomanometer, cuff and stethoscope).

PERFORMANCE EVALUATIONS

Performance During Short Mission Runs (Run Set 1)

The data from run set 1 were obtained for a comparative evaluation of performance for variations of the VSD display feedbacks, control system prefilter, and effects of the SMCS under constant task conditions, including levels of turbulence and terrain routes AF 8 and CAL 6201. The results are summarized in table V for the different test situations. The TF performance measurements used were the altitude deviation from set clearance, Δh_e, and flight path angle, γ, over the selected peaks. In addition to the TF performance measurements, pilot ratings in the form of Cooper-Harper handling quality scale and other pertinent pilot comments are tabulated. The following significant results were obtained:

(1) The TF performance data showed a slight increase in altitude over the peaks as turbulence was increased, but were relatively constant for variations in VSD feedback systems with the SMCS on or off (figure 21).

(2) The effects of turbulence on pilot ratings were examined by comparing the Cooper-Harper and ride quality ratings against the level of turbulence-induced motion. These are shown in figures 22 and 23, indicating slight deterioration in Cooper-Harper rating above 0.9 m/sec (3 ft/sec) turbulence for the SMCS-on case. The SMCS-off case shows a rating deterioration with turbulence in a linear manner. The ride quality rating versus turbulence is

similar to the handling quality rating versus turbulence. This is probably due to the fact that the Cooper-Harper and ride quality rating scales are both indicating difficulties due to environmental parameters. (Refer to appendix B, and note the similarity in word descriptions.)

(3) The subjective pilot evaluation (i.e., pilot ratings) indicated sensitivity to the dynamics of the VSD feedback signals, as shown in figure 24. Examinations of the pitch stick activity from strip chart recorded data and PSD plots (figure 55) reveal considerable stick movement in the frequency region of 0.04 to 0.5 Hz. The stick activity from 0.04 to 0.1 Hz is related to terrain g-command. The stick activity from 0.1 to 0.5 Hz is due to the effects of the dynamics associated with VSD feedback. Phase shifts of the VSD feedback signals per stick input at 0.25 Hz were computed and plotted against Cooper-Harper rating (figure 24). The figure suggests that the deterioration of pilot rating may be attributed to the phase lag of the pilot display interface.

(4) The pilot ratings also indicated sensitivity to the crew discomfort-related parameter, as shown in figure 25. The prefilter and SMCS reduce the pilot excitation of the structural modes and thereby provide the pilot adquate control of the aircraft without inadvertent excitation of structural modes. With the prefilter-out and SMCS-off conditions, the pilot inputs excited the first structural mode, which resulted in an unacceptable pilot-induced oscillation (PIO) and pilot/structural mode coupling (refer to table V). With the SMCS on and prefilter out, significant reduction of the coupling was noted.

Performance During Long Mission Flights (Run Sets 2 and 3)

Three factors encountered during the test program limited the amount of data available for analysis:

(1) Several parameters were lost during FM tape recording. The Δh in the long mission run was available for only one pilot in run set 3.

(2) Simulation anomalies were experienced during the lateral steering runs, and these data were omitted from this study.

(3) Run sets 2 and 3 were planned in a manner that did not allow pilot ratings to be obtained as the program parameters were varied.

Performance versus mission duration.- The σ and mean values of all the recorded parameters were computed for each minute as an intermediate step. Data from approximately half of the parameters (table III) were recomputed for the duration of the segments, as shown in table VI. In table VI, the relationships between terrain and mission time are shown for each 4-hour run. Generally, the segment number which corresponds to CAL 6201 terrain has 5 to 7 minutes, and AF 8 terrain has 12 to 13 minutes elapsed time.

Figures 26 through 38 are the plots of σ and mean values of various performance measures obtained for each segment number for run sets 2 and 3. For clarity, five different symbols in the plots are used to differentiate between terrains. The following trends were noticed from the data:

(1) TF performance data, σ, and mean values of Δh (figure 26) show about the same performance level for a given terrain throughout the 4-hour flight. This characteristic level of performance is similar to that obtained for ATF flight, as will be discussed in more detail in later sections. Within the accuracy of measurement, the TF statistical performance is not a function of the mission duration. A detailed examination of the specific performance over the terrain peaks may be more sensitive than the statistical measures, but was not accomplished in this study.

(2) The $\sigma_{n_{x_{ps}}}$, $\sigma_{n_{y_{ps}}}$ values shown in the figures also indicate that the g-range is not a function of the mission duration. The maneuver load, $\sigma_{\Delta n_{z_{cg}}}$, is used as an indication of terrain roughness.

(3) A low variation in $\sigma_{\Delta M_n}$ (less than 0.02 ΔM_n with mission time) was observed over all the conditions tested. This indicates that the pilot was controlling aircraft mach number accurately throughout the 4-hour flight. The pilot was instructed to maintain a mach number variation to within 0.05 M_n from reference mach number.

(4) The $\sigma_{\Delta h}$, $\sigma_{\text{horiz bar}}$, $\sigma_{\Delta n_z}$, and $\sigma_{\dot{\chi}_\theta}$ parameters showed some variation with mission time. The variations observed were relatively large for flight over water/flat terrain. In particular, the control stick activity $\sigma_{\dot{\chi}_\theta}$ and $\sigma_{\text{horiz bar}}$ showed a consistent increase with mission time for flight over flat terrain.

(5) Pilot comments on the questionnaires indicate significant muscular fatigue during the long-duration runs. The B-1 aircraft has a relatively high stick force control gradient of 35.6 newton/g (10 lb/g) in the pitch axis.

TF performance versus terrain roughness and turbulence.- TF performance is a very strong function of the terrain roughness (maneuver load factor), as shown in the correlation of $\sigma_{\Delta h}$ and $\sigma_{\Delta n_z}$ from run set 3, subject A. These data are plotted in figure 39, using six segments of water, two segments of flat, six segments of CAL 6201, and seven segments of AF 8 terrain route data. The correlation between these two measures is very high, as indicated by a coefficient of correlation equal to 0.91. The coefficient of correlation was computed using Pearson's product-moment coefficient (reference 5), as follows:

$$R_{xy} = \frac{\Sigma xy}{N \sqrt{(\Sigma x^2)\ (\Sigma y^2)}}$$

where

R_{xy} = correlation between x and y

x = deviation of any x-score from the mean in test x

y = deviation of the corresponding y-score from the mean in test y

Σxy = sum of all the products of deviations, each x-deviation times its corresponding y-deviations

N = number of data samples

The coefficient of correlation indicates a degree of correlation between two sets of parameter measurements and can vary from a value of 1, which means perfect correlation, to zero, which means complete independence or no correlation. The maneuver load is related to terrain roughness. The rougher the terrain, the greater the aircraft maneuvering required for TF and, therefore, it becomes more difficult to follow terrain contour within a given aircraft maneuver load and speed limitations. The mean value of the $\sigma_{\Delta n_{z_{cg}}}$ for each terrain type is indicated by an arrow symbol in figure 39. The AF 2 data shown in the figure have a very large $\sigma_{\Delta h}$ value. This is due to the fact that the terrain segment selected for AF 2 is very short, 37 km (23 miles), and rugged (figure 7), which negates the use of a statistical value. In planning the simulation program, the turbulence was statistically correlated with terrain. This correlation for run sets 2 and 3 is shown in figure 40. The mean values (indicated by circle) of σ_{turb} and the maximum and minimum of the measured σ_{turb} values (indicated by bar) are shown plotted against the terrain roughness factor.

The TF performance measure, $\sigma_{\Delta h}$, is also shown with respect to the σ_{turb} in figure 41. The figure indicates that the TF performance is not a direct function of turbulence for the level of turbulence that was simulated. The maximum simulated turbulence induced acceleration at the pilot station was 0.082 g rms. Other studies (such as reference 11) show that the TF performance was not degraded with acceleration levels up to 0.3 g rms.

Pilot performance versus terrain roughness and turbulence.- Significant correlations were found between the pilot tracking performance, $\sigma_{Horiz\ Bar}$, with the maneuver load, $\sigma_{\Delta n_z}$, or terrain roughness, showing that increasing amounts of tracking error are associated with terrain difficulty. This is expected, since the more difficult the terrain, the more frequent and larger the maneuver commands and, hence, more maneuvering error. There is no definitive explanation as to why pilot A performs better with SMCS off than SMCS on (figure 42). The $\sigma_{Horiz\ Bar}$ values computed from each segment number are plotted against turbulence level (σ) for a given terrain in figures 43 through 46 for four flights (run sets 2 and 3). The lines in the figures are average lines drawn through the σ values for each terrain type. The figures indicate that the effects of turbulence in flights over contour terrains (CAL 6201 and AF 8) are different from flights over level terrain. In the contour terrains, the pilot tracking performance is relatively constant with an increase in turbulence level. However, the pilot's tracking performance deteriorates consistently as turbulence level increases in flat terrain. The pilot performance measures, $\sigma_{Horiz\ Bar}$, versus pilot's stick activity, σ_{χ_θ}, are plotted in figures 47 and 48. The figures show that the $\sigma_{Horiz\ Bar}$ increases with stick activity. This relationship is mainly caused by the terrain roughness. Marked differences between the SMCS-on and -off cases are observed from the figures (both pilots), showing that there is some discontinuity pattern in $\sigma_{Horiz\ Bar}$ versus σ_{χ_θ} for SMCS-on cases. For the SMCS-on case, there are greater corrective stick movements for smoother terrain than for rougher terrain. The number of subjects in the long mission flight where data are available is limited. Five is generally necessary for a good set of data samples.

Physiological/biodynamic measures and results.- Respiratory rate and pulse rate are presented in figure 49, for subject A, and in figure 50, for subject B. The data are plotted separately for SMCS on and SMCS off. The following observations and general comments can be made from examination of the data.

Pulse rate data for both subjects show that SMCS on produced a slightly lower value than SMCS off. For both subjects, the SMCS-on testing followed the SMCS-off condition. Both subjects showed an initial pulse rate increase which may be seen by comparing the preflight level to the first several readings after the onset of vibration. Subject B showed a small increase in pulse rate during the SMCS-off condition run and a larger increase during SMCS on; for subject A, this was reversed.

Although pulse rate became somewhat elevated at the onset of vibration, it did not rise further, as evidenced by the SMCS-on and -off data for subject B and the SMCS-off data for subject A. The SMCS-on data for subject A show a gradual return to resting levels. Postflight pulse rate for subject A was lower than preflight and run level data for both SMCS conditions. For subject B, postflight pulse rate is higher than preflight, but almost equal to that observed during the runs with SMCS on and off.

Respiratory rate data showed no systematic variation as a function of mission duration, SMCS condition, or preflight/postflight factors.

The physiological data for both subjects (pulse and respiration) fall within normal limits (references 7 and 8) before, during, and after each run.

The lower pulse rate for the SMCS-on condition (as opposed to SMCS off) may be due to a familiarization effect, since it was conducted after the SMCS-off condition, or it may be due to the lower vibration levels associated with SMCS on, or it may be due to the combined effect of both factors.

The initial pulse rate increase that was evidenced by both subjects is predictable and is in accordance with the classical anticipatory fear response pattern typically shown in this setting (references 6 and 9).

The gradual return of the pulse level of subject A to resting level during the course of the SMCS-on run has been observed in prior research (references 6, 9, and 10).

The respiratory rate data, although somewhat higher than those shown in prior studies, are not judged to differ significantly. This must be tempered by the fact that the data were taken for two subjects over two runs; a small sample in light of individual differences.

The pulse and respiratory data reveal no significant stress effects due to the vibration conditions used in this study. These same data also fail to differentiate mission duration and task difficulty level effects.

Manual Terrain-Following (MTF) and Automatic Terrain-Following (ATF) Performance Comparison (Run Set 4)

ATF performance was measured to provide a base level of performance. The MTF and ATF performance comparisons were made over two types of terrain: CA1 6201 and AF 8 routes. A 6-minute flight of segment 2 (pilot A, SMCS on) data for a CAL 6201 route and a 12-minute flight of segment 7 (pilot A, SMCS on)

data for an AF 8 route were used for MTF cases. For the ATF case, the terrain segments that are equivalent to the MTF terrain routes were used so that the comparison can be made over the same terrain.

A comparison on the $\Phi_{\Delta h}$, data between MTF and ATF is shown in figures 51 and 52 for CAL 6201 and AF 8, respectively. Large differences in the frequency range of 0.04 to 0.1 Hz are observed between the two $\Phi_{\Delta h}$ plots. The frequency compositions of the CAL 6201 and AF 8 altitude profiles have a relatively high power spectral density. The predominant frequency for CAL 6201 is approximately 0.07 (i.e., 15 seconds flight time between terrain peaks), as observed from figure 51. Thus, this large difference in $\Phi_{\Delta h}$ is a clear indication of the aircraft trajectory path differences existing between MTF and ATF runs. There are probably many reasons for this, but one logical explanation is that of pilot reaction time. The pilot reacts slower than and differently from the automatic system. Since the B-1 TF command algorithm was developed from autopilot response time, equivalent performance may be achievable if proper pilot lead compensation is provided in the TF algorithm for MTF operation.

A comparison of the Φ_{δ_H} for MTF and ATF flights is shown in figures 53 and 54 for CAL 6201 and AF 8 routes. An interesting observation from the figures is the increased control surface activity above 0.1 Hz in MTF due to the pilot's extraneous stick movements. This stick activity is not actually affecting the TF performance, as seen in figure 51. This effect may be attributable to several factors, including possible PIO tendencies which were observed from strip chart data. The TF algorithm was not optimized for MTF, and additional extraneous motions may be due to improperly phased display feedbacks.

The $\Phi_{\text{Horiz Bar}}$ and Φ_{χ_θ} data are shown in figure 55 for manual TF over route CAL 6201. This figure clearly indicates that there is some coupling induced between the VSD signals and pilot/aircraft system above 0.1 Hz, due to display feedbacks. The terrain maneuver command above 0.1 Hz is very small. Therefore, the coupling must be through the stick and/or aircraft normal g feedbacks in the VSD system.

CONCLUSIONS

The analysis of simulation data acquired during the B-1 development program has provided preliminary validation of existing ride quality criteria, and has added to the technology base for the design of future aircraft. The data available for analyses were limited, in that the data from long mission flights were available only from two subjects and adequate statistical analyses of the performance and environmental parameters were not possible. However, the experimental data and the data analyses have shown results consistent with past studies

and new relationships between parameters which may be significant in specification of new criteria.

The simulation program was designed to provide flight crew evaluation of manual TF under conditions representative of the B-1 ride qualities. The subjective evaluation by all pilots who participated in the program indicated that the ride qualities were satisfactory. Therefore, it was generally concluded that these results provided preliminary validation of the levels of both the crew sensitivity index ($\bar{H}$) and rms discomfort due to control excitation ($\sigma_{D_{\delta H}}$) which were simulated in this program. The following conclusions were also derived from the data analyses:

(1) There was no indication of TF performance deterioration with mission time for the conditions tested. The pilot's subjective comments did indicate various levels of fatigue for the 4-hour runs.

(2) The turbulence and terrain were programmed according to a specific schedule such that low turbulence existed for mild terrain, and high turbulence existed over rough terrain. This factor caused difficulty in determining the variation in performance with turbulence level. Therefore, the statistical data obtained indicated no degradation of performance for variations in the turbulence-induced vibration levels up to 0.11 maximum total g rms at the pilot's station. Discrete performance parameters such as altitude clearance over a specific peak did show an increase (deterioration) with turbulence-induced motion increase. More detailed examination of the discrete performance parameters should be included in future studies. However, subjective ride quality ratings did vary with levels of vibration, and these ratings were acceptable for the conditions tested.

(3) TF performance varies significantly with terrain differences but remains relatively constant for a given terrain. The maneuver load factor can be used as a good indicator of terrain roughness.

(4) TF performance did not vary significantly with variations in the control/display dynamics for the conditions tested in this study, but pilot rating did show sensitivity to display variations. A control/display dynamic parameter was identified which exhibited strong correlation with pilot handling quality ratings. This parameter was the phasing of the display signal due to stick input at the pilot's control frequency.

(5) Performance and pilot ratings appear to vary significantly with the rms discomfort due to control excitation ($\sigma_{D_{\delta H}}$). However, the variations in $\sigma_{D_{\delta H}}$ and related pilot comments were not available for correlation from the results of this program. A new parameter similar to $\sigma_{D_{\delta H}}$ did correlate well with pilot handling quality ratings. The new parameter, identified as a strong

handling quality, ride quality, PIO predictor in the MTF task simulated in this program, is the peak of the frequency response of pilot seat acceleration to stick input at the first structural mode.

(6) The conditions simulated did not result in workload or stress conditions which would cause respiratory rate or pulse rate to exceed normal limits during the 4-hour flight.

(7) Four-hour flights of MTF should be possible without adverse fatigue for the conditions simulated. Comments indicated muscular fatigue toward the end of 4-hour flights, but the data show little reflection of this muscular fatigue affecting the pilot's tracking ability.

(8) Slight variations and deterioration in pilot tracking occurred over the water/flat terrains which have been attributed to either muscular fatigue or boredom.

The preceding results in general concur with the results reported in previous studies of references 6, 9, 10, and 11. In reference 6, the turbulence levels were varied up to 0.2 g rms in a mission time of 4 hours, with no apparent changes in TF performance or respiratory and pulse rates. Slight deterioration of performance due to boredom has been reported in references 9, 10, and 11.

APPENDIX A.- BASIC AND AUGMENTED HANDLING QUALITY PARAMETERS

Parameter	Configuration	
	Basic	Augmented
ω_n, rad/sec	2.06	4.45
ζ	0.58	0.64
$1/T_{\theta_2}$, 1/sec	1.00	2.15
Fs/g, newton/g (lb/g)	35.6 (10.0)	28.5 (8.0)
ω_d, rad/sec	2.2	2.0
ζ_D	0.1	0.5
T_R, sec	0.51	0.12
$L_{\delta_{H'}}\left(\delta H'\right)_{max}$, rad/sec^2	1.9	1.9
$(\omega_\phi/\omega_d)^2$	0.89	0.95

a. Cooper-Harper rating scales

1	Excellent highly desirable	Pilot compensation not a factor for desired performance.
2	Good negligible deficiencies	Pilot compensation not a factor for desired performance.
3	Fair - some mildly unpleasant deficiencies	Manual pilot compensation required for desired performance.
4	Minor but annoying deficiencies	Desired performance required moderate pilot compensation.
5	Moderately objectionable deficiencies	Adequate performance required considerable pilot compensation.
6	Very objectionable, but tolerable deficiencies	Adequate performance requires extensive pilot compensation.
7	Major deficiencies	Adequate performance not attainable with max tolerable pilot compensation. Controllability not in question.
8	Major deficiencies	Considerable pilot compensation is required for control.
9	Major deficiencies	Intense pilot compensation is required for control
10	Major deficiencies	Control will be lost during some portion of required operation.

Increase of pilot effort with turbulence	Deterioration of task performance with turbulence	Rating
No significant increase	No significant deterioration	A
More effort required	No significant deterioration Minor Moderate	B C D
Best efforts required	Moderate Major (but evaluation tasks can still be accomplished) Large (some tasks cannot be performed)	E F G
Unable to perform tasks		H

b. Ride quality rating scales

APPENDIX C.- PILOT QUESTIONNAIRE SHEET

Set No._____ Run No._____ Pilot _____ Date _____

Conditions

1. SMCS: On____Off_____
2. Turbulence: Present_____ Absent_____
3. SCAS Failure: Yes_____ No_____ (Not applicable for this report)

Ratings

1. Cooper-Harper ratings

   (a) MTF Task_____
   Primary basis of rating (check one): Vertical Control_____
   Lateral Control_____
   Both_____

   (b) SCAS Failure Recovery Task_____ (Not applicable for this report)

2. Ride Quality Rating _____

3. Steering Cross Sensitivity Rating (Not applicable for this report)

	Too Low			About right	Too High		
	Extreme	Moderate	Slight		Slight	Moderate	Extreme
Vertical							
Lateral							

4. PIO Tendencies Rating

	Not noticeable	Slight	Moderate	Severe
Vertical				
Lateral				

Comments:

REFERENCES

1. Rustenburg, J.W.: Development of Tracking Error Frequency Response Function and Aircraft Ride Quality Design Criteria for Vertical and Lateral Vibration, ASD-TR-70-18, Jan. 1971.

2. Flight Control Analysis: Flight Control System Description, Rockwell International, TFD-71-807, 1972.

3. Saunders, K.D.: B-6613 Low Level Gust Study, Vol. I, Technical Analysis, WADP TR60-305, Vol. 5, Mar. 1961.

4. Bergmann, G.E.; and DeBacker, G.L.: Terrain Following Criteria, AFFDL-TR-73-135, 1974.

5. Guildford, J.P.: Fundamental Statistics in Psychology and Education, McGraw-Hill Book Company, Inc., 1956.

6. Lefritz, N.M.: Pilot Performance Capabilities in Low-Altitude, High-Speed (LAHS) Flight, NA-65-1006, May 1966.

7. Bioastronautics Data Book, NASA SP-3006, 1973.

8. McFarland, R.A.: Human Factors in Air Transportation, McGraw-Hill, 1953.

9. Holland, C.L.: Performance and Psychological Effects of Long Term Vibration, AMR-TR-66-143, Oct. 1966.

10. Dudek, R.A.; Ayoub, N.M.; and El-Nawawi, M.A.: Optimal Work-Rest Schedules Under Prolonged Vibration, Ergonomics, 1973, 16, 469-479.

11. Soliday, S.M.; and Schohan, B.: A Simulator Investigation of Pilot Performance During Extended Periods of Low-Altitude, High-Speed Flight, NASA CR-63, June 1964.

TABLE I.- SUMMARY OF TEST CONDITIONS

Run set	Terrain	Turbulence (a)	Vertical situation display	SMCS	Prefilter	Duration (min)	Purpose
1	CAL 6201	0 0.5 1.0	X_θ + lag n_z + filter	Off On	Out In	7	TF display, prefilter performance
2	AF 8 Composite (b)	0 Variable (b)	Combination (c)	Off	In	240	TF/ride qualities long-mission length
3	AF 8 Composite	0 Variable	Combination	On	In	12 240	TF/ride qualities/ SMCS long-mission length
4	CAL 6201 AF 8 AF 2	0	Not applicable	On	In	7 12 4	Automatic terrain-following (ATF) performance

[a]Factor on 2.1 m/sec (7 ft/sec) RMS combined w_g and v_g

[b]Terrain and turbulence scheduled for long runs

[c]1/2 (X_θ + lag) + 1/2 (n_z + filter)

TABLE II.- PARAMETERS RECORDED ON STRIP CHARTS

Recorder No. 1		Recorder No. 2	
1.	Aircraft and terrain altitude	1.	n_z (pilot seat)
2.	Δh (aircraft minus terrain)	2.	X_θ
3.	n_z (turbulence only)	3.	n_y (pilot seat)
4.	γ (flight path angle of vehicle)	4.	X_ϕ
5.	γ_C (command)	5.	Bank angle error (vertical bar)
6.	Vertical acceleration command	6.	Vertical acceleration error (horizontal bar)
7.	$n_{Z_{cg}}$	7.	ECG (pulse)
8.	n_Z (pilot seat)	8.	Thermocouple (respiration)
Recorder No. 3		Recorder No. 4	
1.	δ_H	1.	n_Y } platform acceleration (monitor only)
2.	$\delta_{CV(S)}$	2.	n_Z }
3.	$\delta_{CV(A)}$	3.	$\ddot{\theta}$ }
4.	Δ Mach No.	4.	$\ddot{\psi}$ }
5.	Throttle No. 2	5.	$\ddot{\phi}$ }
6.	Velocity	6.	α (angle of attack)
7.	ϕ (roll angle)	7.	q (pitch rate)

TABLE III.- PARAMETERS RECORDED ON FM TAPE

No.	Parameter	No.	Parameter
1.	$n_{Z_{PS}}$ (normal acceleration at pilot seat)	13.	Δ Mach No.
2.	$n_{Y_{PS}}$ (lateral acceleration at pilot seat)	14.	Clearance alt (H-HTX)
3.	$n_{X_{PS}}$ (fore-and-aft acceleration	15.	δ_H (horizontal tail deflection)
4.	n_{Z_H} (vertical acceleration helmet mounted)	16.	δ_{RL} (lower rudder panel deflection
5.	n_{Y_H} (lateral acceleration helmet mounted)	17.	$\delta_{H'}$ (rolling tail differential deflection)
6.	n_{X_H} (axial acceleration helmet mounted)	18.	$\delta_{cv}^{(S)}$ (SMCS symmetric vane deflection)
7.	$n_{Z_{cg}}$ due to maneuver only	19.	$\delta_{cv}^{(A)}$ (SMCS antisymmetric vane deflection)
8.	X_θ (pitch stick)	20.	n_Z (due to turbulence only)
9.	X_ϕ (roll stick)	21.	ECG (pulse)
10.	Bank angle error	22.	Thermocouple (respiration)
11.	Vertical acceleration error	23.	Rudder pedal (X_Y)
12.	Throttle No. 2	24.	(spare)

TABLE IV.- CREW SENSITIVITY INDEX VALIDATION

		Quasi-steady aero & gust with factors	Unsteady aero & gust	Simulator (measured)
$\bar{H}_Z$	SMCS off	0.0363	0.0316	0.0305
	SMCS on	0.0333	0.0278	0.0265
		Quasi-steady aero & gust with factors	Quasi-steady aero unsteady gust	Simulator (measured)
$\bar{H}_Y$	SMCS off	0.0149	0.0120	0.0123
	SMCS on	0.0068	0.0069	0.0063

TABLE V. - SUMMARY OF TF AND PILOT PERFORMANCES FROM RUN SET 1

Terrain	σTurb level m/sec (ft/sec)	SMCS	VSD	Prefilter	TF Performance over peak (a)		Pilot ratings (b)		Other pilot comments		
					Δh_e m (ft)	γ (deg)	Cooper-Harper	Ride quality	PIO*	Pilot acceptability	Safety
CAL 6201	1.067 (3.5)	Off	X_θ + lag	Out			7.5	D	Yes	Poor	Unsafe
	1.067 (3.5)	On	X_θ + lag	Out			6	C-	Yes		
AF 8	0	Off	X_θ + lag	In	5.5 (18.0)	2.6	3		No	Good	Unsafe in out-of-trim condition
	1.067 (3.5)	Off	X_θ + lag	In	6.1 (20.0)	2.2	4	D	No	Good	
	2.134 (7.0)	Off	X_θ + lag	In	9.8 (32.0)	2.5	5	E-	No	Good	
	0	Off	$n_{z_{SMCS}}$ + lag	In	5.2 (17.0)	2.1	4		Slight	Poor	Good
	1.067 (3.5)	Off	$n_{z_{SMCS}}$ + lag	In	7.0 (23.0)	2.3	4.5	D	Slight	Poor	
	2.134 (7.0)	Off	$n_{z_{SMCS}}$ + lag	In	8.5 (28.0)	2.2	5	E-	Slight	Poor	
	1.067	Off	Combination	In	5.2 (17.0)	1.5	3.5	C-	No	Good	Good
CAL 6201	0	Off	X_θ + lag	In	4.4 (14.4)	0.5	3.5	A	No	Good	Unsafe in out-of-trim condition
		On	X_θ + lag	In	4.6 (15.1)	0.5	3.5	A	No	Good	
	1.067 (3.5)	Off	X_θ + lag	In	3.1 (10.2)	1.0	4.0	C-	No	Good	
		On	X_θ + lag	In	5.5 (18.0)	0.5	3.5	D	No	Good	
	2.134 (7.0)	Off	X_θ + lag	In	7.3 (24.0)	1.2	5.0	E	No	Good	
		On	X_θ + lag	In	6.7 (22.0)	1.2	4.5	E-	No	Good	

[a]Average value obtained over selected terrain peaks.

[b]Average value obtained from five subjects over selected terrain peaks.

*Pilot-induced oscillations

**Terrain following

TABLE VI.- RELATIONSHIPS OF SEGMENT NUMBER TO ELAPSED TIME

Segment No.	Subject A, SMCS on				Subject B, SMCS on				Subject A, SMCS off				Subject B, SMCS off			
	Terrain	Mission time (min)			Terrain	Mission time (min)			Terrain	Mission time (min)			Terrain	Mission time (min)		
		From	To	Lapse time		From	To	Lapse time		From	To	Lapse time		From	To	Lapse time
1.	Water	3	8	5	Water	0	4	4	Water	0	4	4	Water	0	4	4
2.	6201	8	16	8	6201	4	11	7	6201	4	12	8	6201	4	12	8
3.	Water	16	29	13	Water	11	25	14	Water	12	26	14	Water	12	26	14
4.	-	-	-	4	6201	25	33	8	6201	26	34	8	6201	26	34	8
5.	6201	33	41	8	Water	33	49	16	-	-	-	2	Water	34	39	5
6.	Water	41	57	16	AF 8	49	62	13	Water	36	49	13	AF 8	60	63	13
7.	AF 8	57	70	13	AF 8	62	75	13	AF 8	52	65	13	AF 8	63	76	13
8.	AF 8	70	83	13	AF 8	-	-	6	AF 8	65	78	13	AF 8	76	89	13
9.	AF 8	83	96	13	AF 8	81	94	13	AF 8	78	91	13	6201	89	97	8
10.	6201	96	103	7	6201	94	101	7	6201	91	99	8	AF 8	97	109	12
11.	AF 8	103	115	13	AF 8	101	114	13	AF 8	99	112	13	-	-	-	5
12.	Water	119	121	3	-	-	-	6	-	-	-	5	6201	114	119	5
13.	6201	121	128	7	6201	120	126	6	6201	117	123	7	Water	123	125	2
14.	Water	128	132	4	Water	126	131	4	Water	125	128	3	6201	125	133	8
15.	6201	132	140	8	6201	131	138	7	6201	130	135	5	Flat	133	137	4
16.	Flat	140	143	3	Flat 1	138	141	3	-	-	-	4	AF 2	137	139	2
17.	AF 2	143	145	2	AF 2	141	144	3	AF 2	139	141	2	6201	139	146	7
18.	6201	145	153	8	6201	144	151	7	o201	141	149	8	AF 8	146	159	13
19.	AF 8	153	165	13	AF 8	151	164	13	AF 8	149	162	13	AF 8	159	172	13
20.	AF 8	165	178	13	AF 8	164	177	13	AF 8	162	175	13	Water	178	220	42
21.	Water	191	227	36	Water	177	225	48	Water	182	219	37	6201	220	227	7
22.	6201	227	233	7	6201	225	233	8	6201	224	230	6	Flat	227	231	4
23.	Flat	236	238	2	Flat	233	237	4	Flat	230	234	4	6201	231	239	8
24.	6201	238	246	8	6201	237	244	7	6201	234	241	7	AF 8	239	251	12
25.	AF 8	246	259	12	AF 8	244	258	14	AF 8	241	252	11				

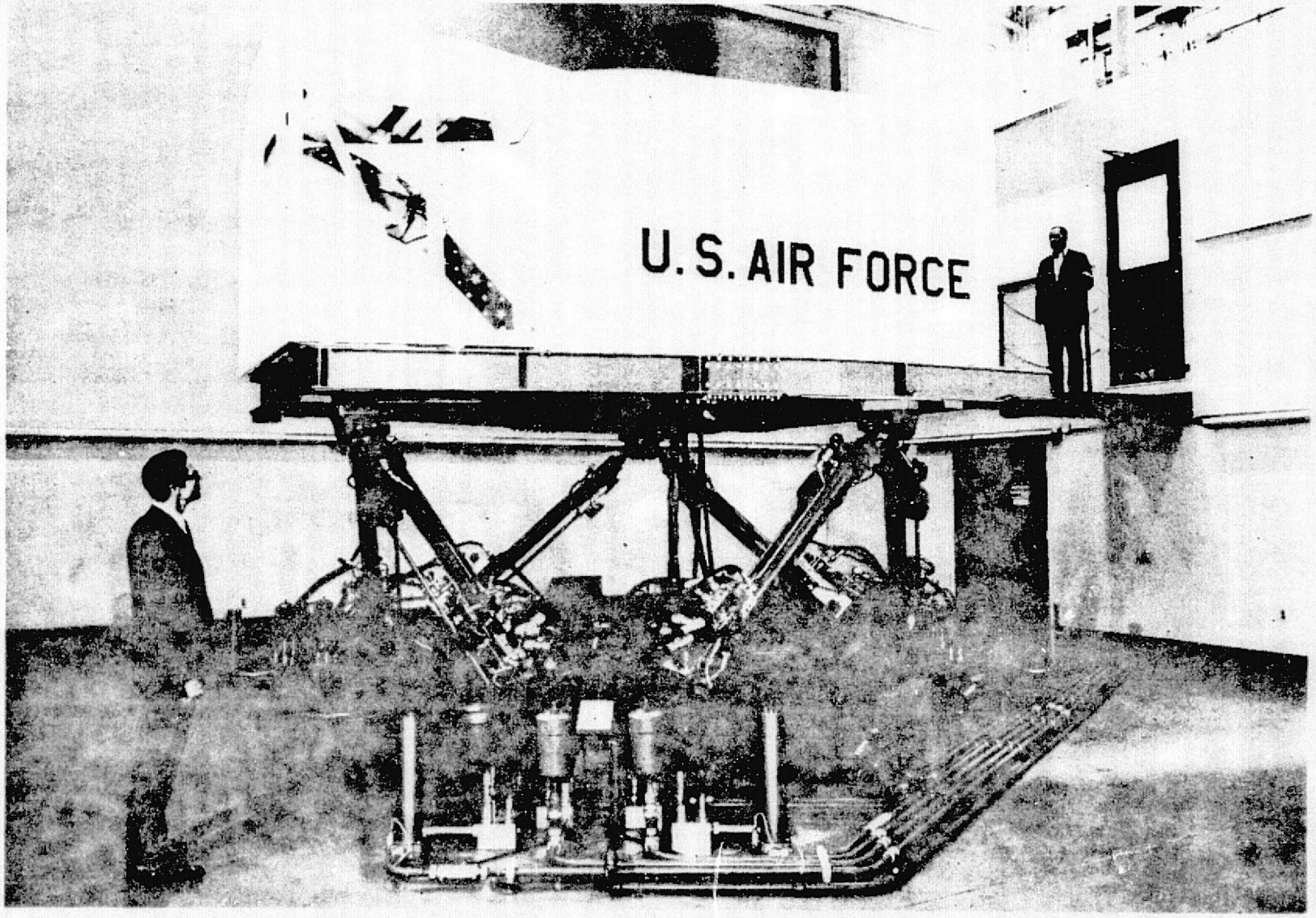

Figure 1.- B-1 moving-base simulator.

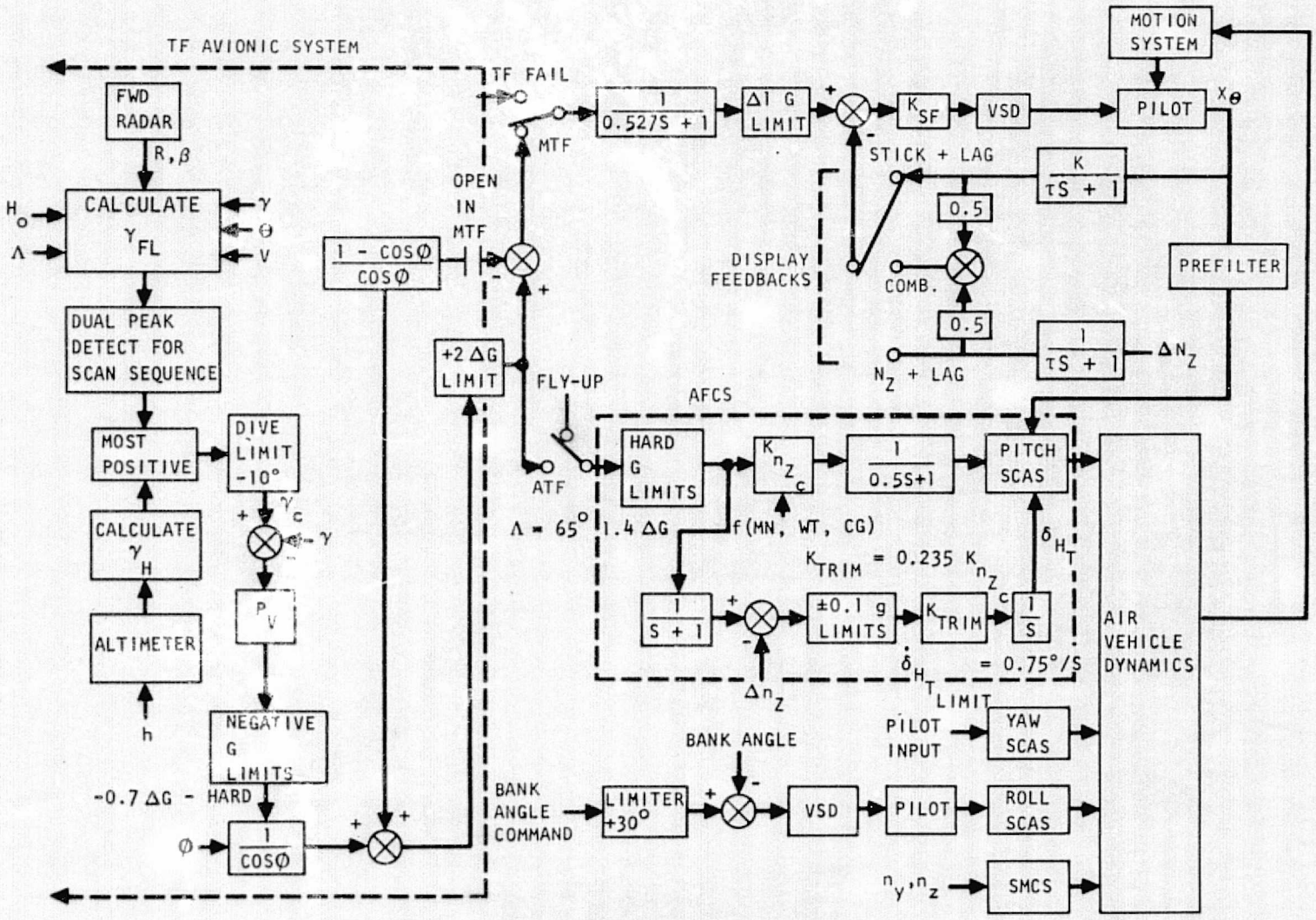

Figure 2.- Functional block diagram of total simulation system.

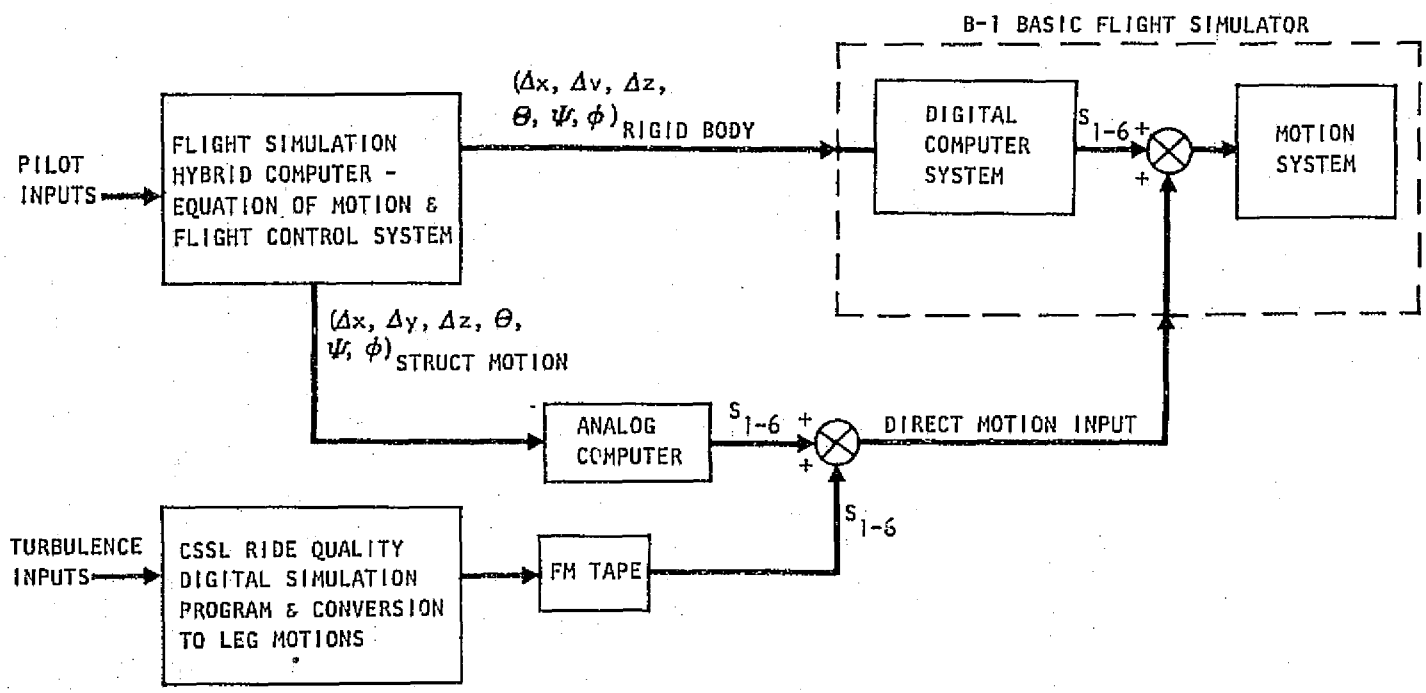

Figure 3.- Schematic of ride quality flight simulation.

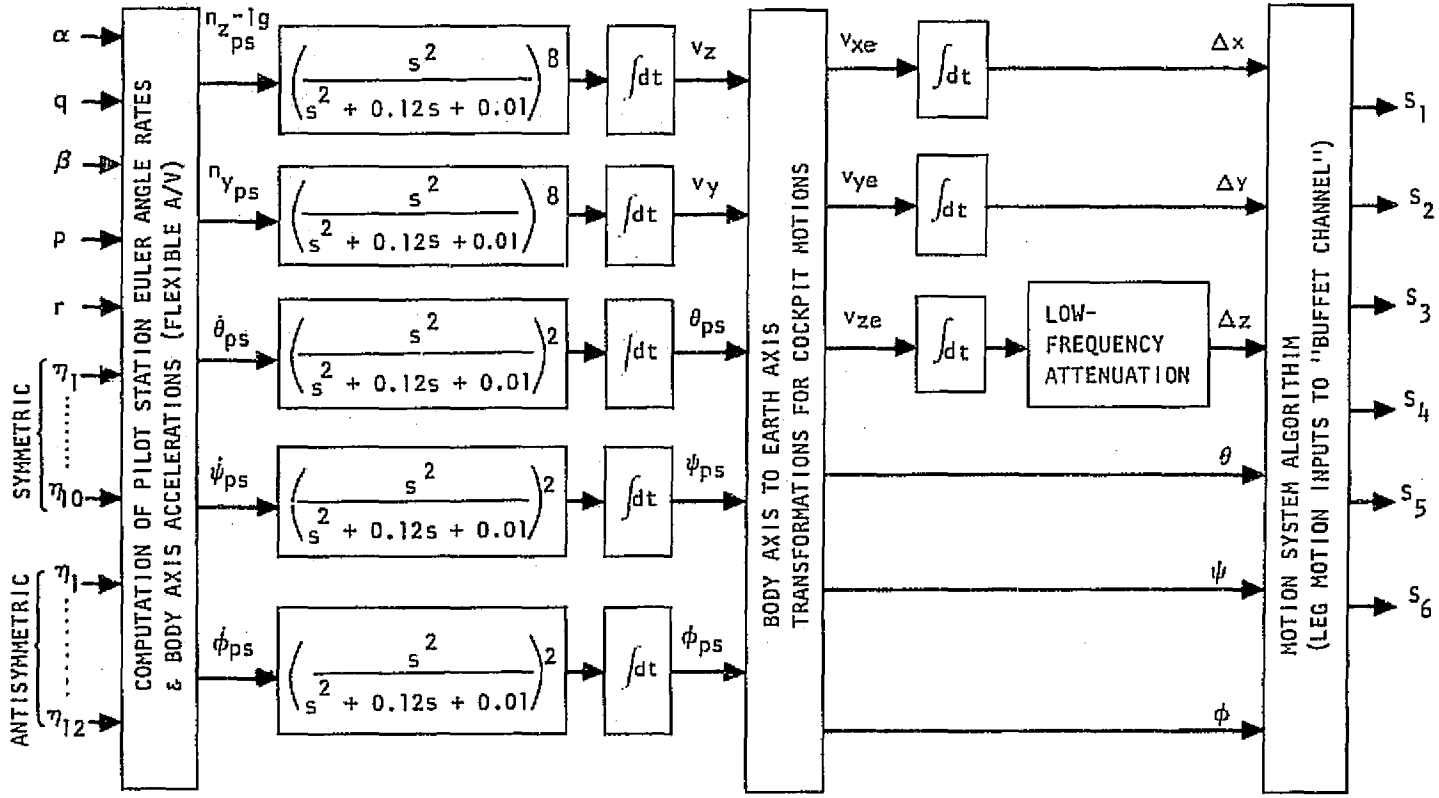

Figure 4.- Digital computation of simulator input variables for turbulence.

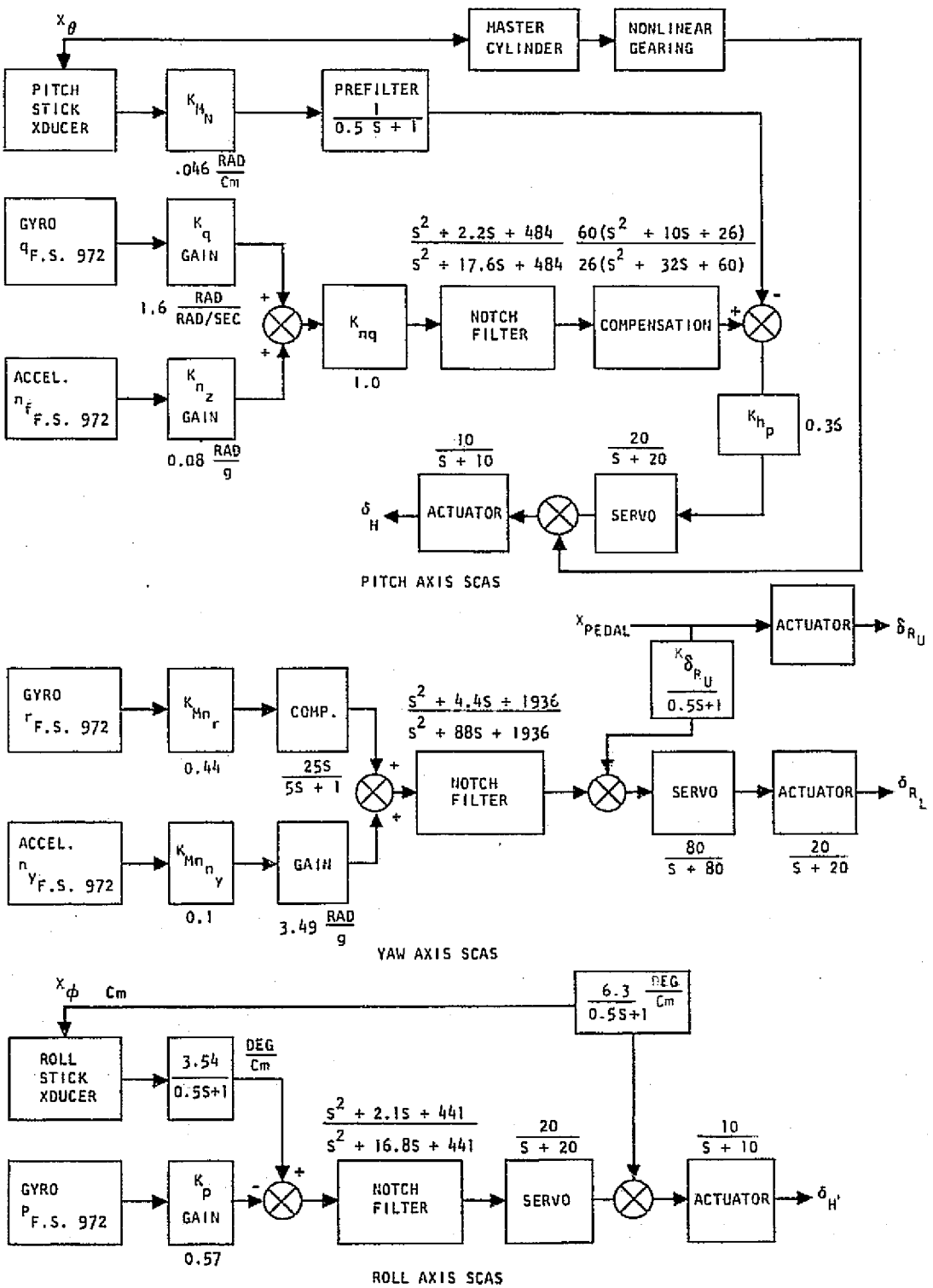

Figure 5.- B-1 stability and control augmentation system (SCAS).

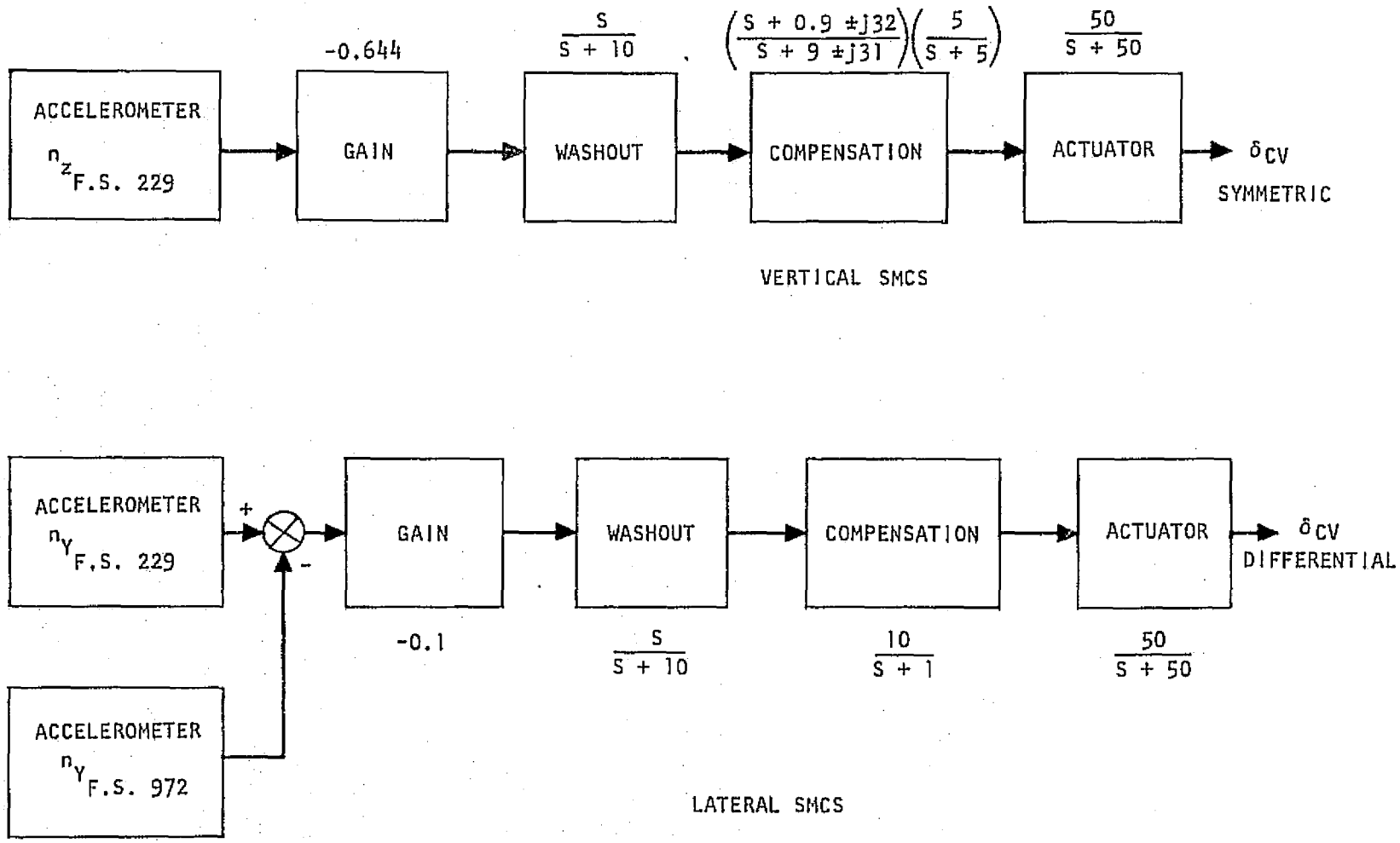

Figure 6.- B-1 structural mode control system.

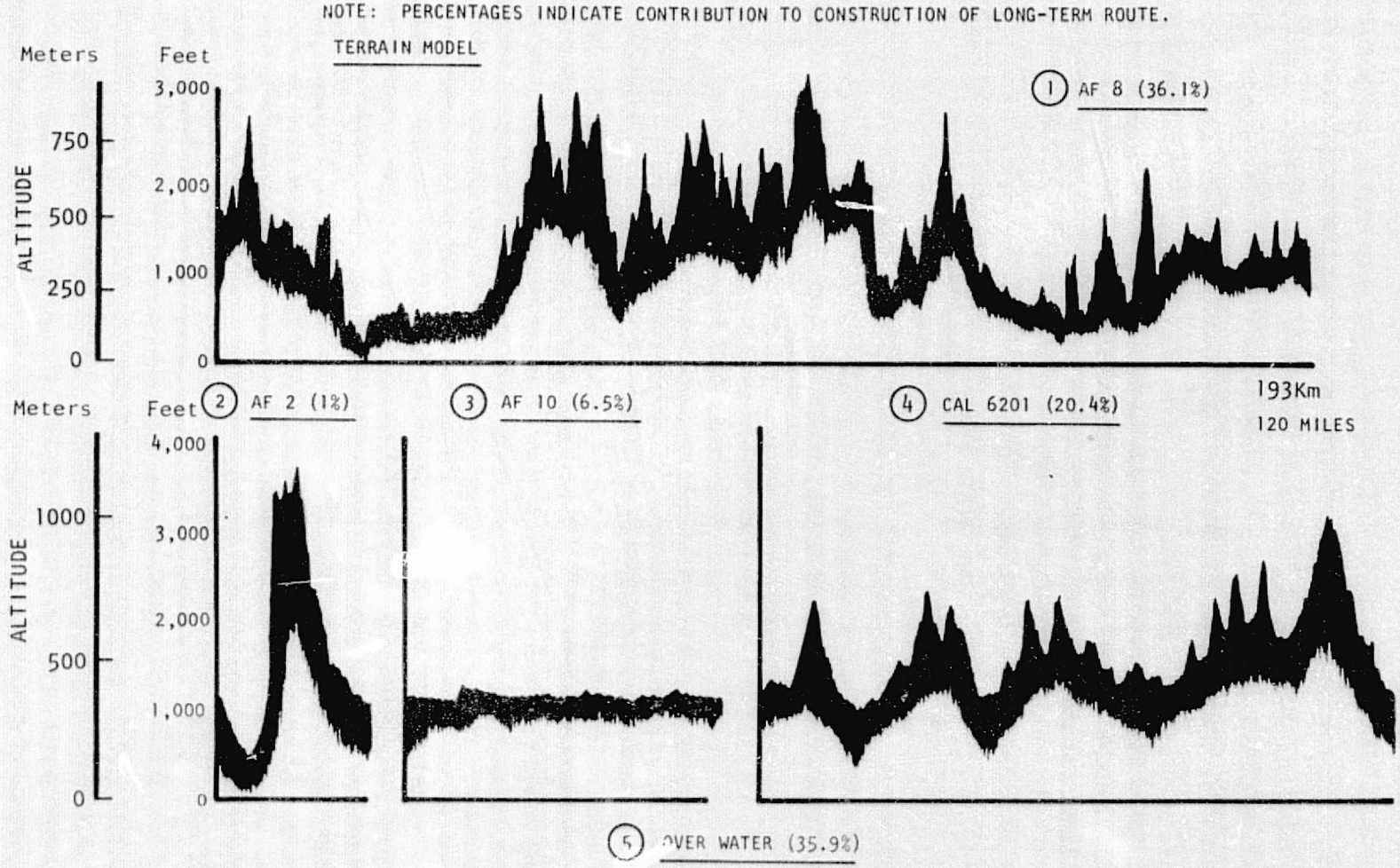

Figure 7.- Terrain model elements.

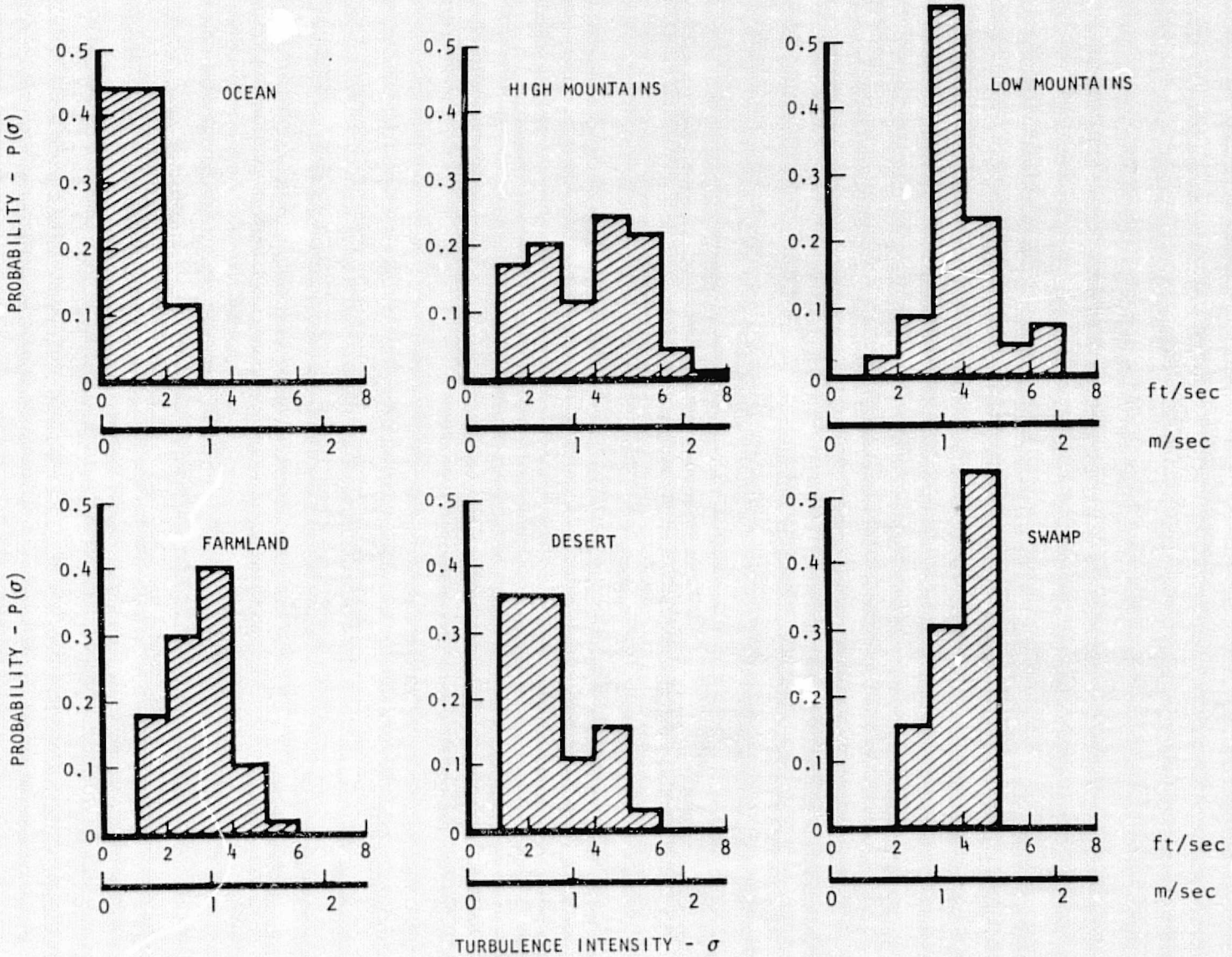

Figure 8.- Correlation of terrain and turbulence.

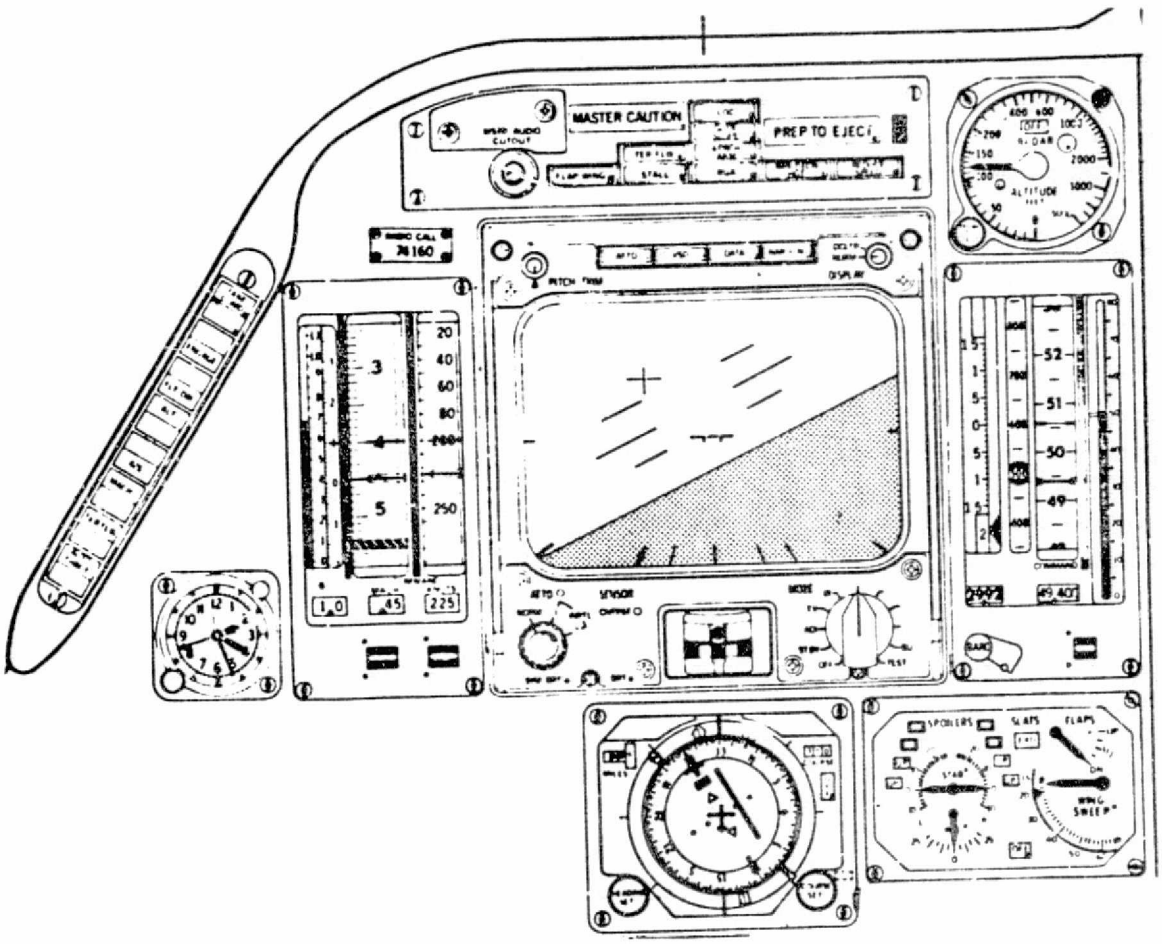

Figure 9.- B-1 instrument panel layout.

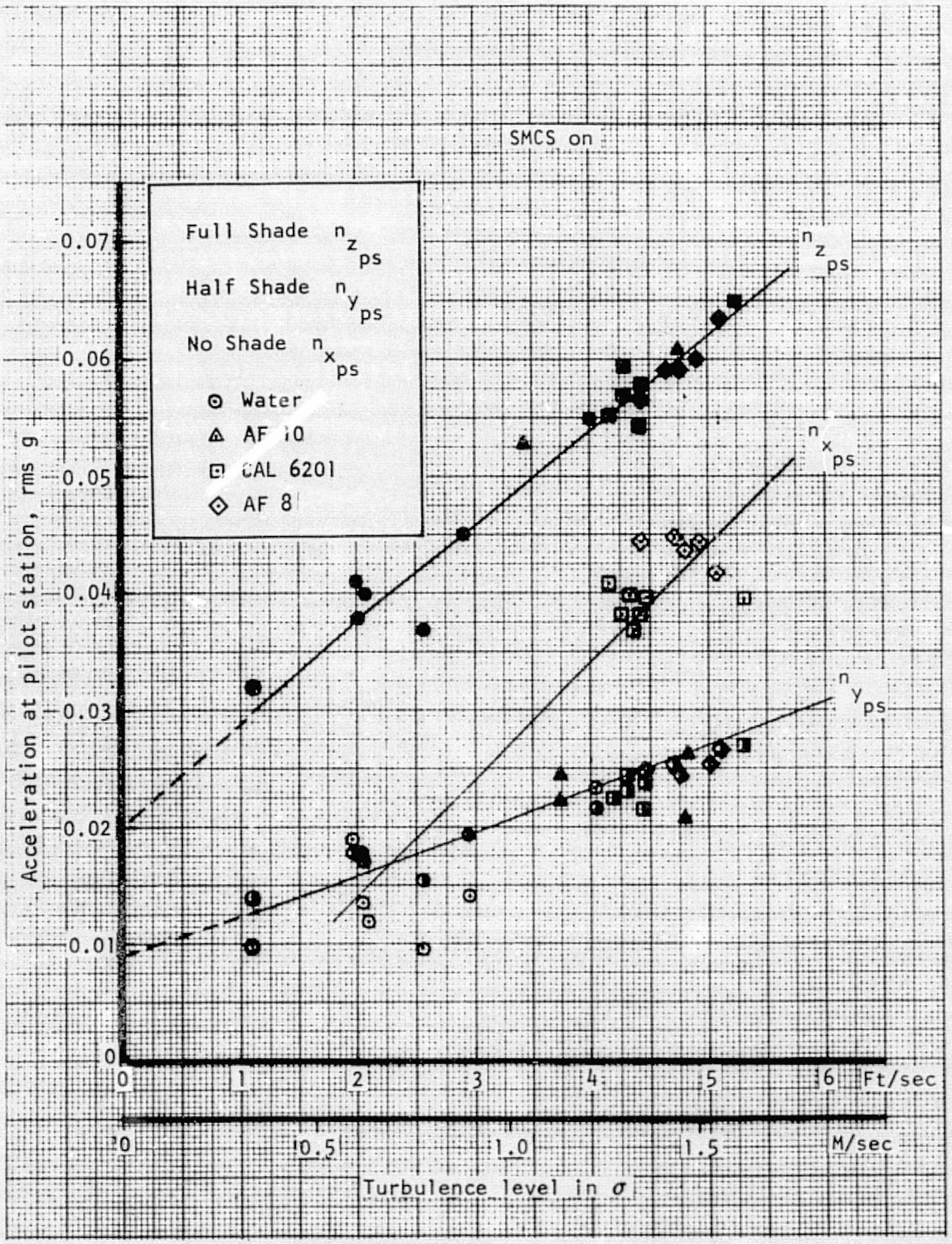

Figure 10.- Measured accelerations at pilot seat versus turbulence (SMCS on).

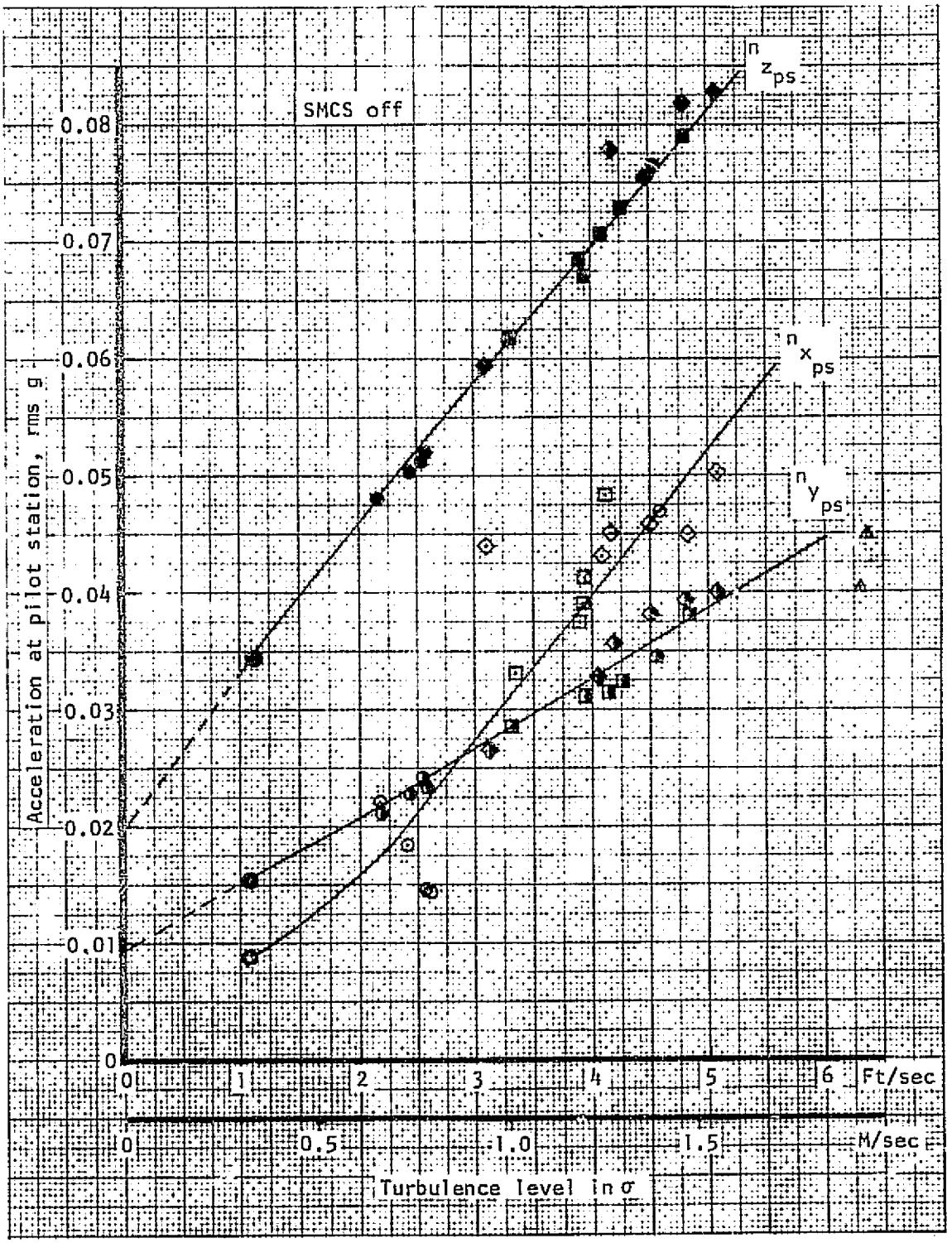

Figure 11.- Measured acceleration at pilot seat versus turbulence (SMCS off).

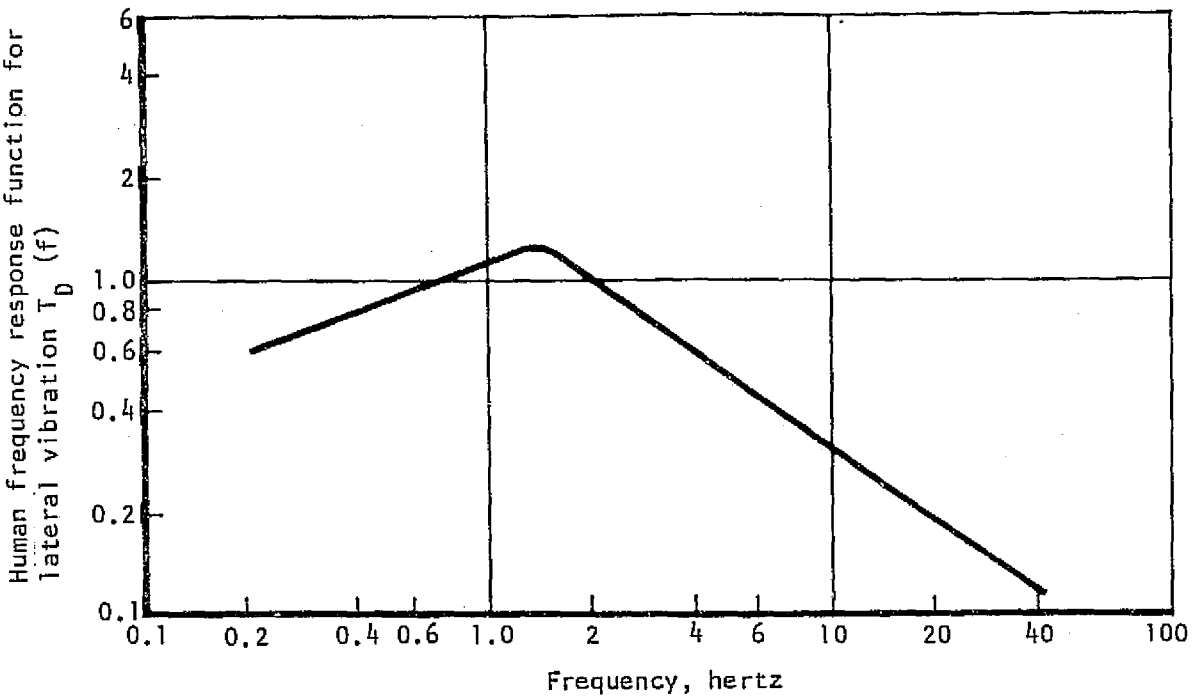

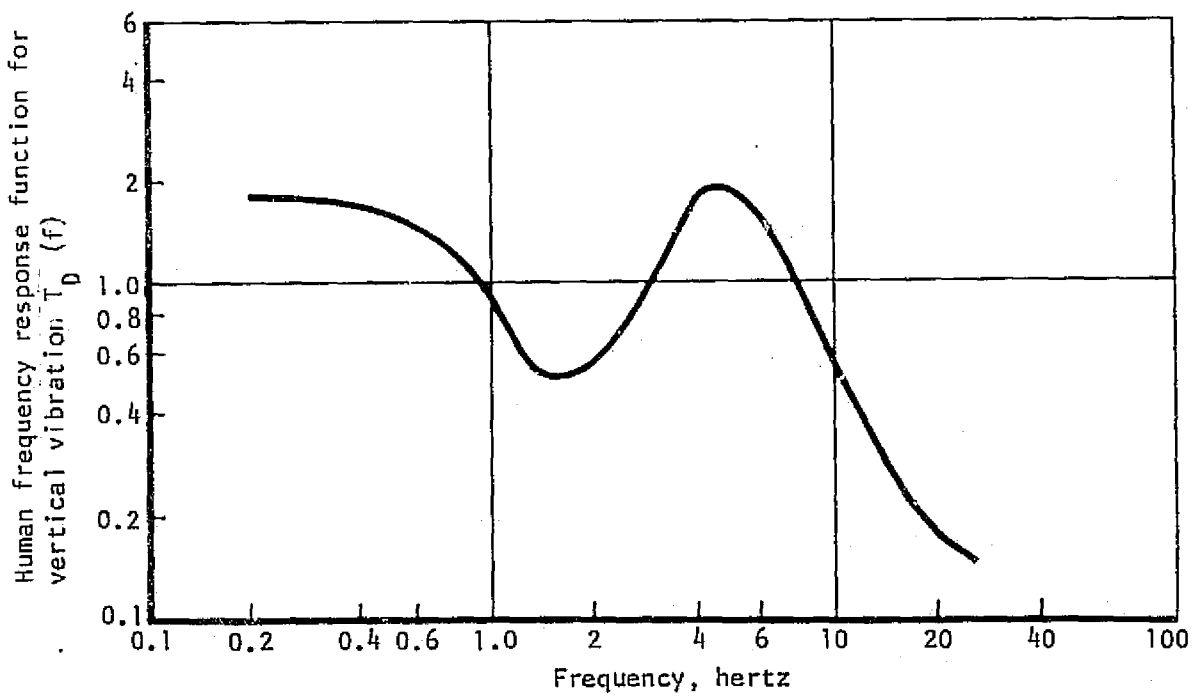

Figure 12.- Human frequency response functions.

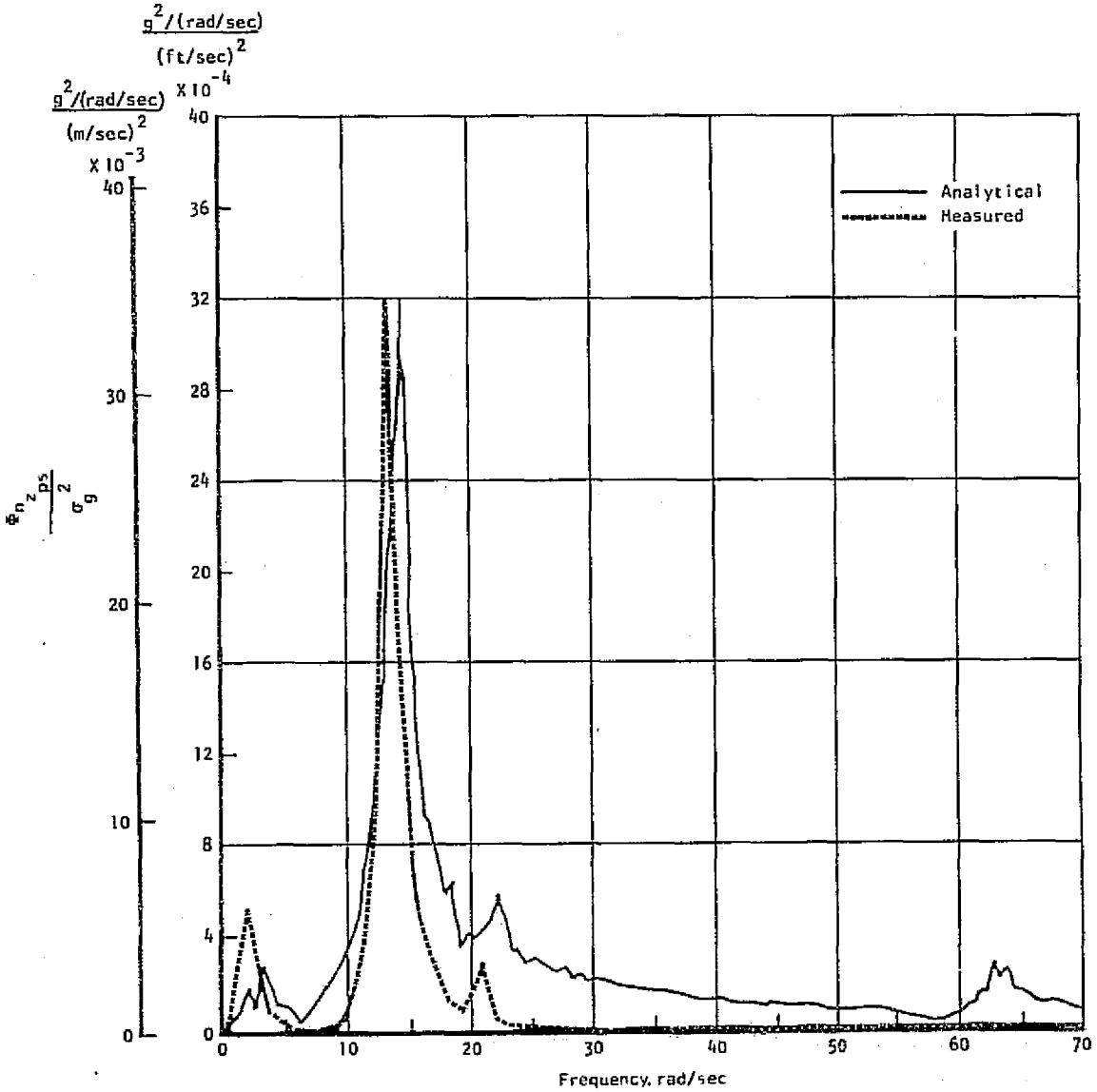

Figure 13.- PSD of vertical acceleration at pilot station - SMCS off.

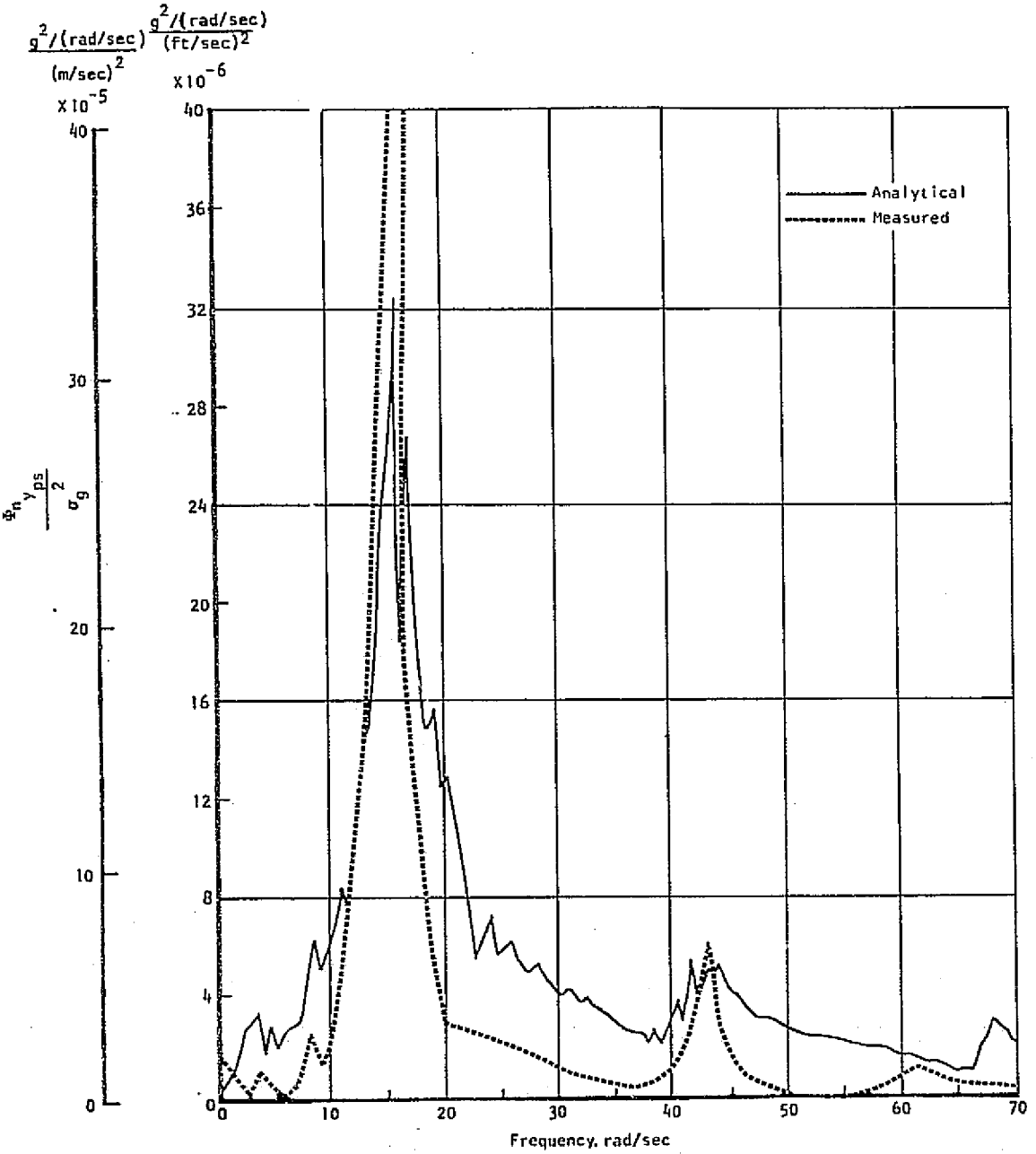

Figure 14.- PSD of lateral acceleration at pilot station - SMCS off.

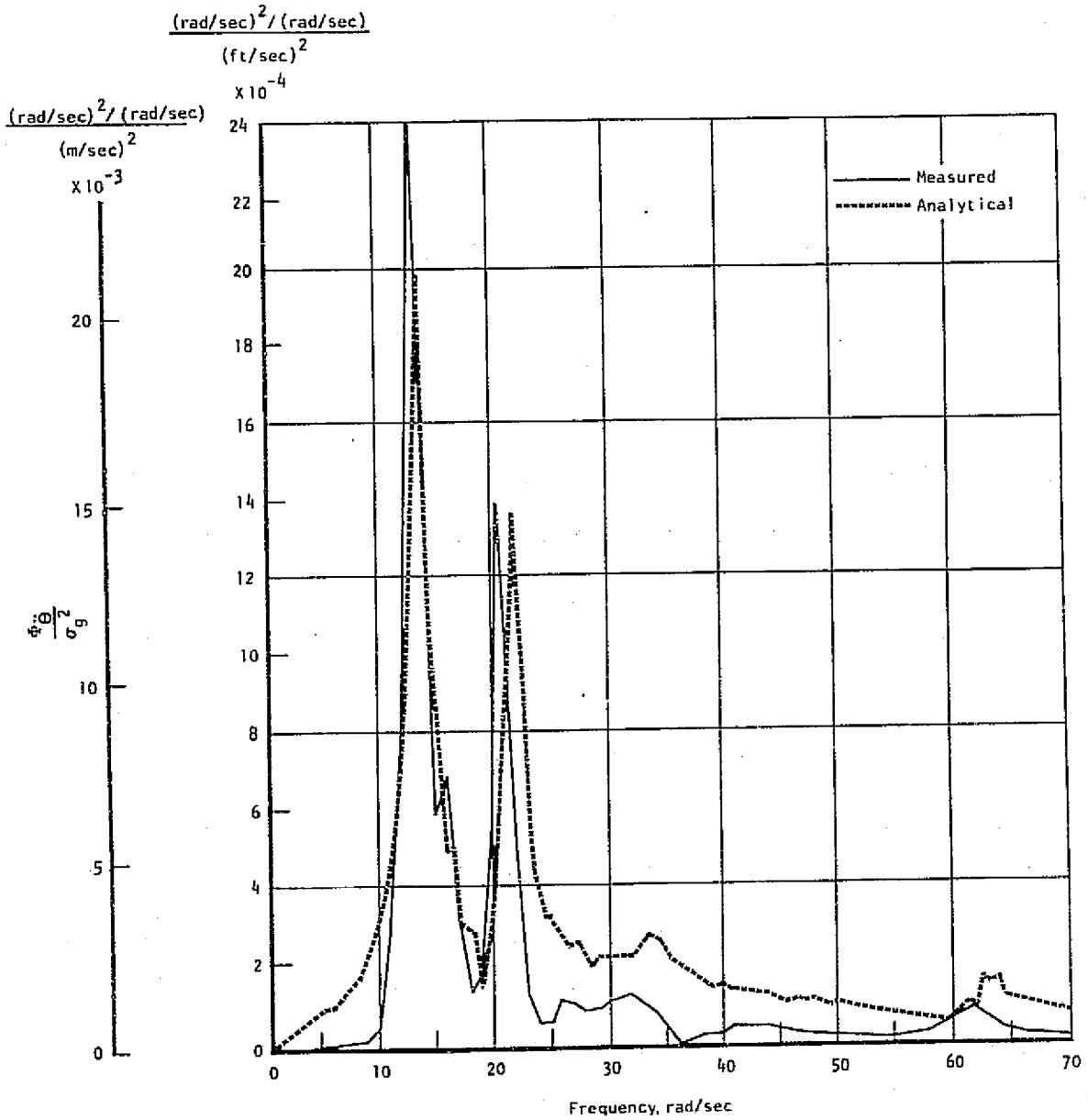

Figure 15.- PSD of pitch acceleration at pilot station - SMCS off.

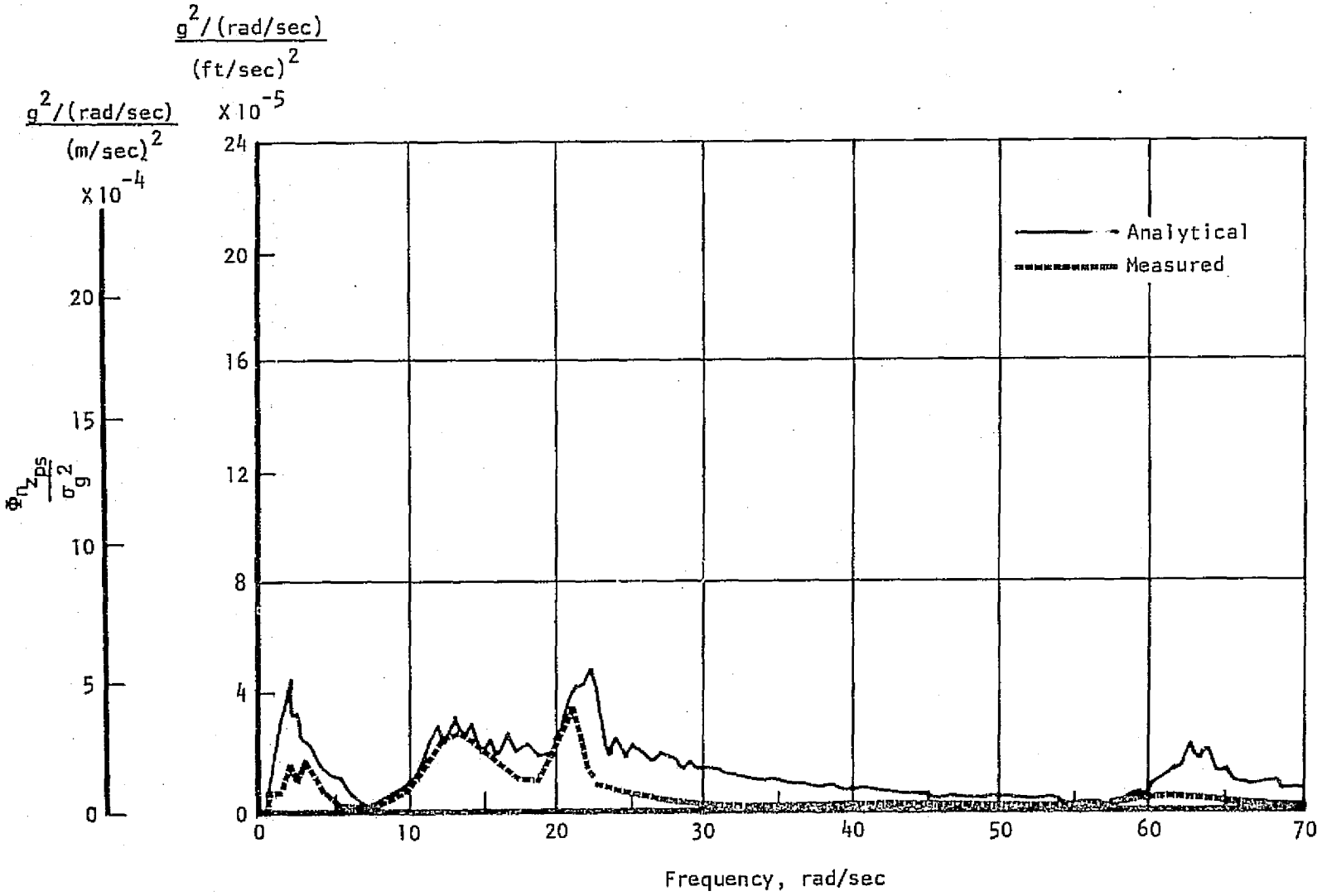

Figure 16.- PSD of vertical acceleration at pilot station - SMCS on.

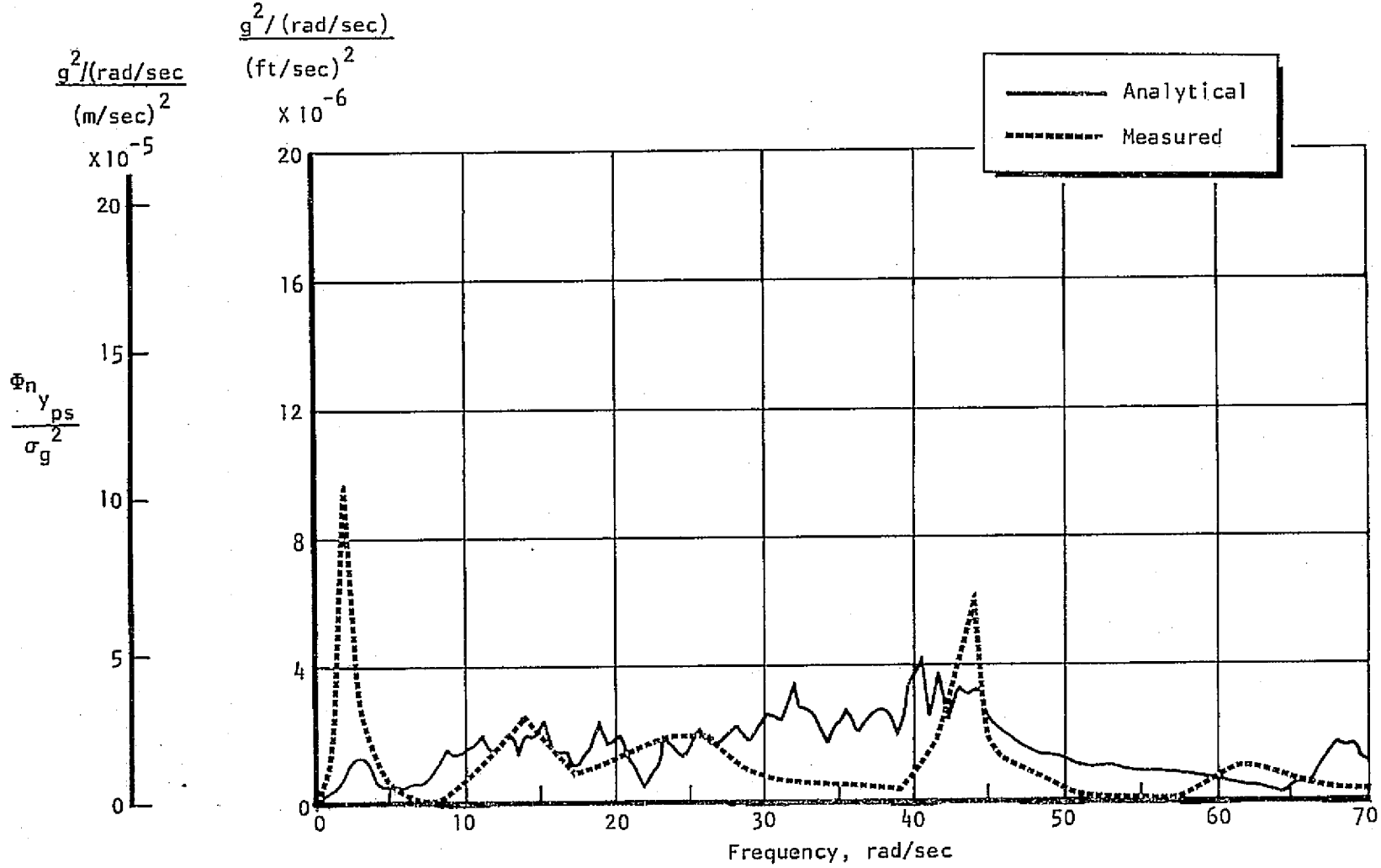

Figure 17.- -PSD of lateral acceleration at pilot station-SMCS on.

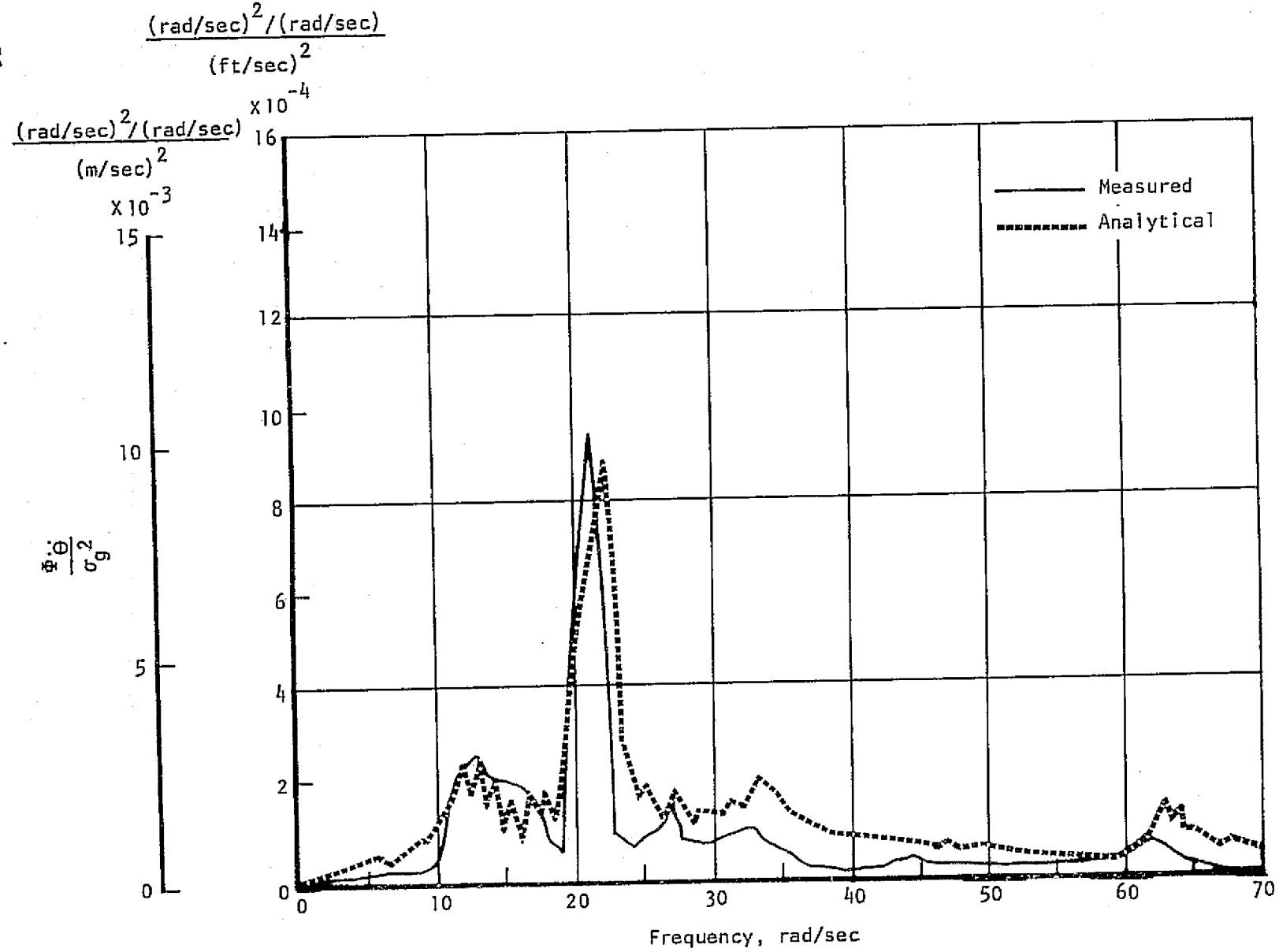

Figure 18.- PSD of pitch acceleration at pilot station - SMCS on.

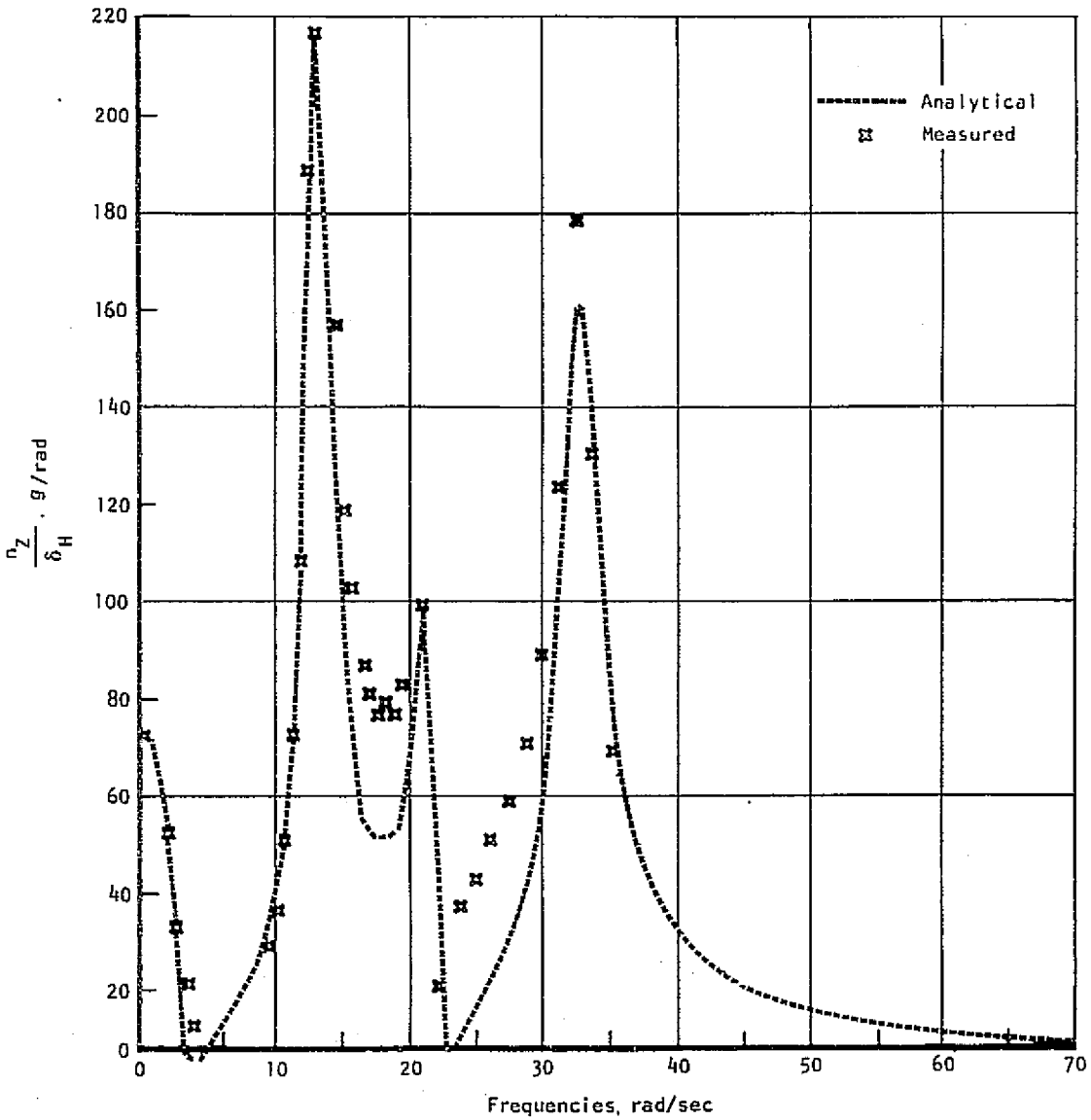

Figure 19.- Frequency response of n_Z/δ_H at control vane station.

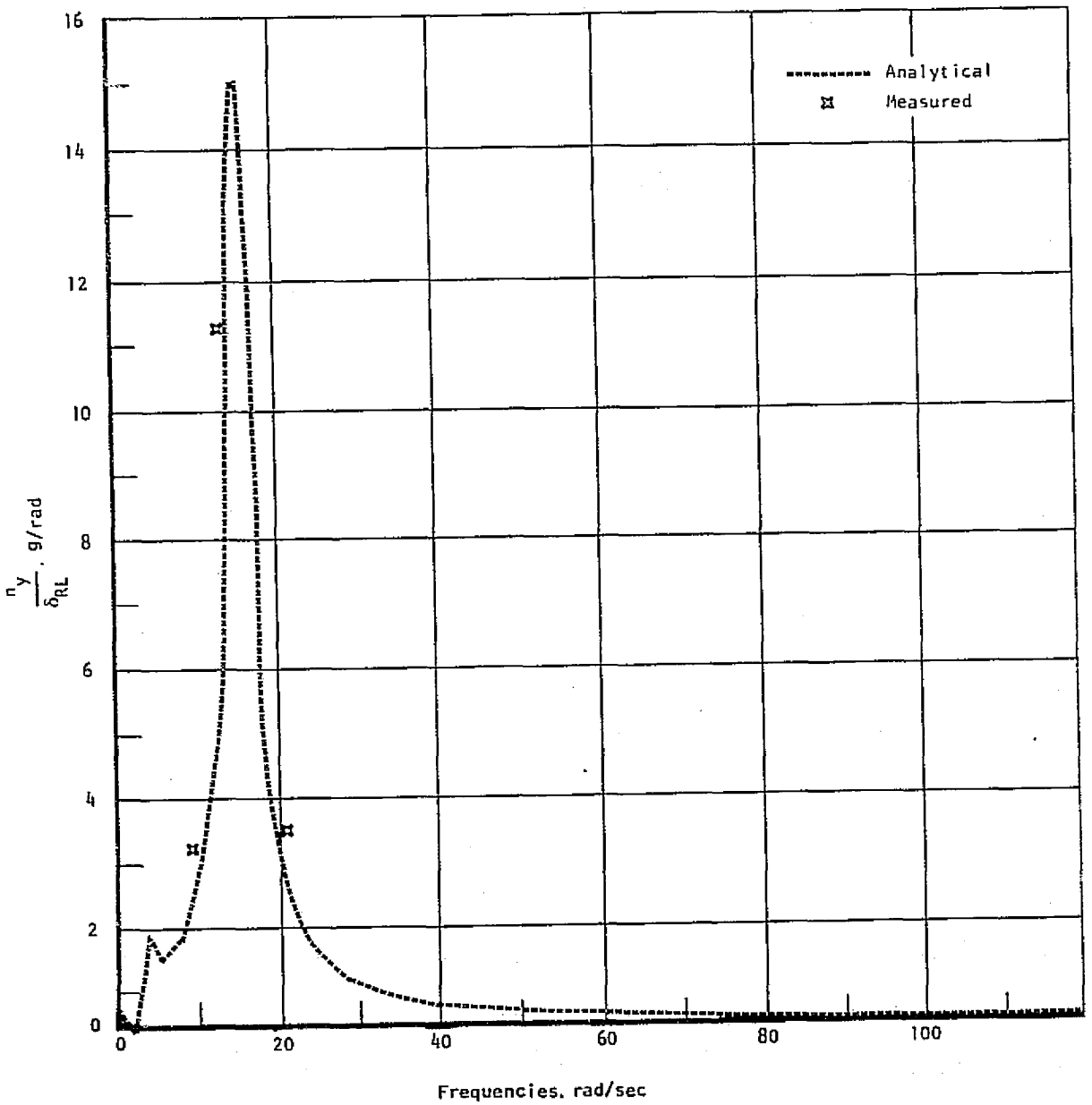

Figure 20.- Frequency response of n_y/δ_{RL} at control vane station.

Legend

⊙ = X_θ + lag
△ = n_Z + lag
⊡ = Combination
Shaded: SMCS on
Unshaded: SMCS off

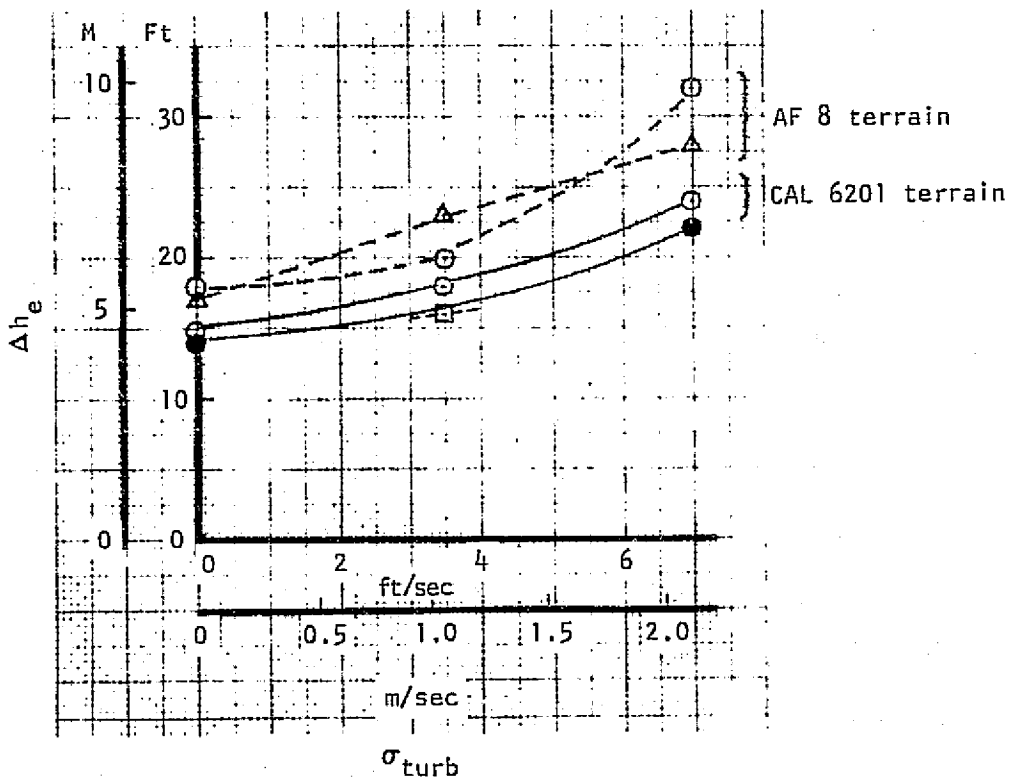

Figure 21.- Altitude performance over peaks versus turbulence.

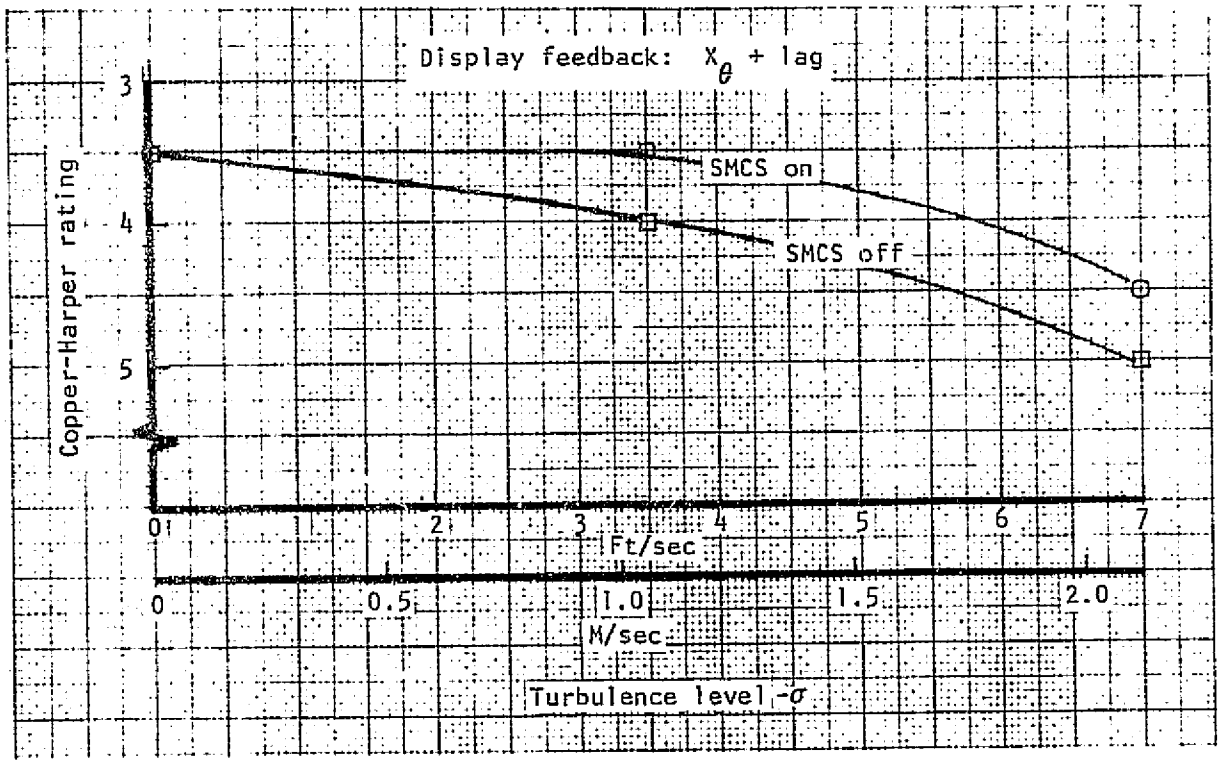

Figure 22.- Pilot handling quality rating versus turbulence.

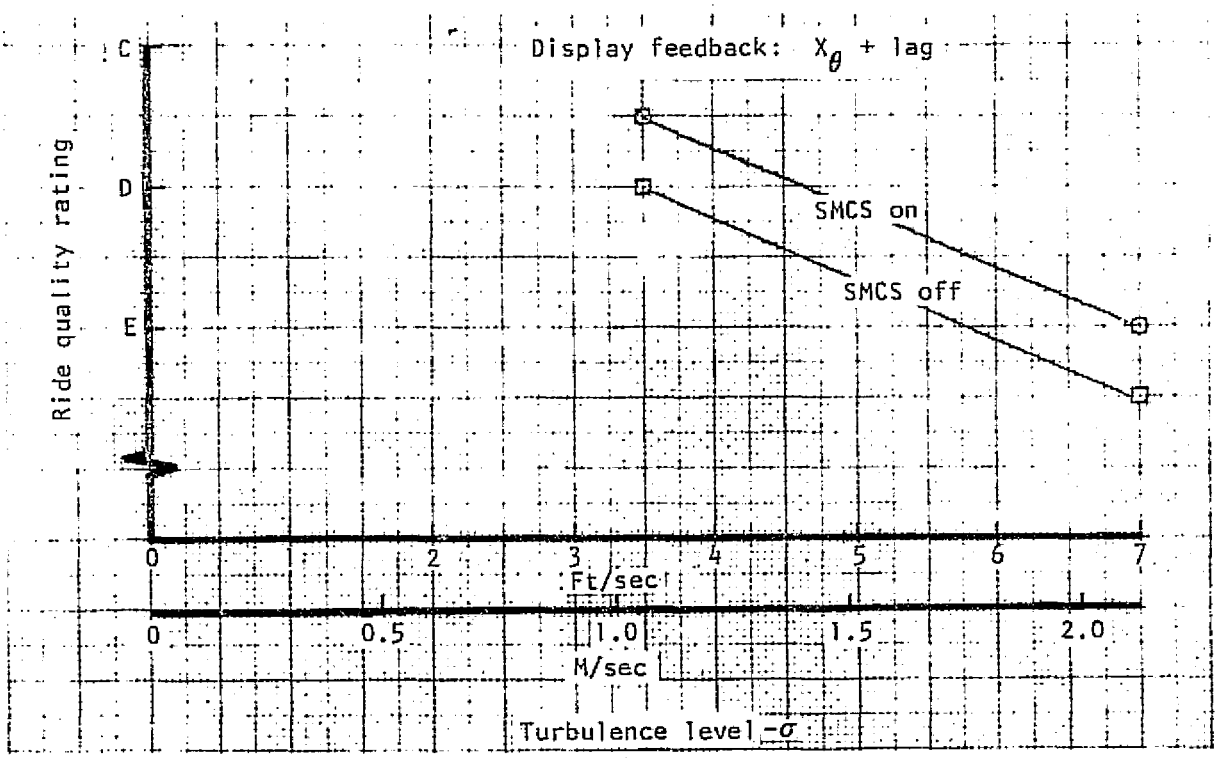

Figure 23.- Pilot ride quality rating versus turbulence.

Test conditions: Terrain AF 8
Turb 1.067 m/sec

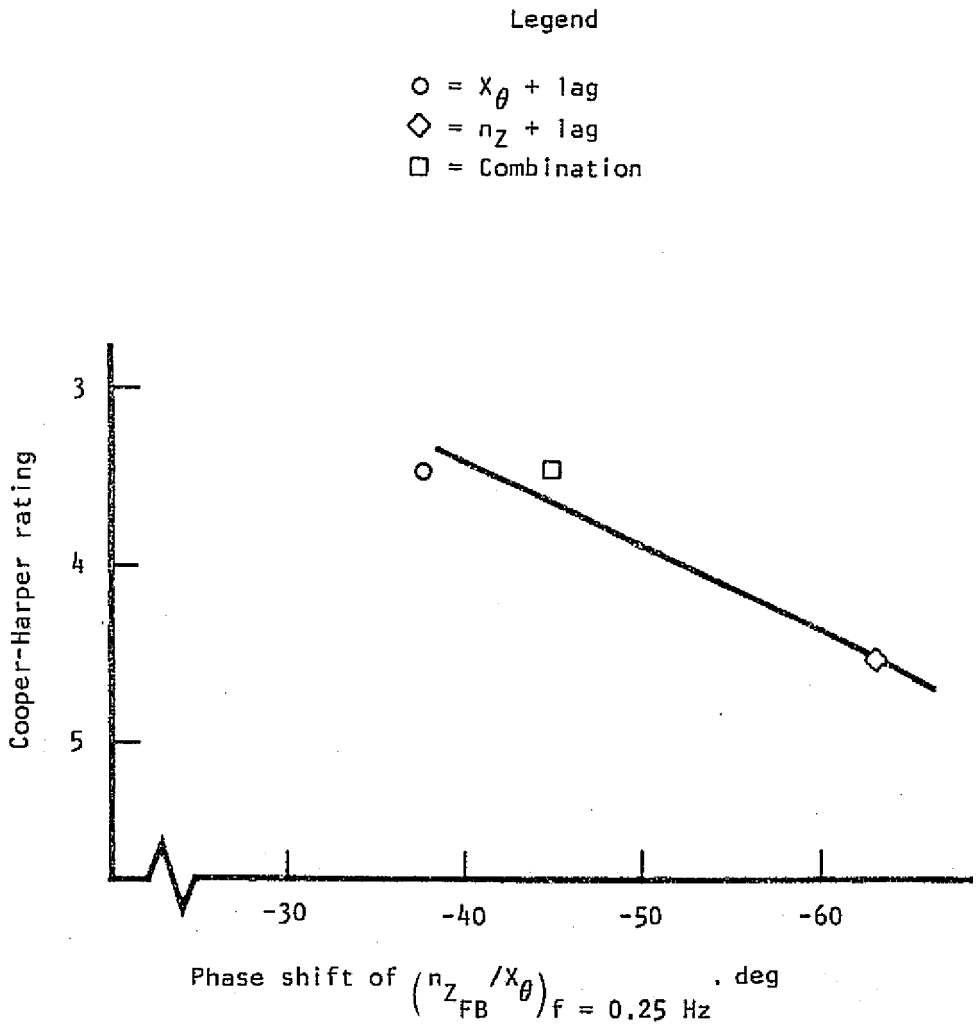

Figure 24.- Handling quality rating versus display parameters.

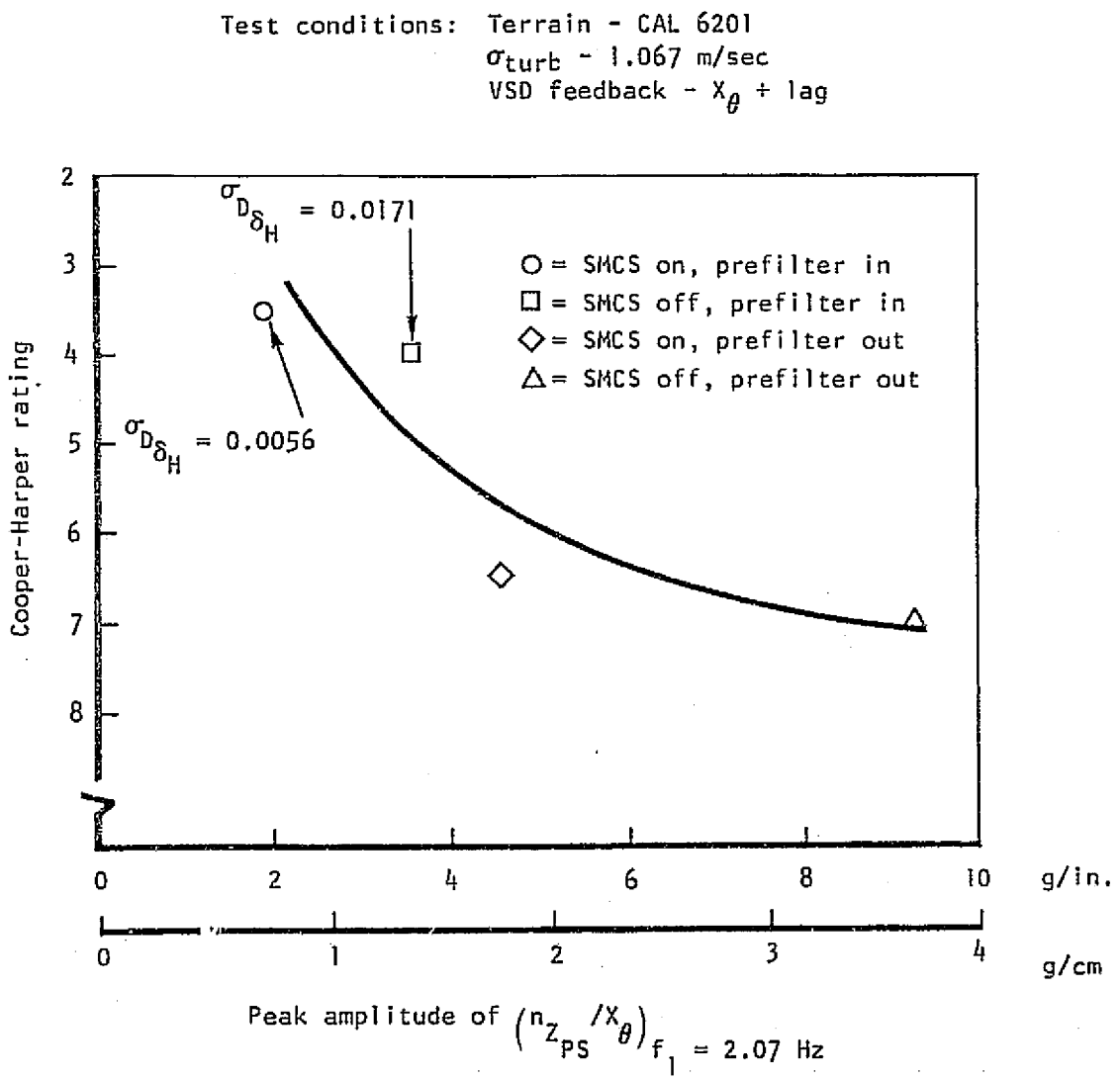

Figure 25.- Handling quality rating versus vehicle/control parameter.

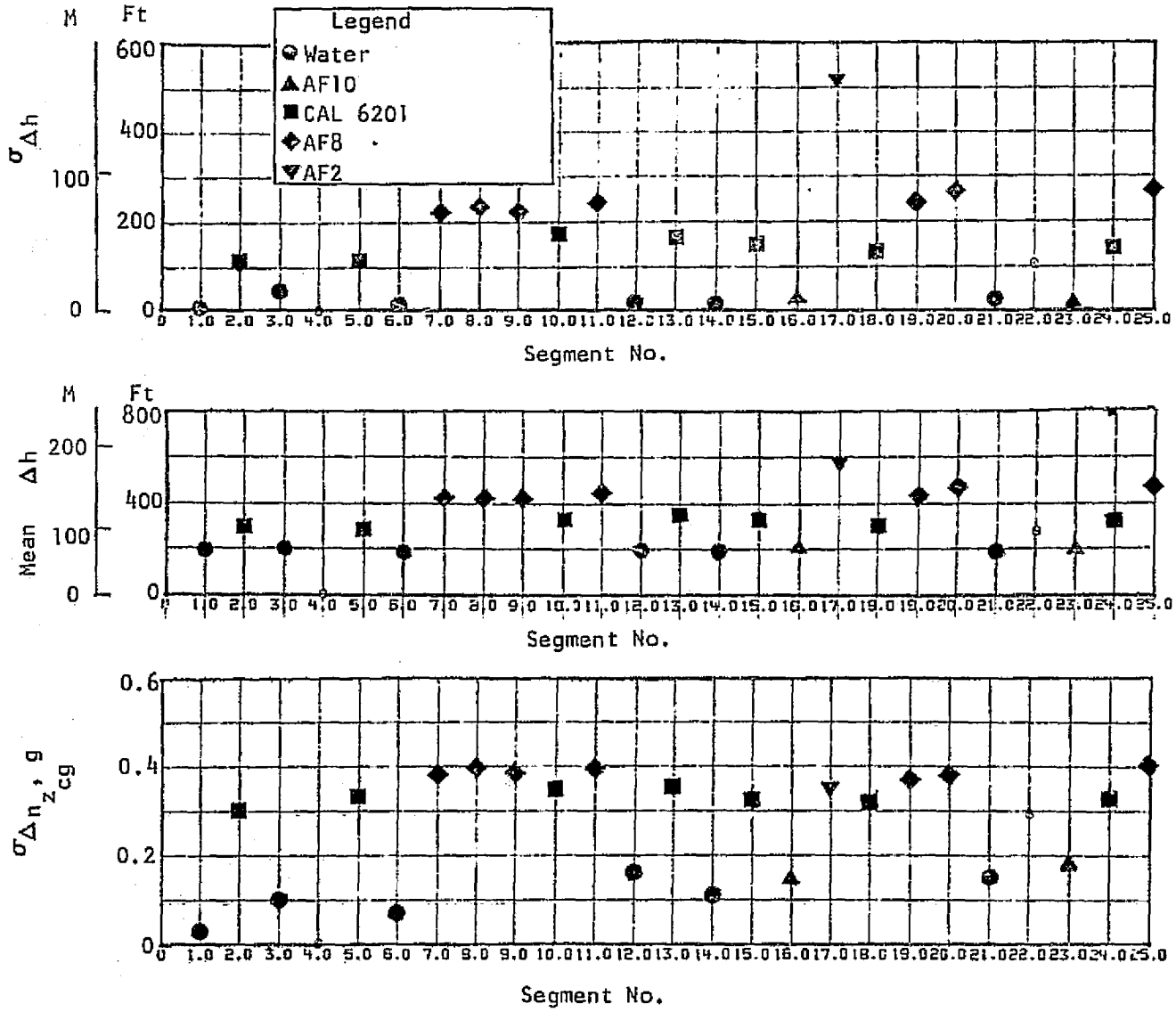

Figure 26.- Standard deviation and mean values of TF performance measures - run set 3, pilot A.

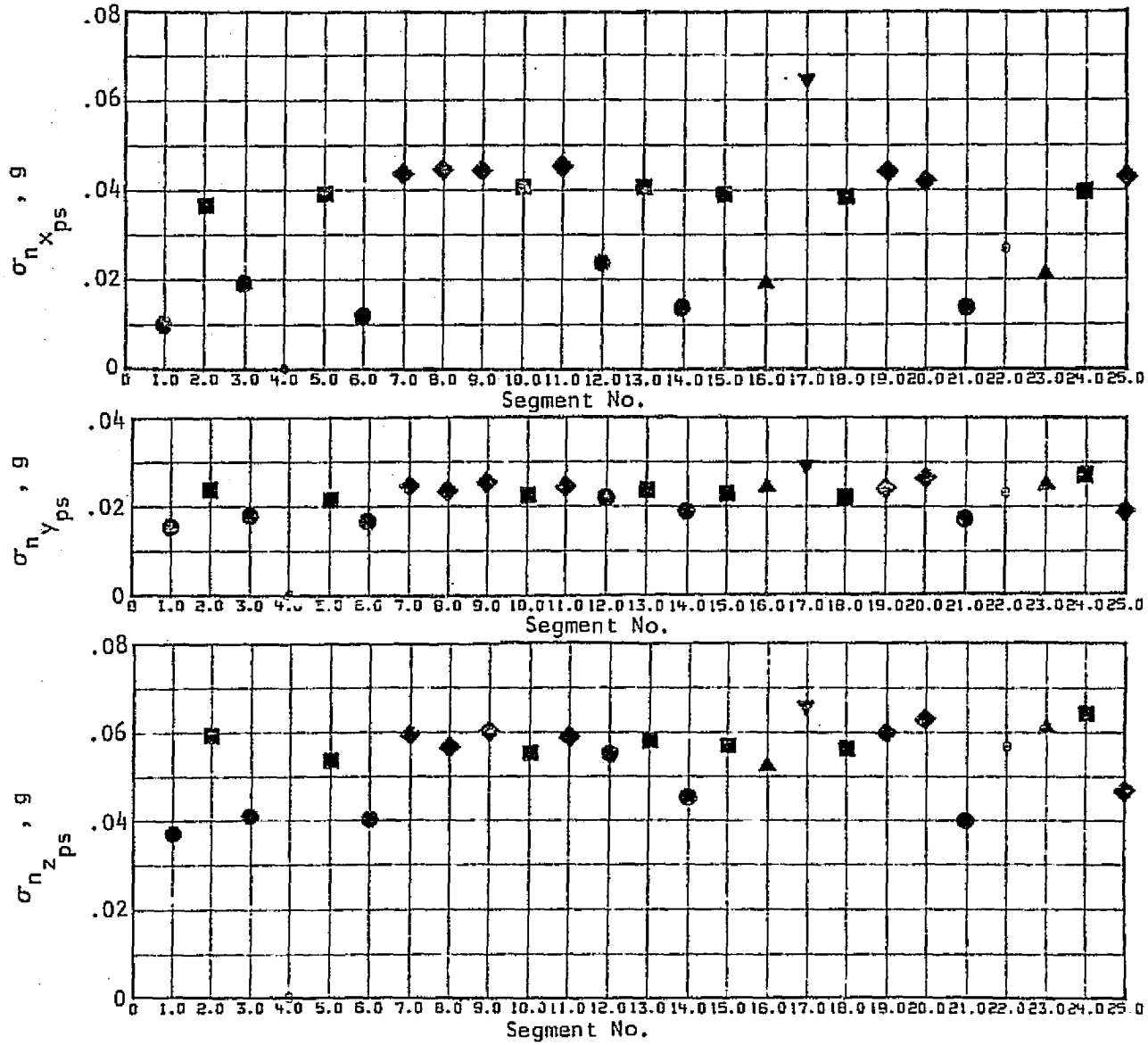

Figure 27.- Standard deviation of accelerations at pilot's seat - run set 3, pilot A.

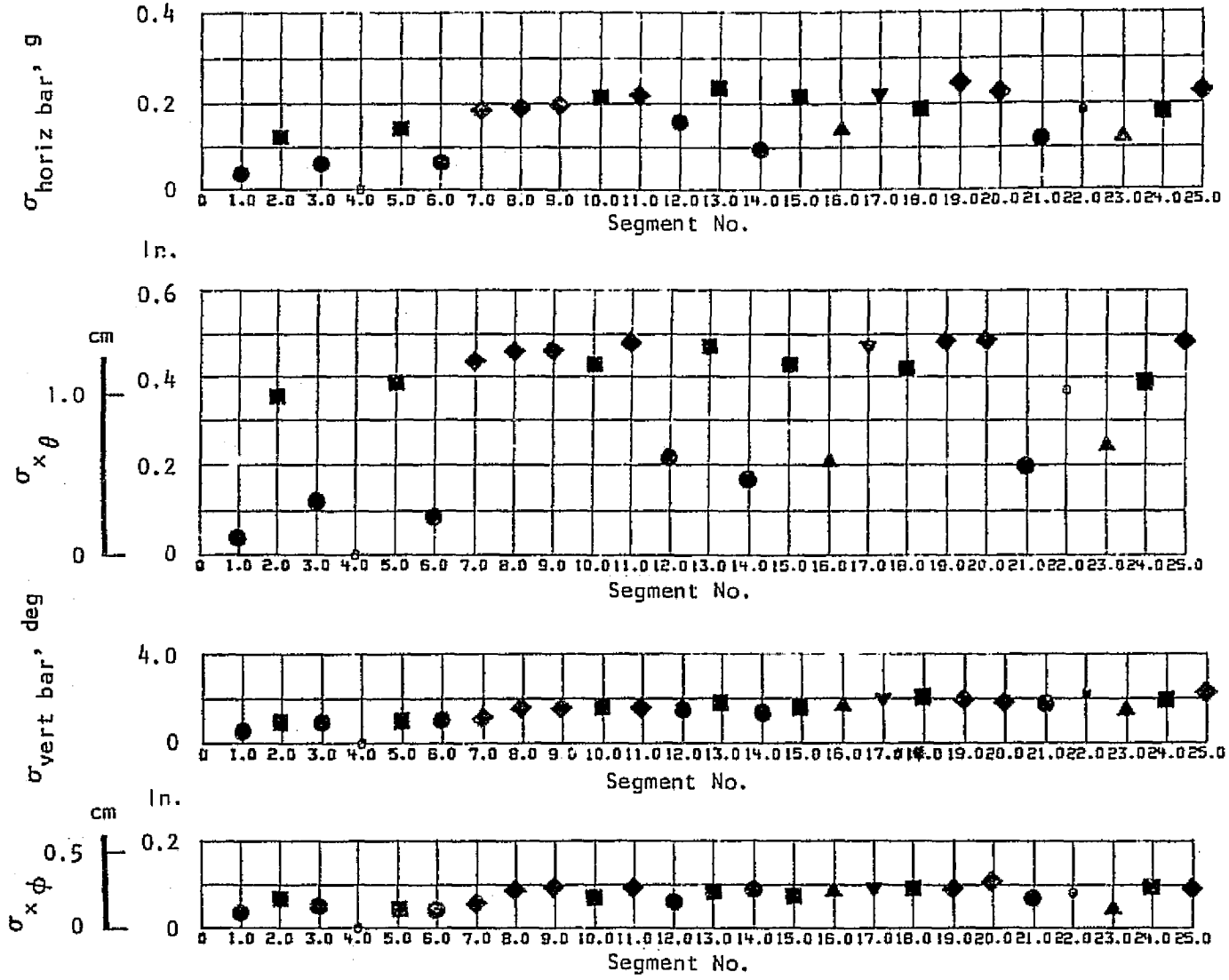

Figure 28.- Standard deviation of pilot tracking errors and stick displacements - run set 3, pilot A.

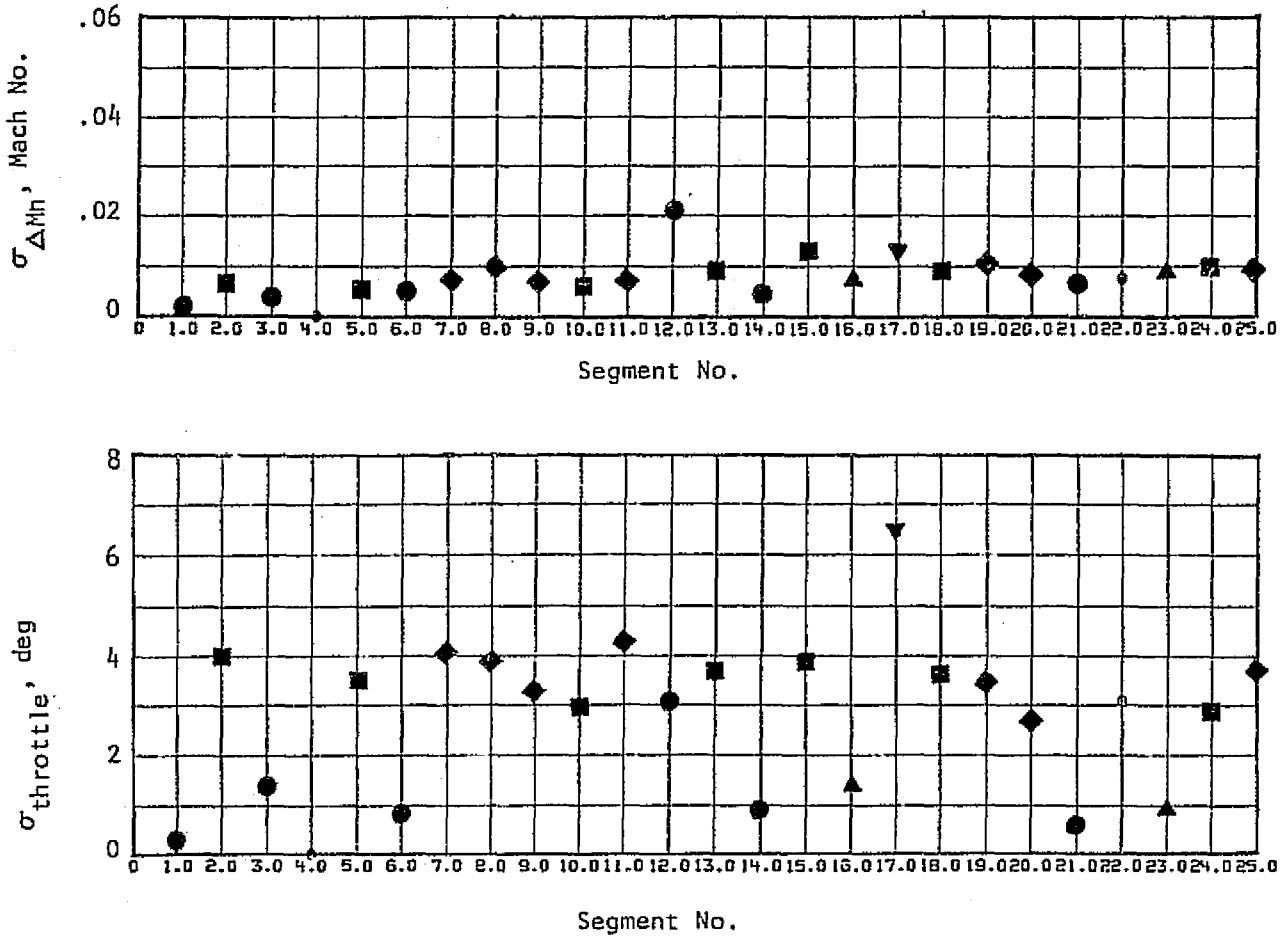

Figure 29.- Standard deviation of speed control parameters - run set 3, pilot A.

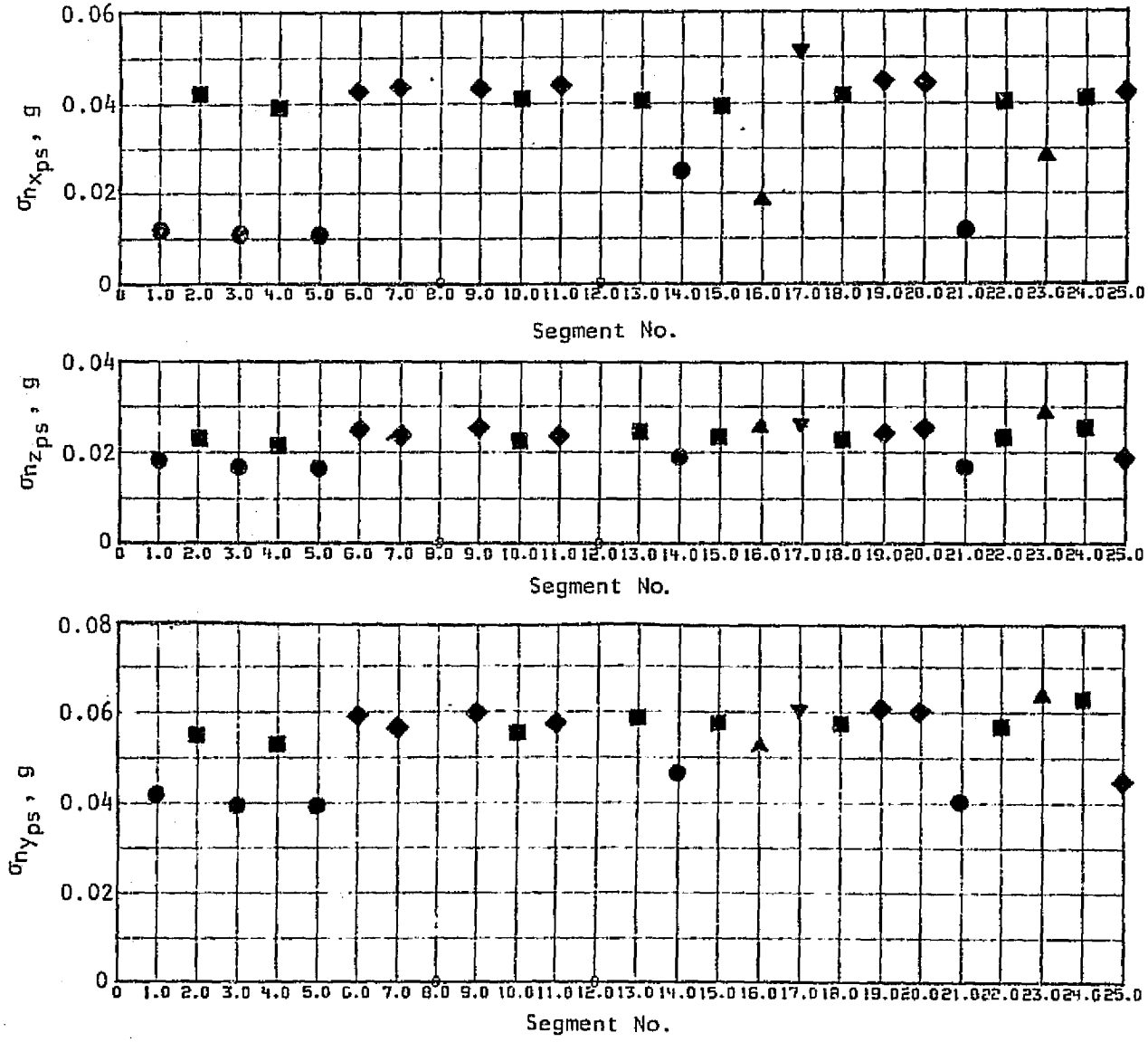

Figure 30.- Standard deviation of accelerations at pilot's seat - run set 3, pilot B.

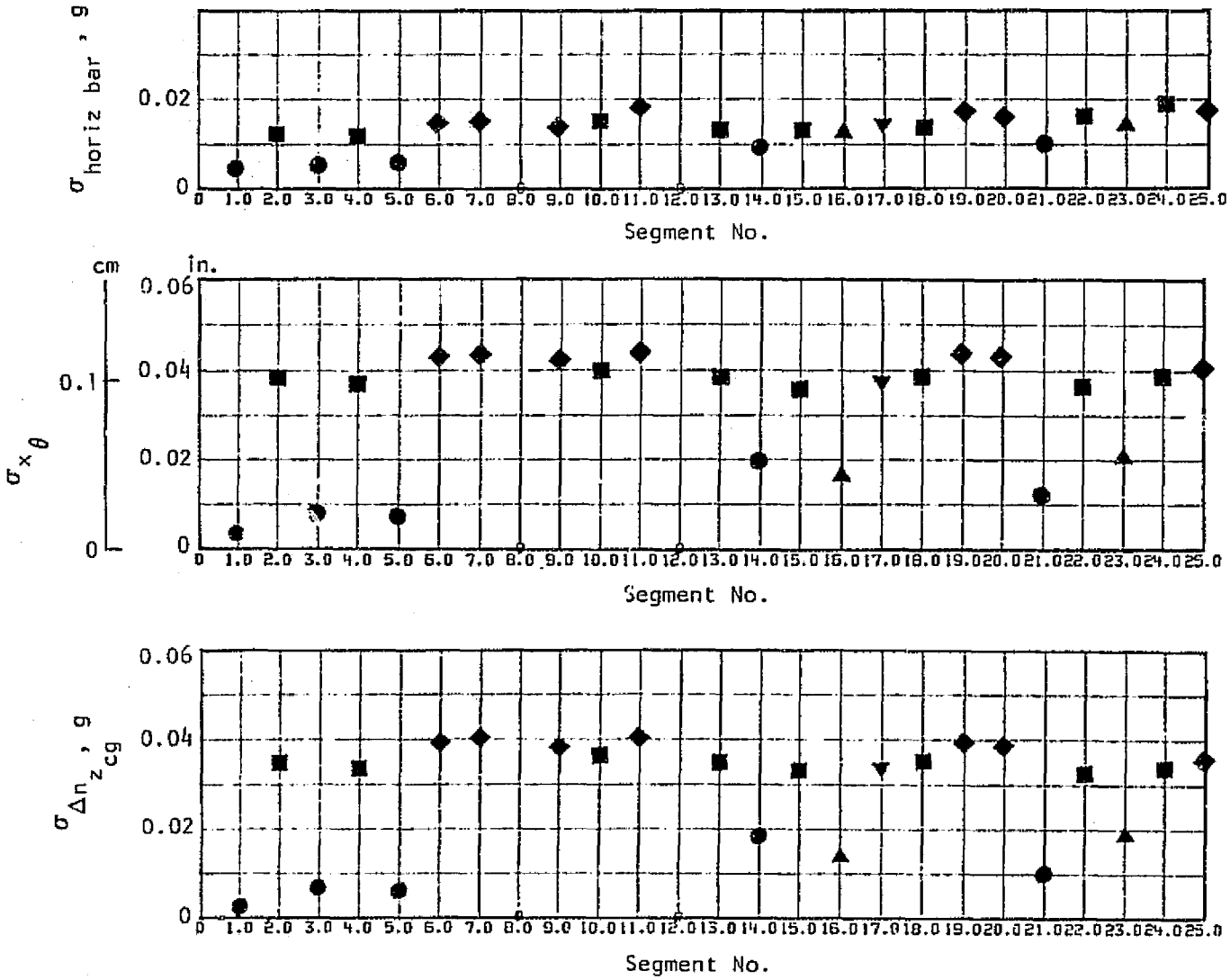

Figure 31.- Standard deviation of pilot tracking error, pilot stick displacement, and maneuver load - run set 3, pilot B.

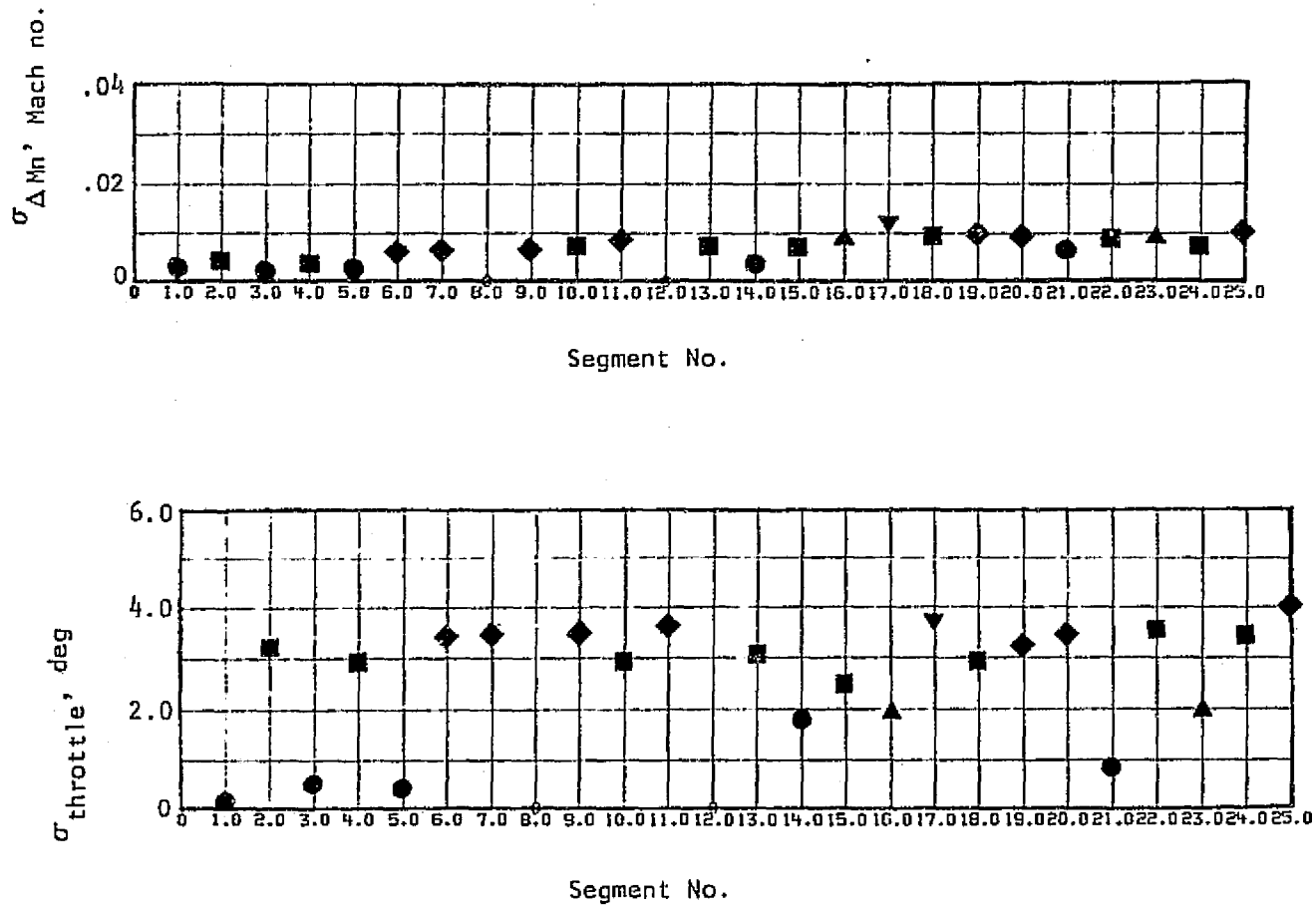

Figure 32.- Standard deviation of speed control parameters - run set 3, pilot B.

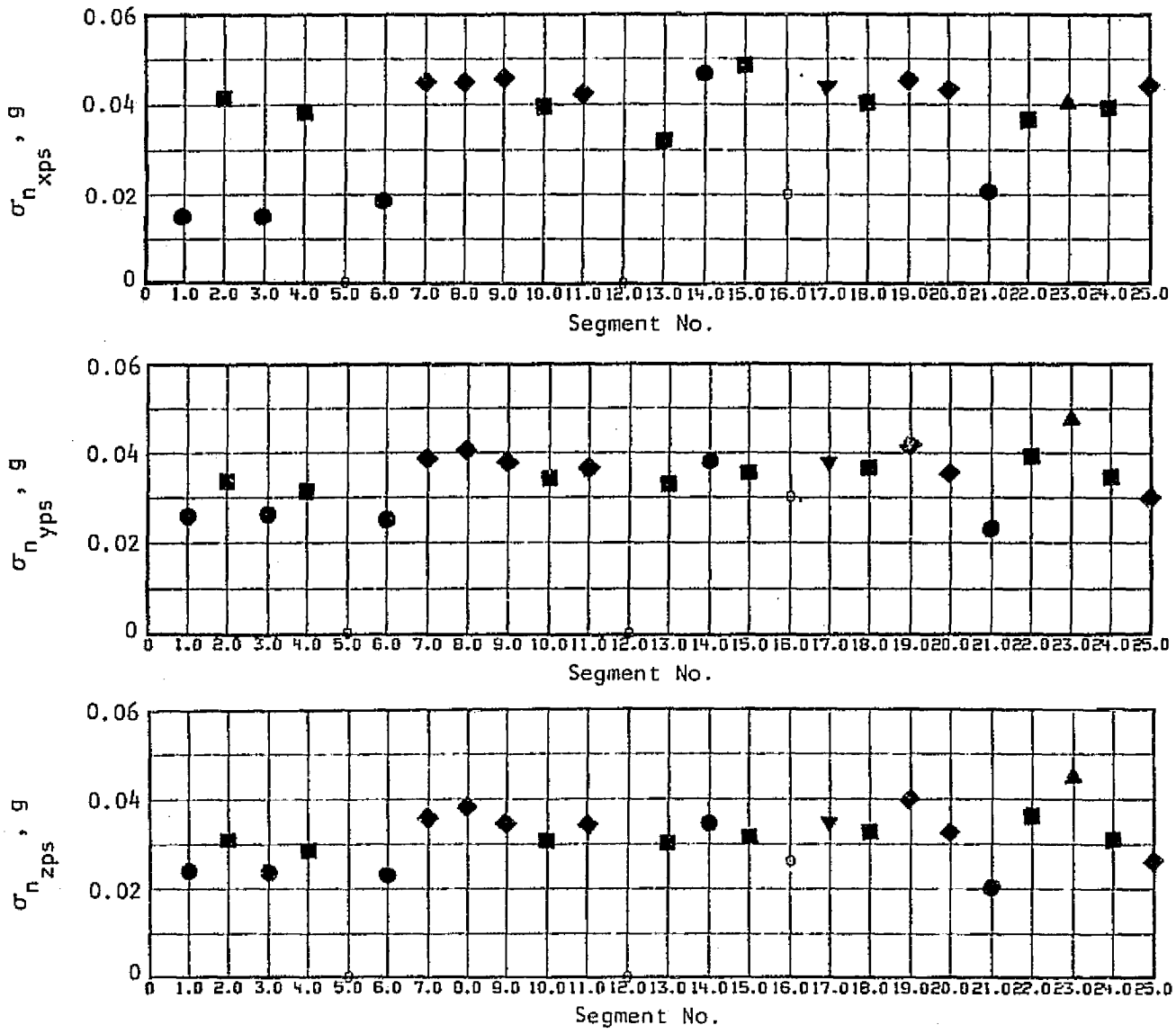

Figure 33.- Standard deviation of accelerations at pilot's seat - run set 2, pilot A.

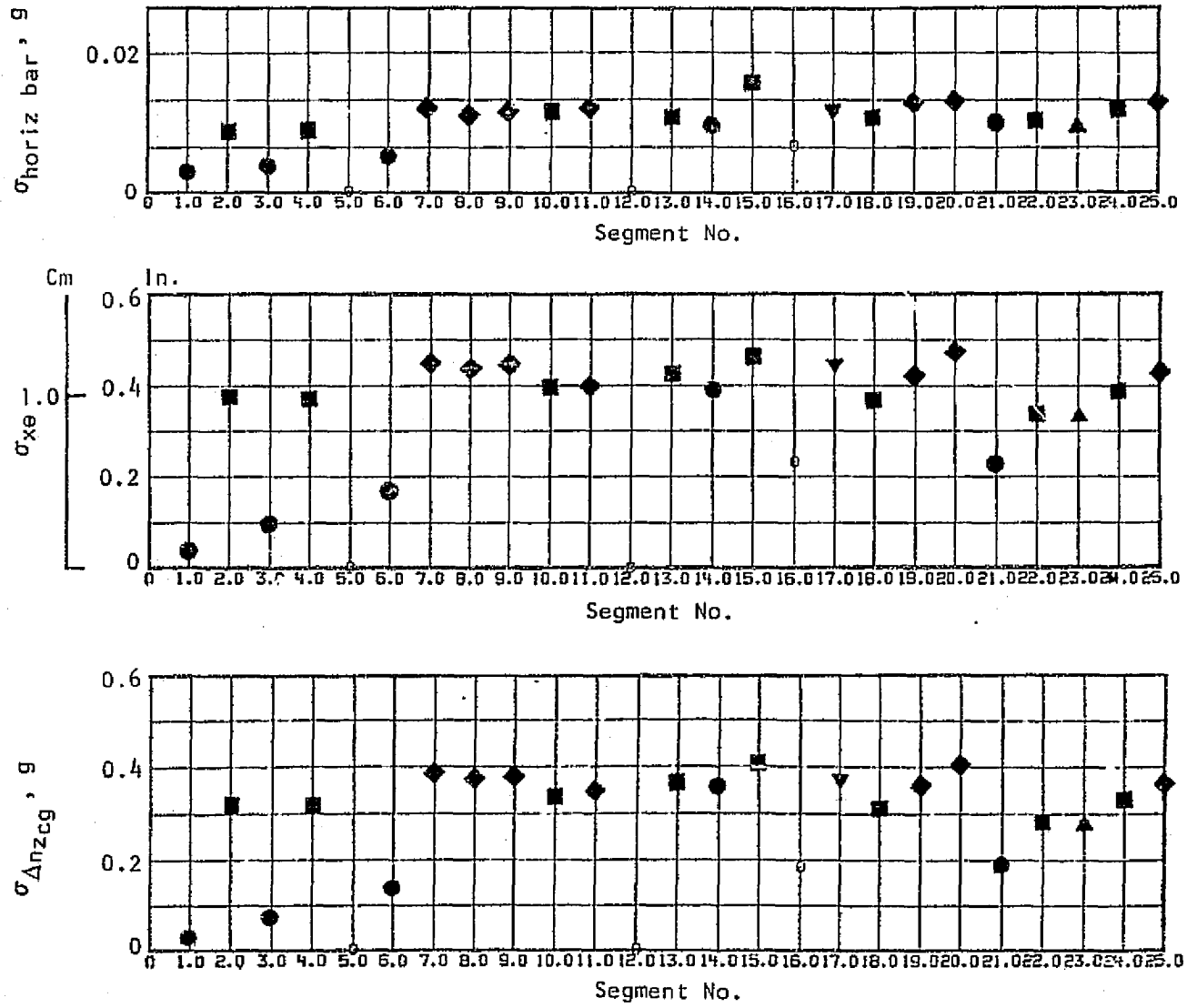

Figure 34.- Standard deviation of pilot tracking error, pilot stick displacement, and maneuver load - run set 2, pilot A.

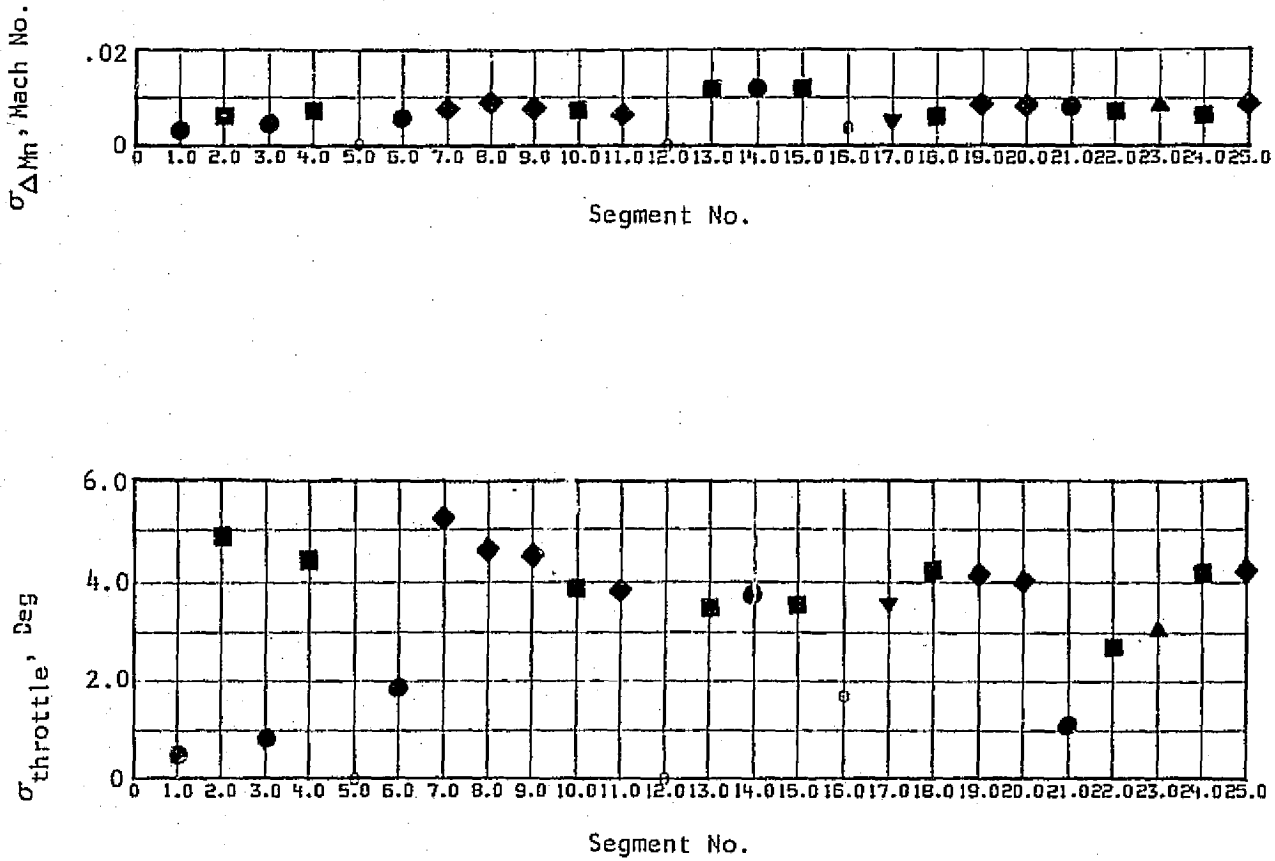

Figure 35.- Standard deviation of speed control parameters - run set 2, pilot A.

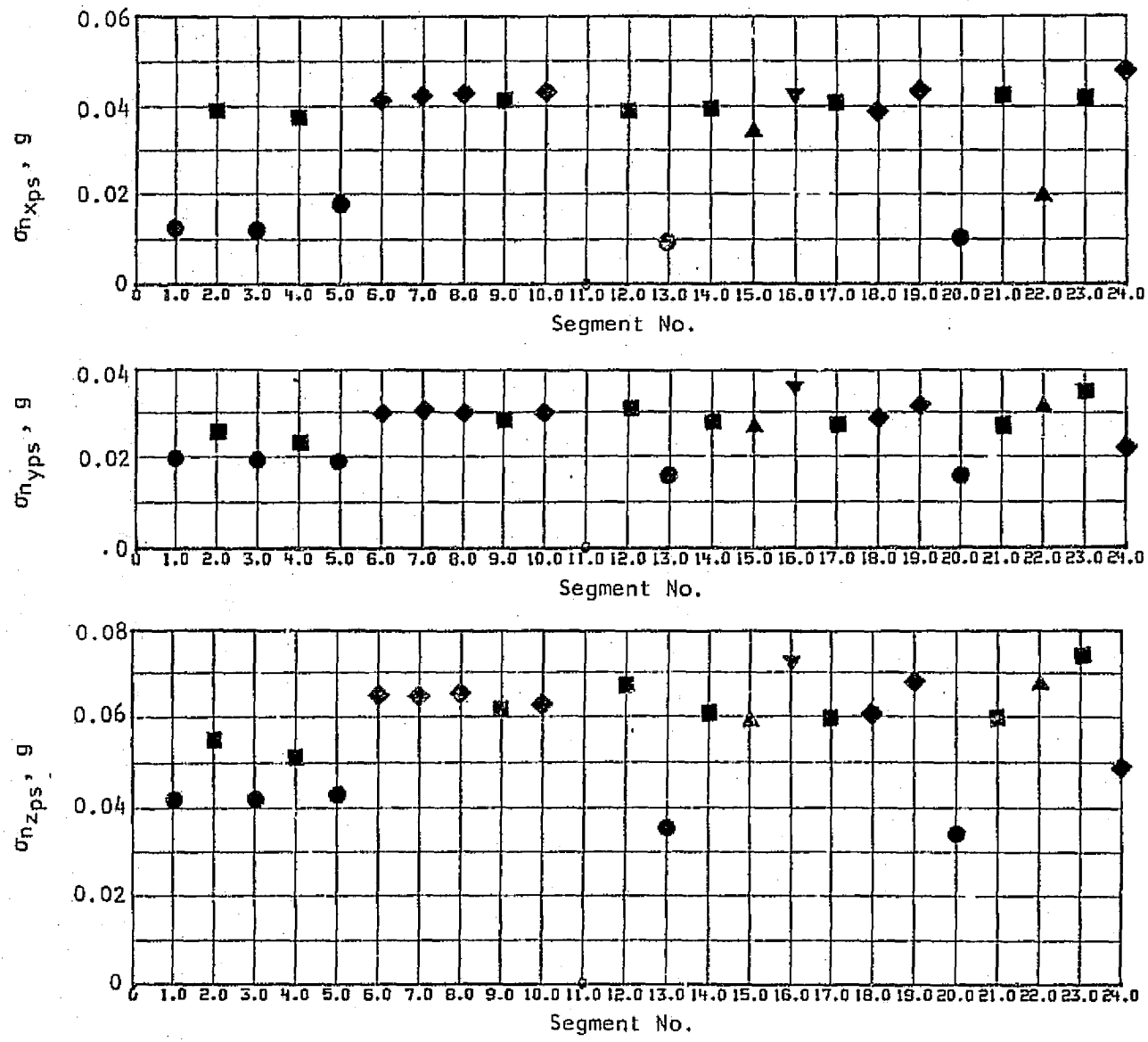

Figure 36.- Standard deviation of acceleration at pilot's seat - run set 2, pilot B.

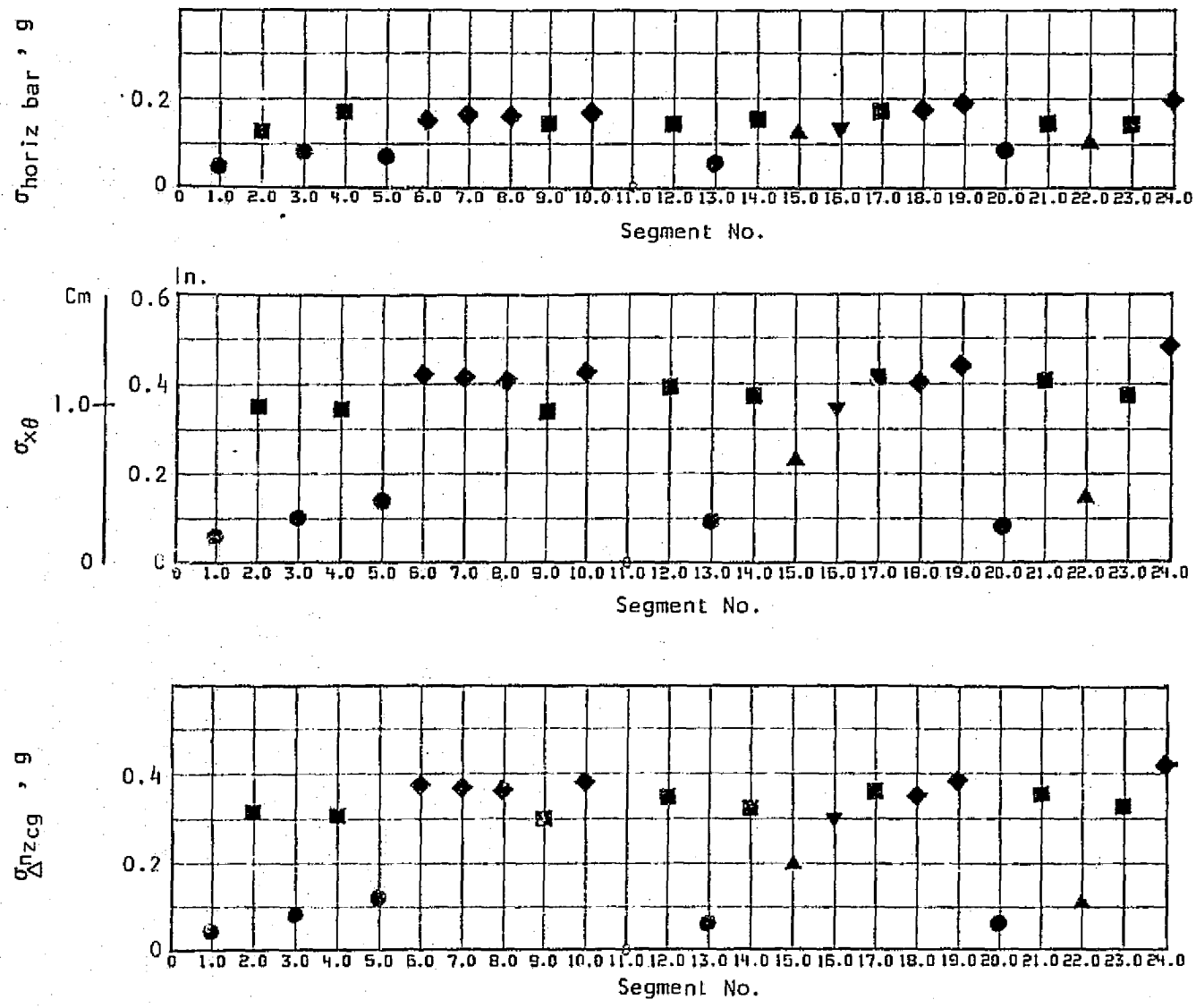

Figure 37.- Standard deviation of pilot tracking error, pilot stick displacement, and maneuver load - run set 2, pilot B.

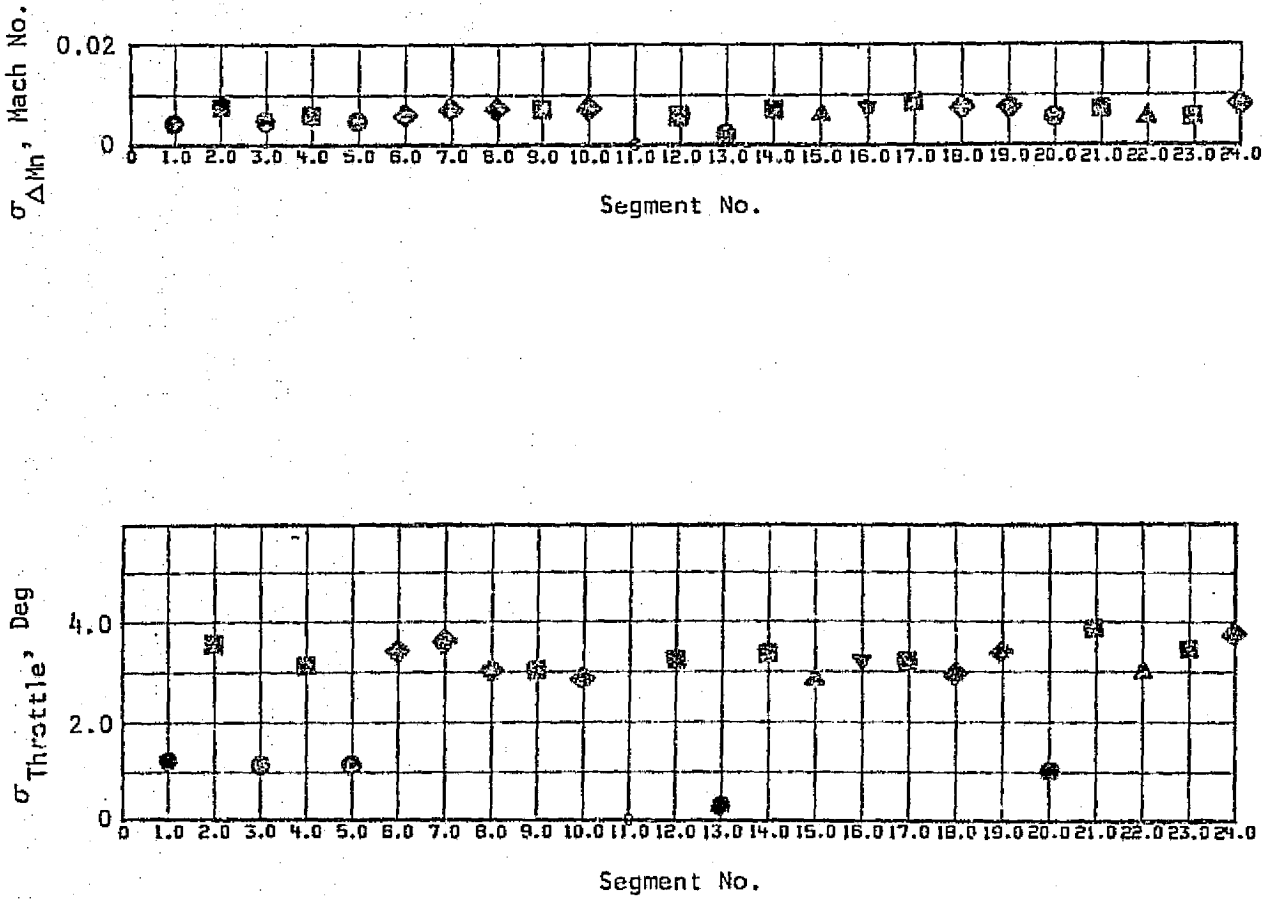

Figure 38.- Standard deviation of speed control parameters - run set 2, pilot B.

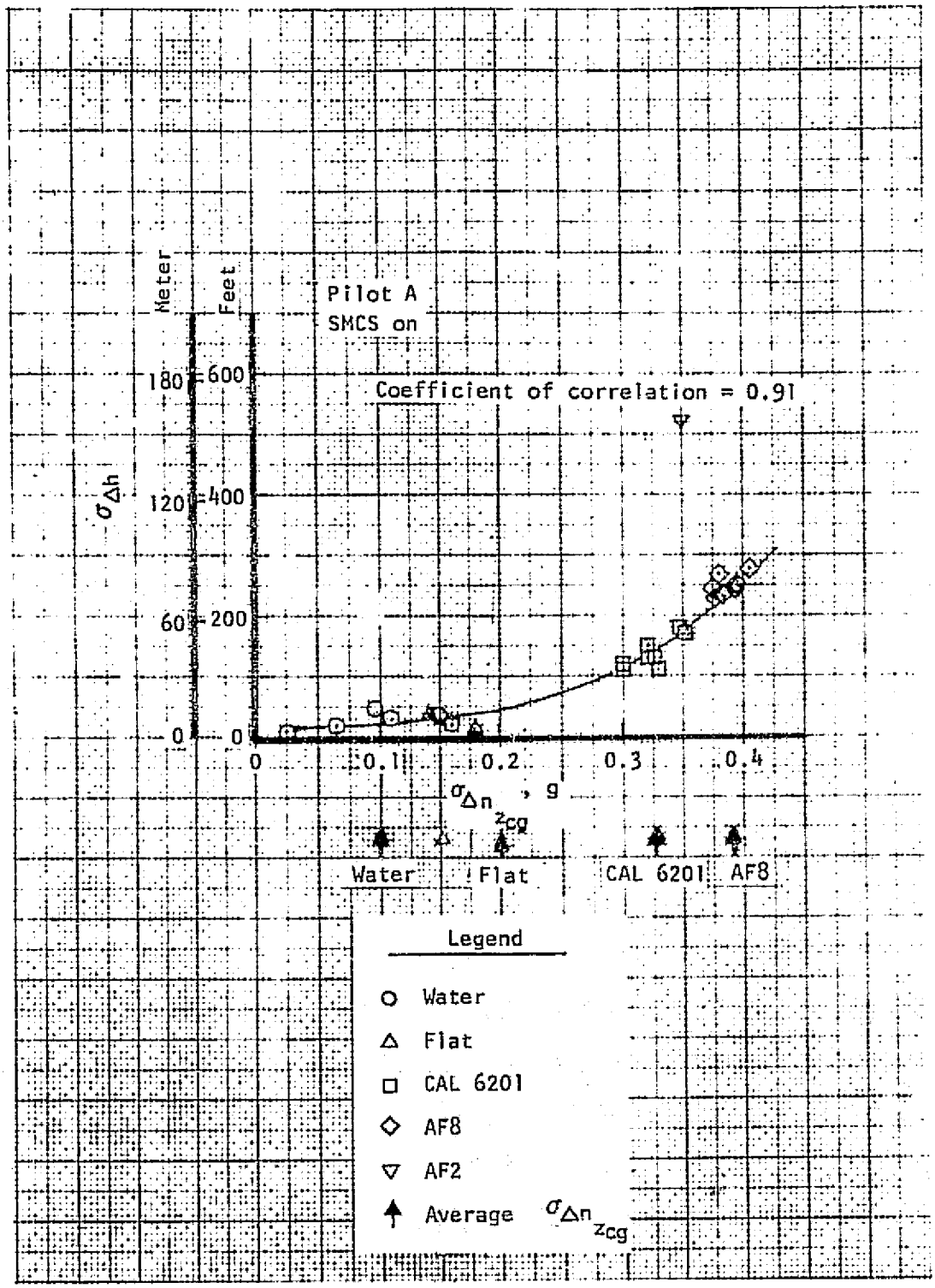

Figure 39.- TF performance versus maneuver load.

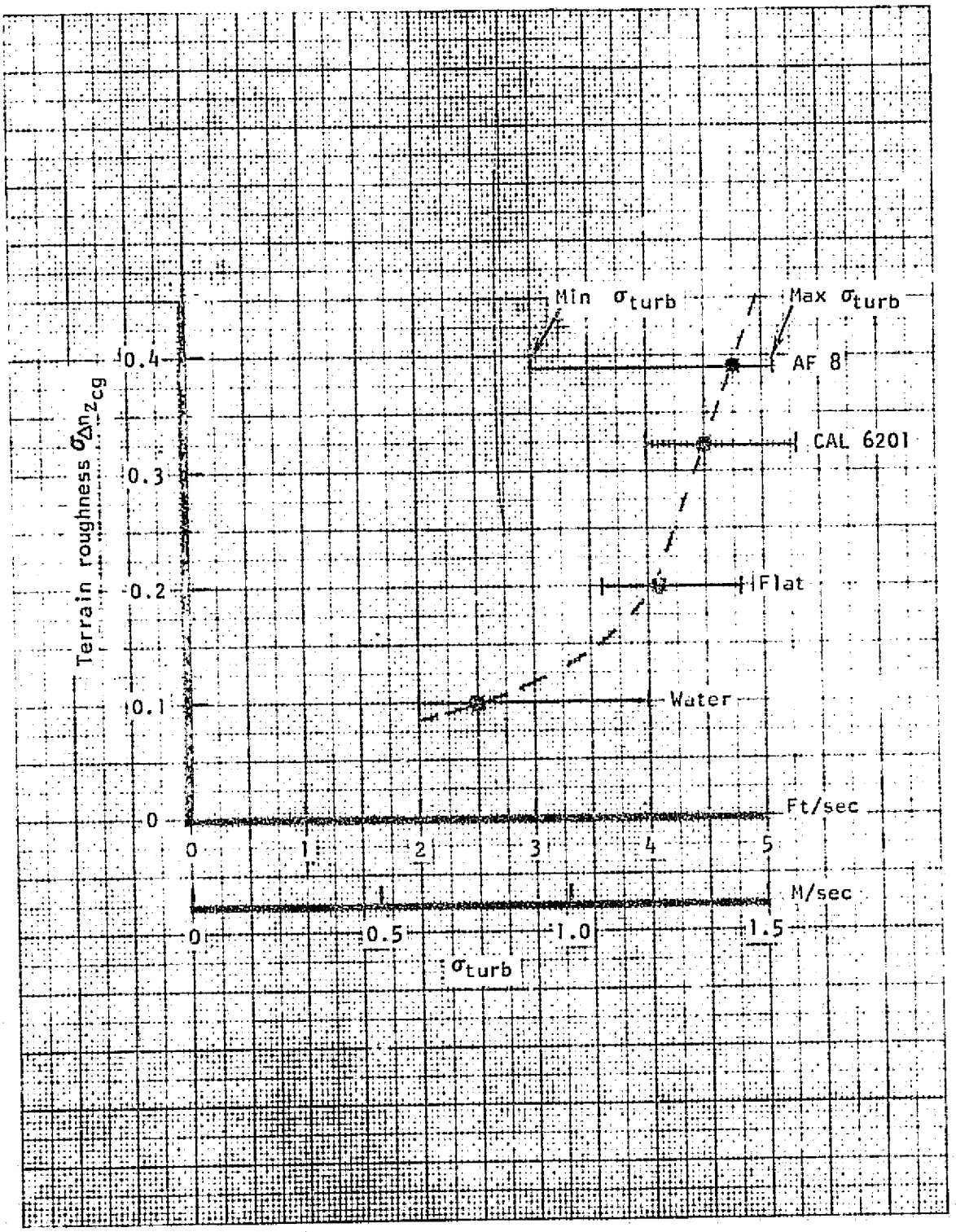

Figure 40.- Terrain roughness versus measured turbulence.

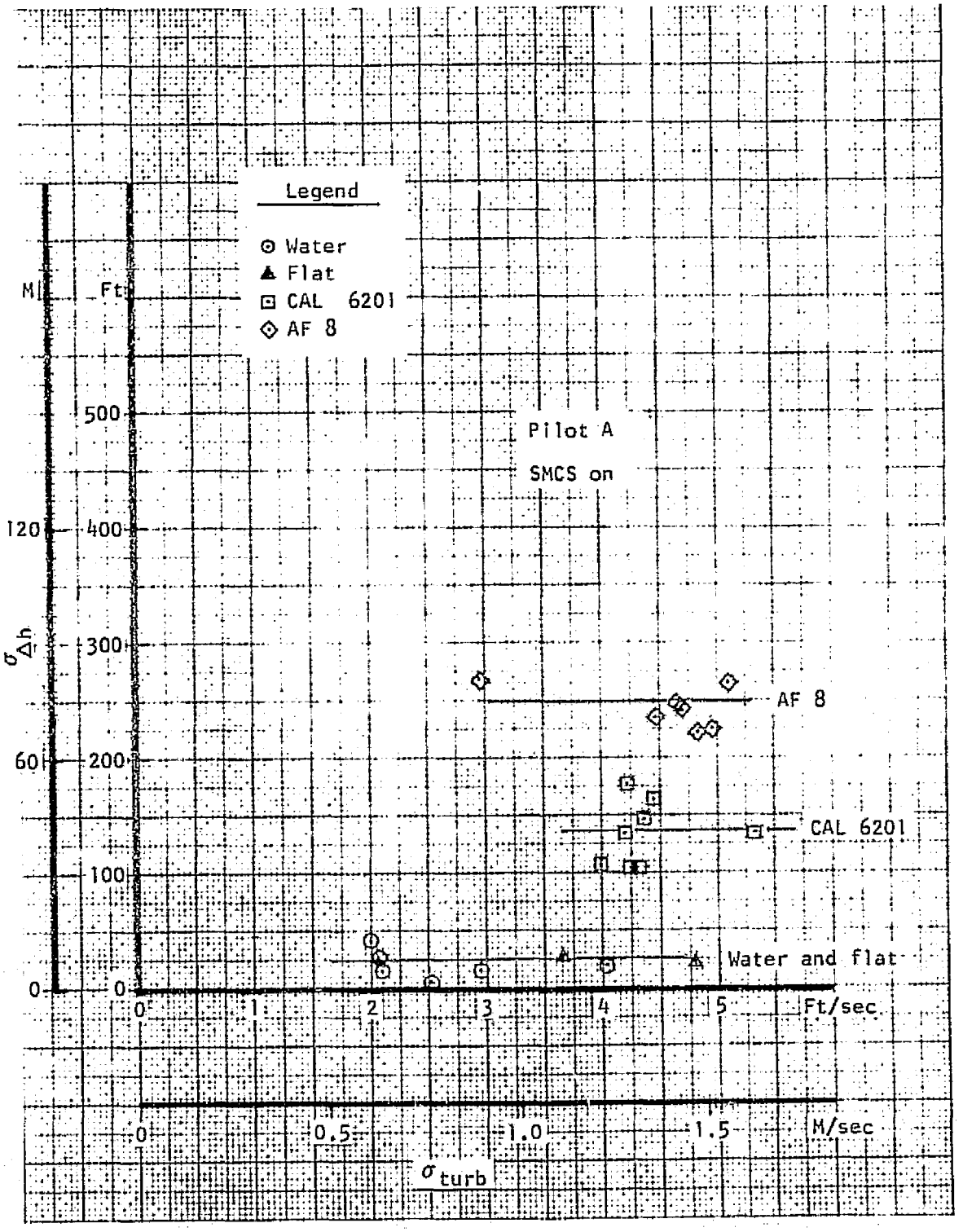

Figure 41. TF performance versus turbulence and terrain.

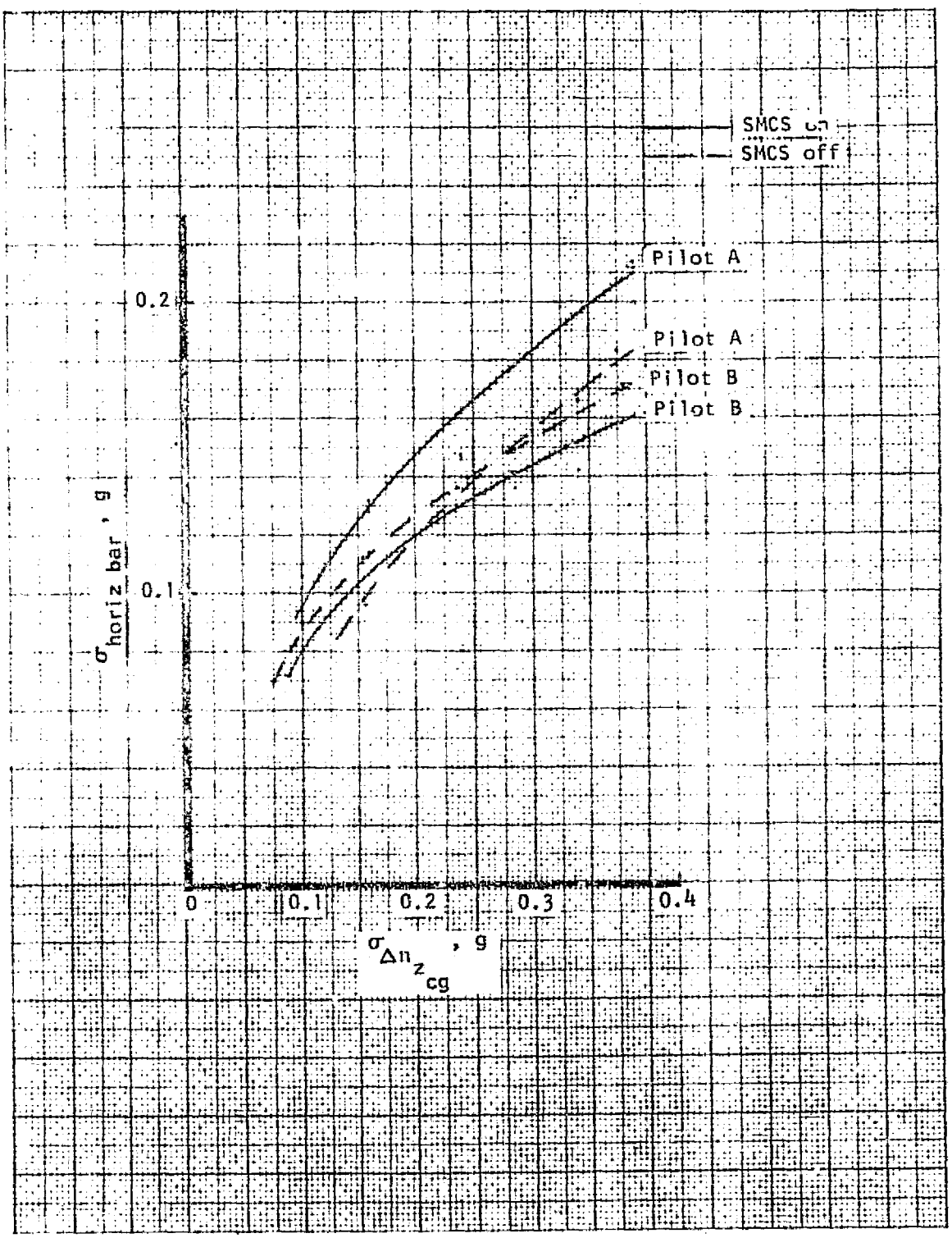

Figure 42.- Pilot TF performance versus maneuver load.

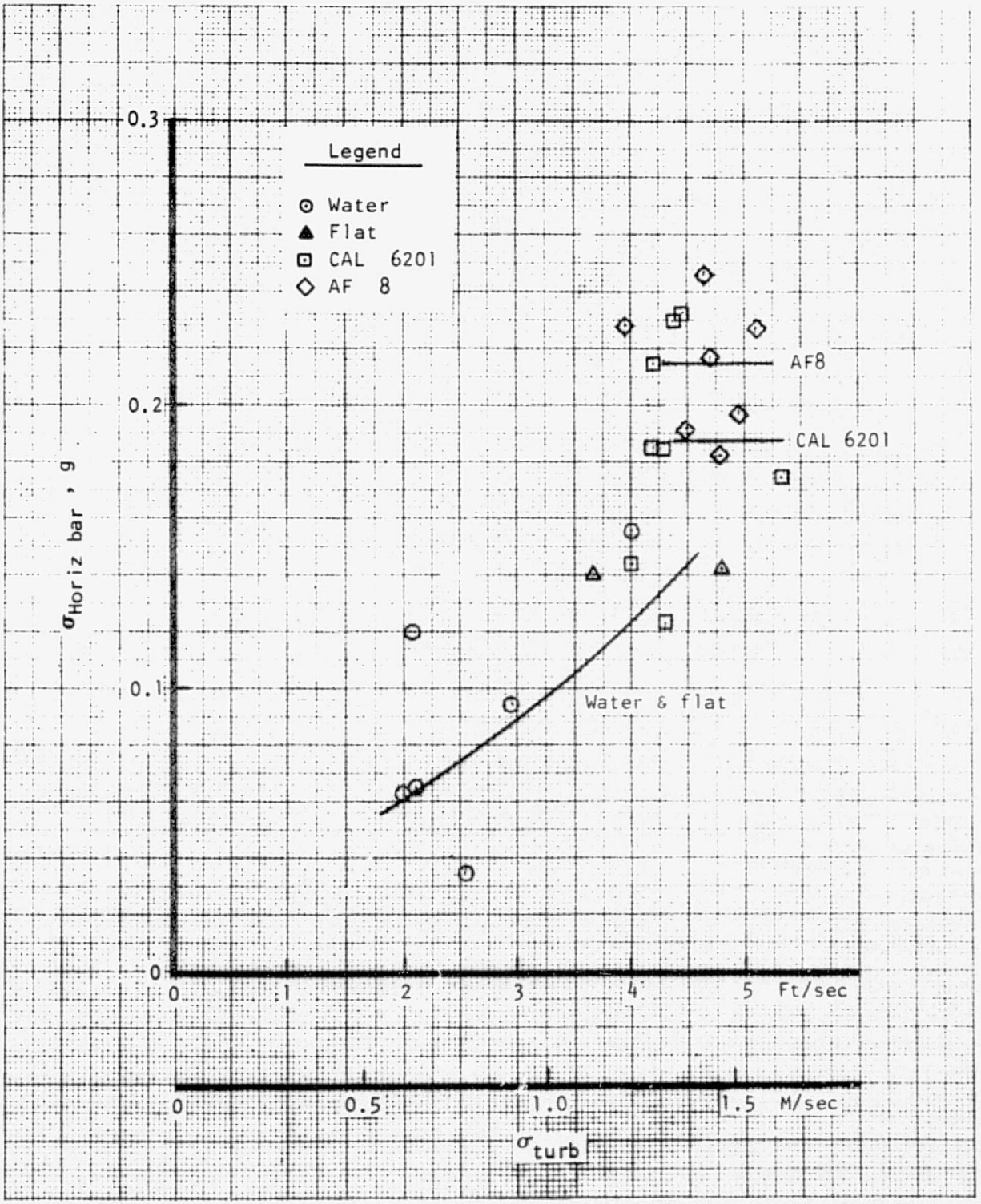

Figure 43.- Pilot [illegible] performance versus turbulence (pilot A, SMCS on).

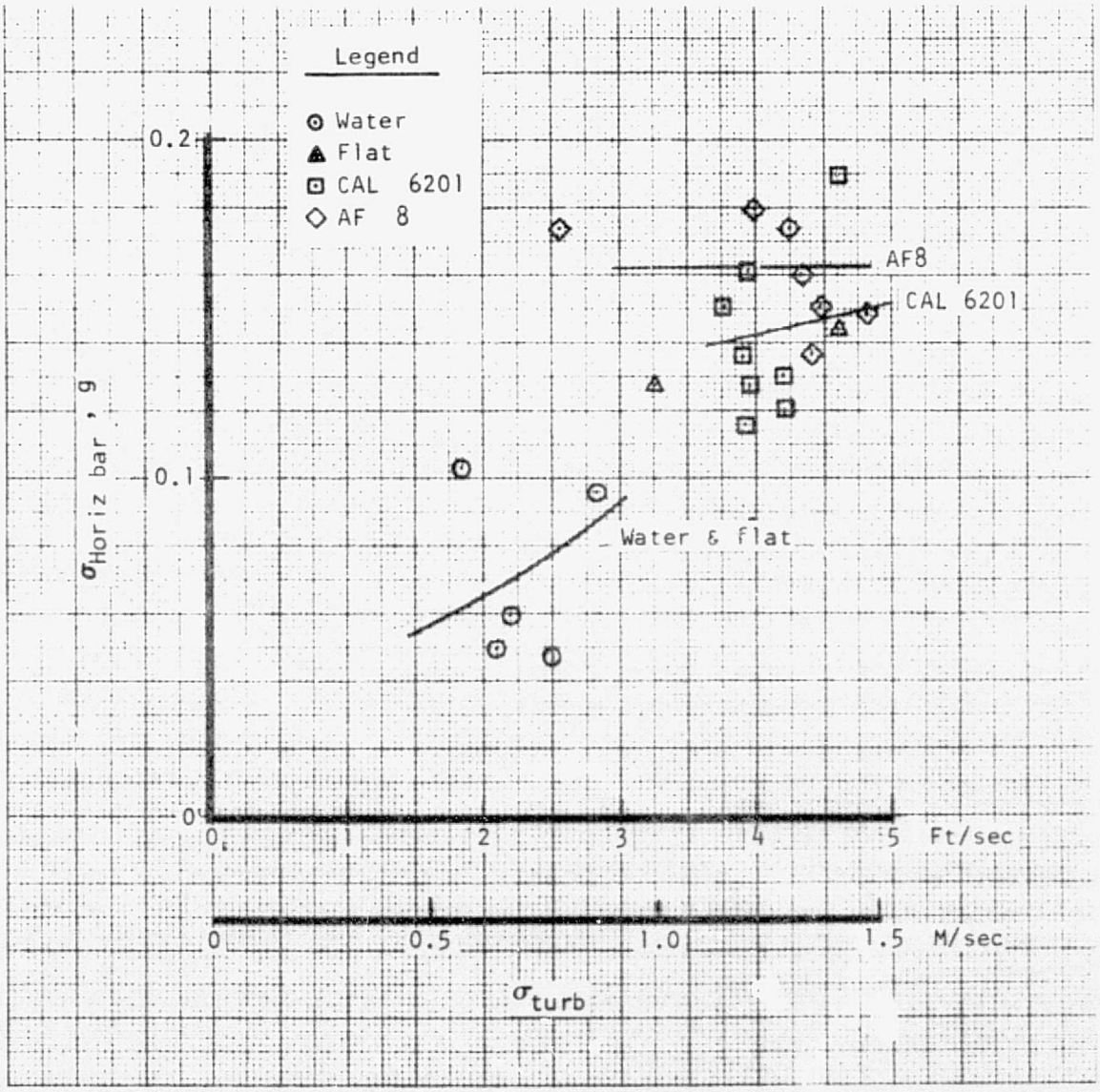

Figure 44.- Pilot TF performance versus turbulence (pilot B, SMCS on).

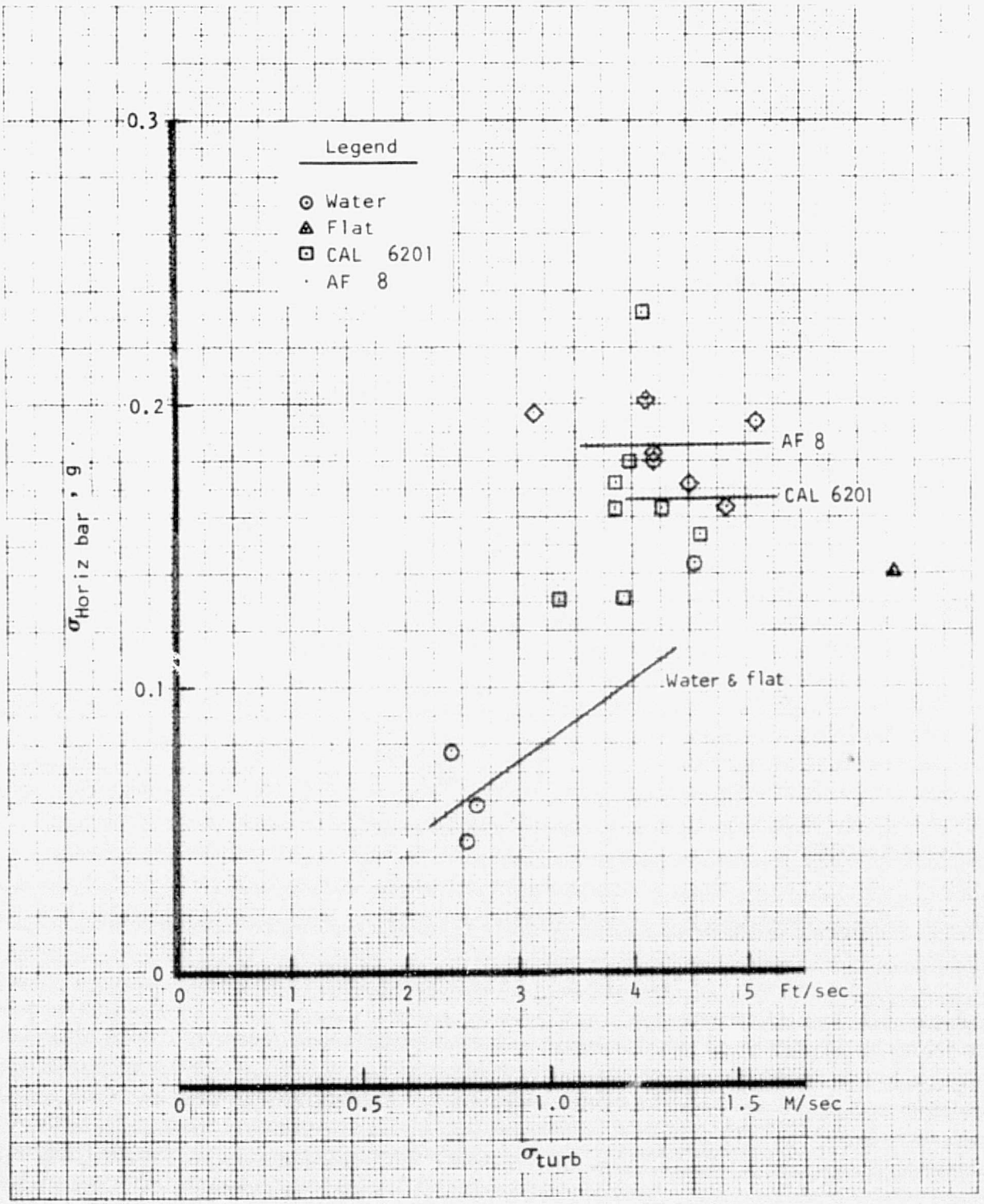

Figure 45.- Pilot TF performance versus turbulence (pilot A, SMCS off).

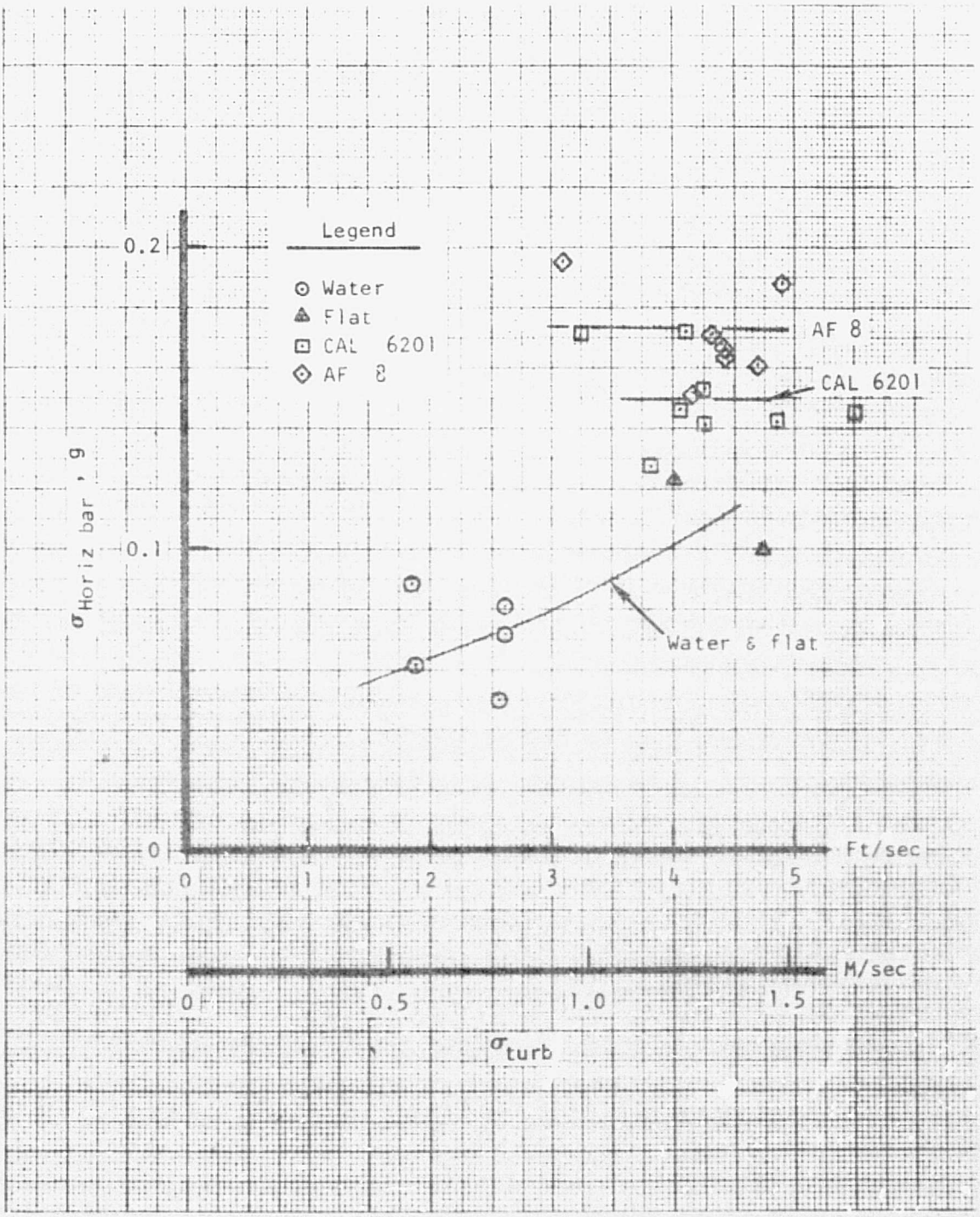

Figure 46.- Pilot TF performance versus turbulence (pilot B, SMCS off).

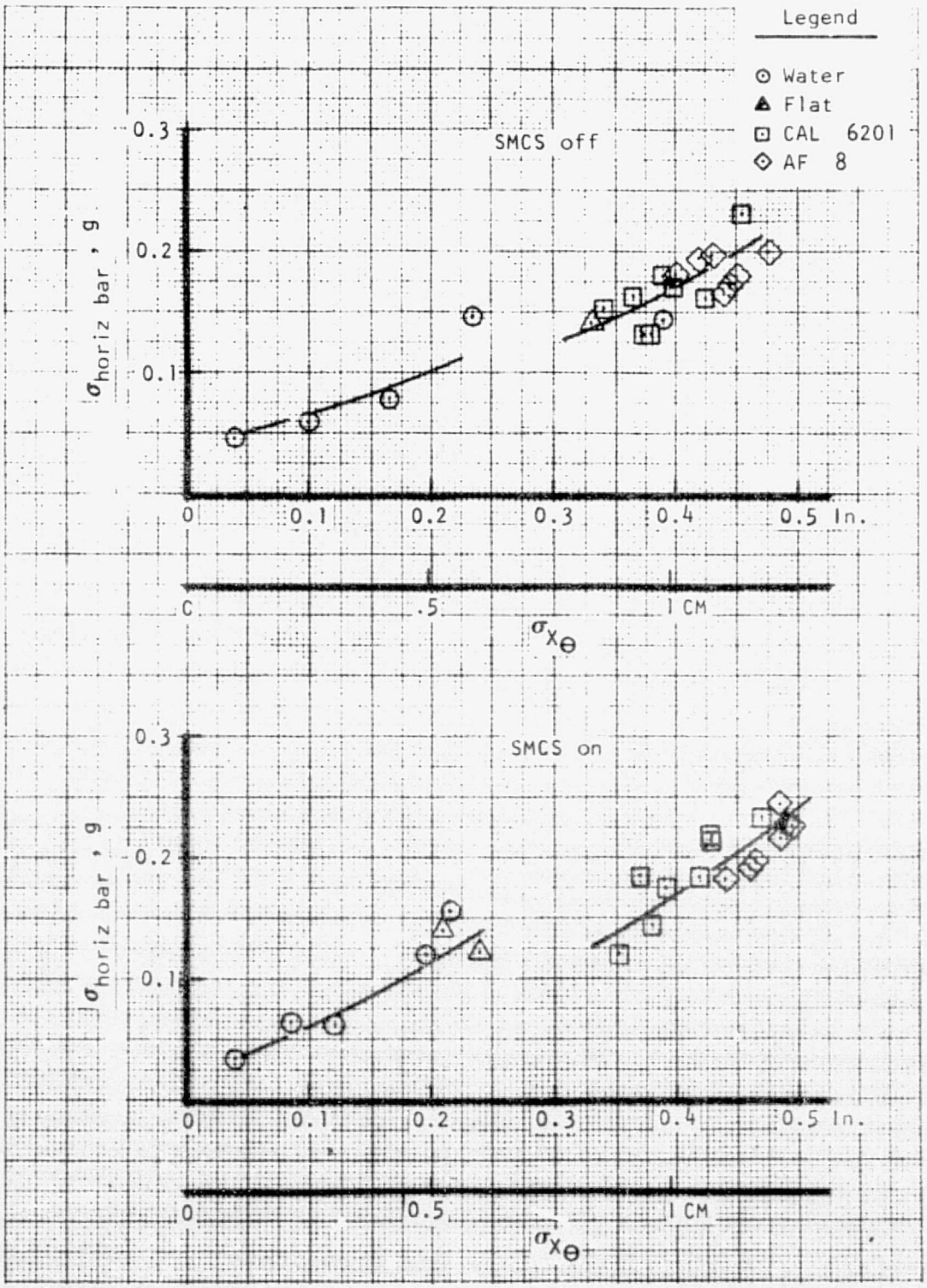

Figure 47. Pilot TF performance versus stick displacement (pilot A).

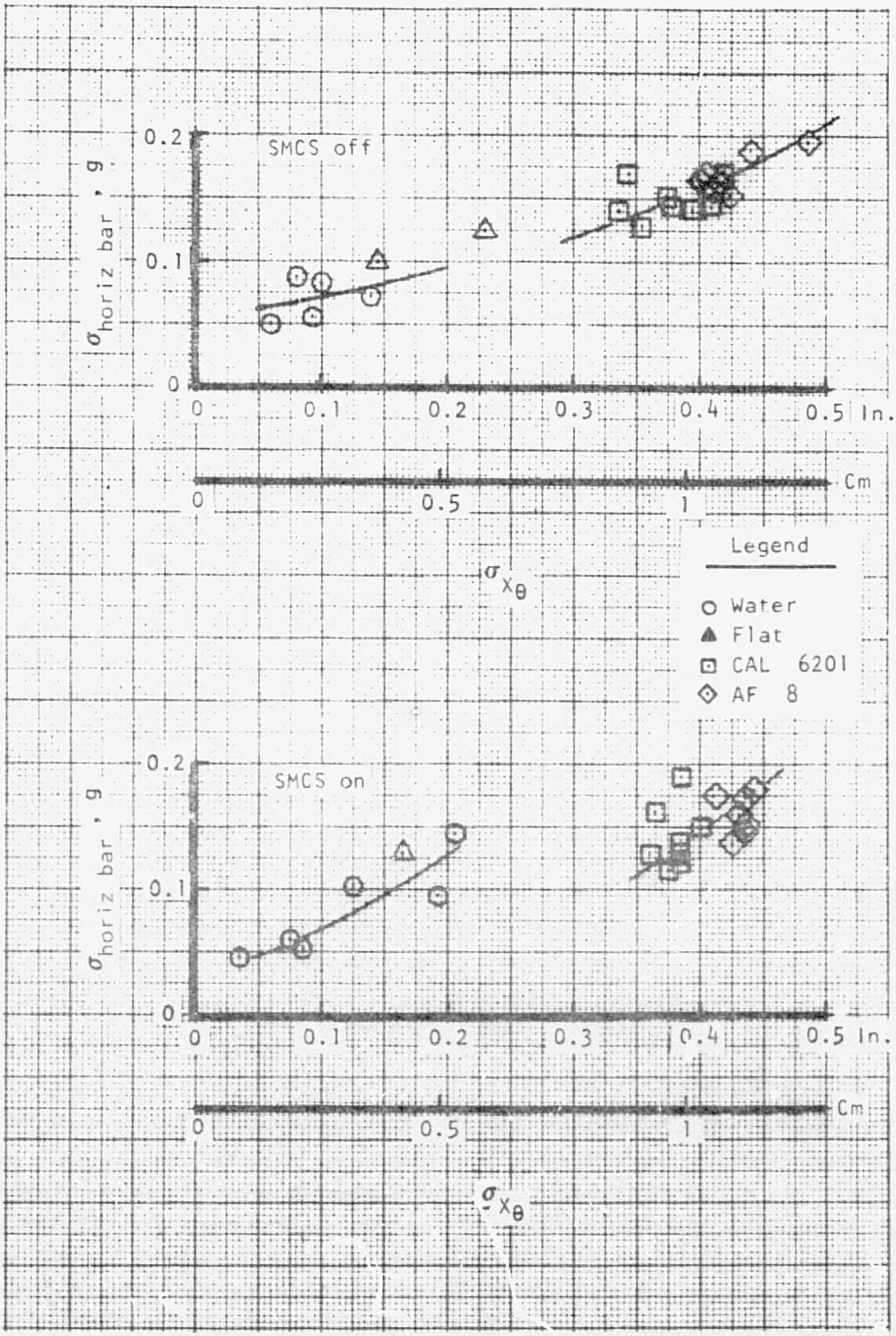

Figure 48.- Pilot TF performance versus stick displacement (pilot B).

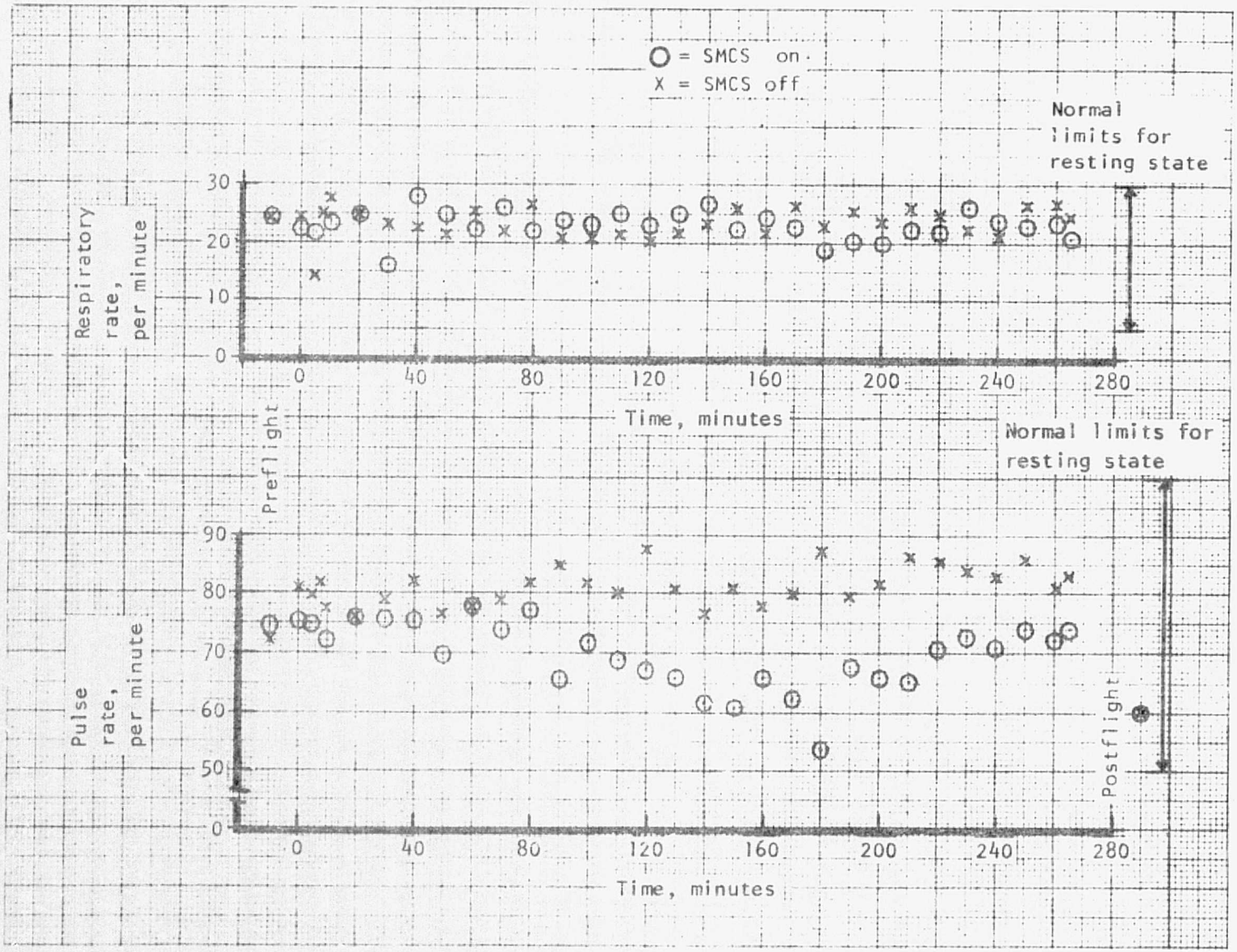

Figure 49.- Respiratory rate and pulse rate versus mission time (pilot A).

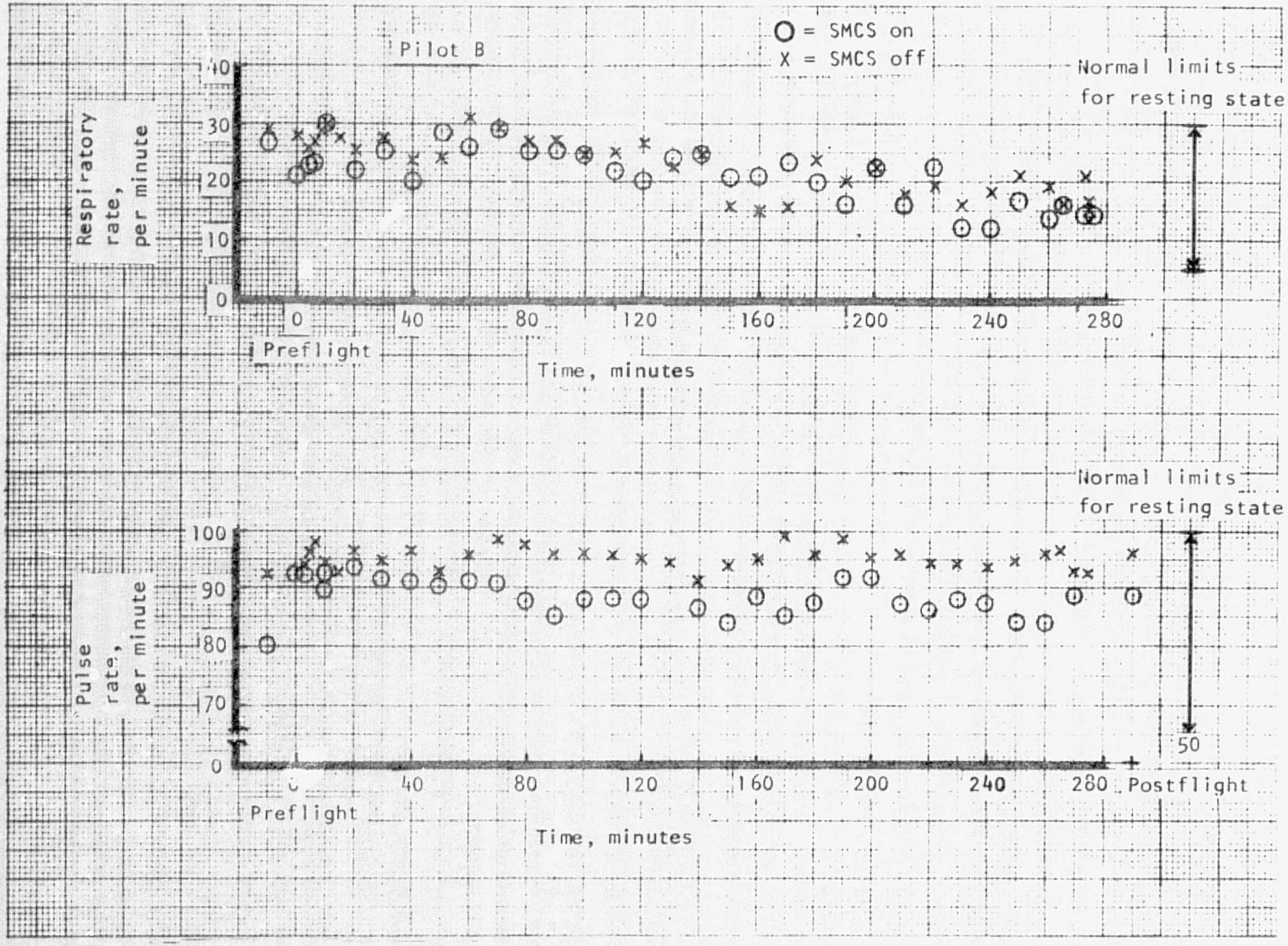

Figure 50.- Respiratory rate and pulse rate versus mission time (pilot B).

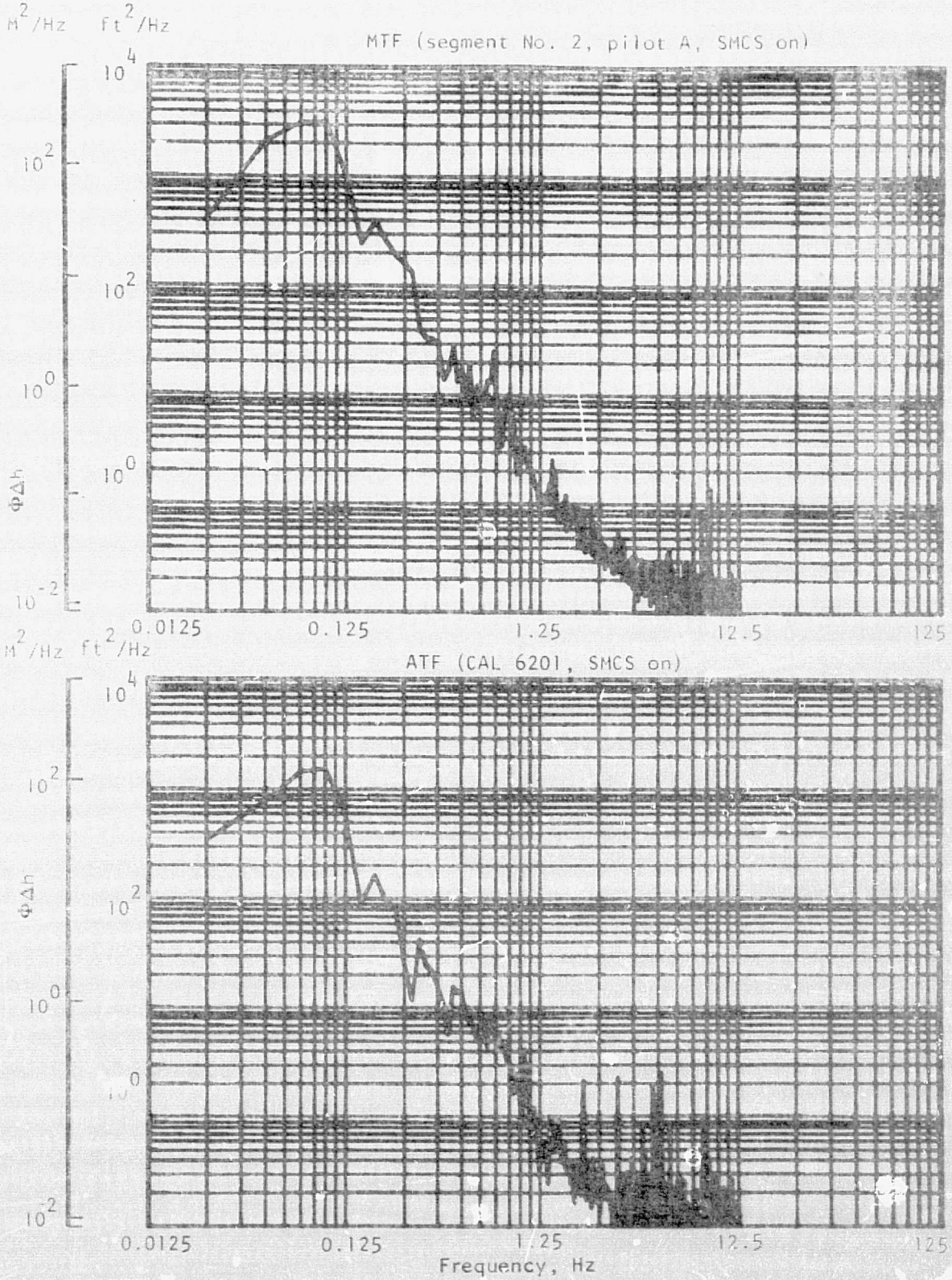

Figure 51.- Power spectral densities of clearance altitude (CAL 62[illegible]).

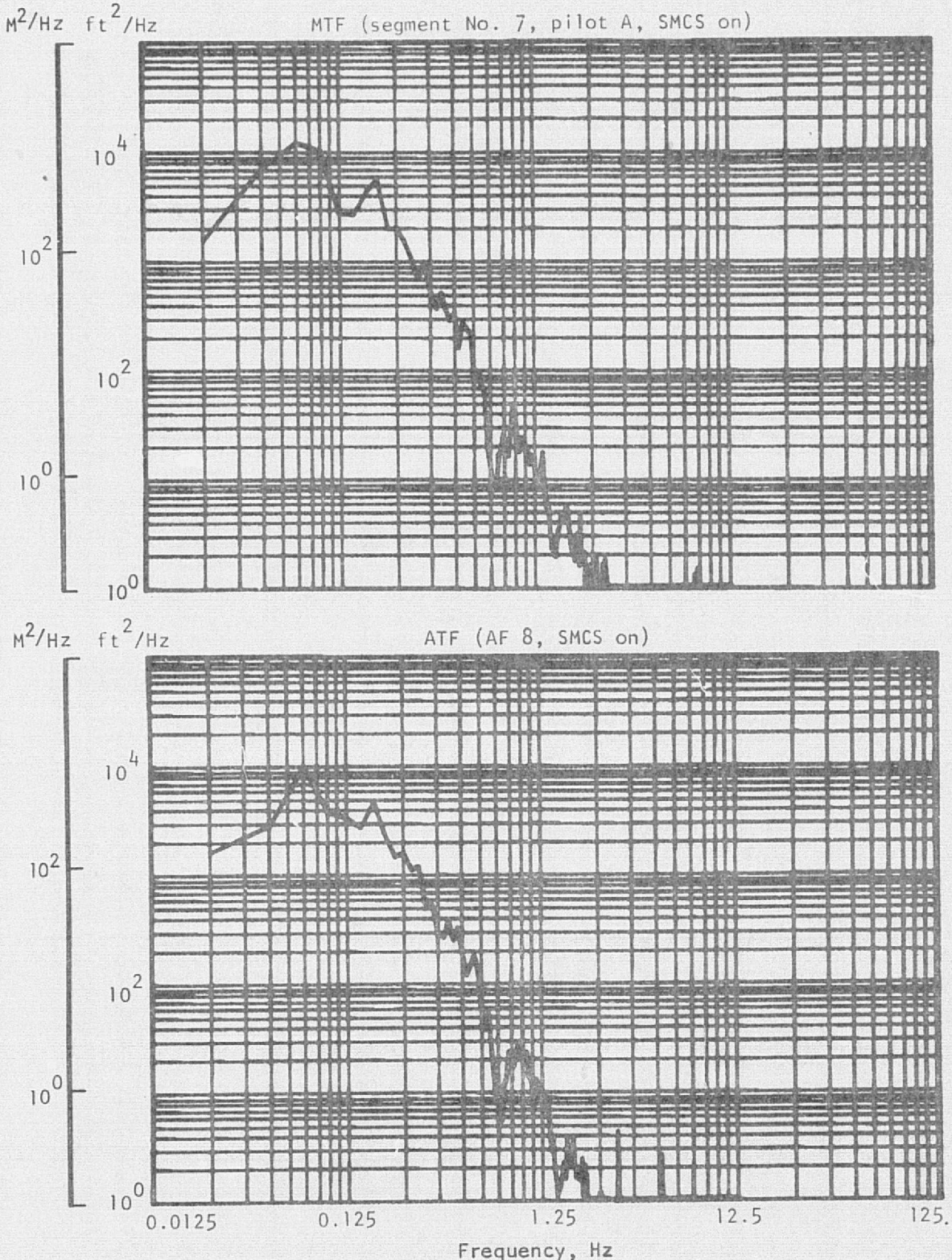

Figure 52.- Power spectral densities of clearance altitude (AF 8).

C.2

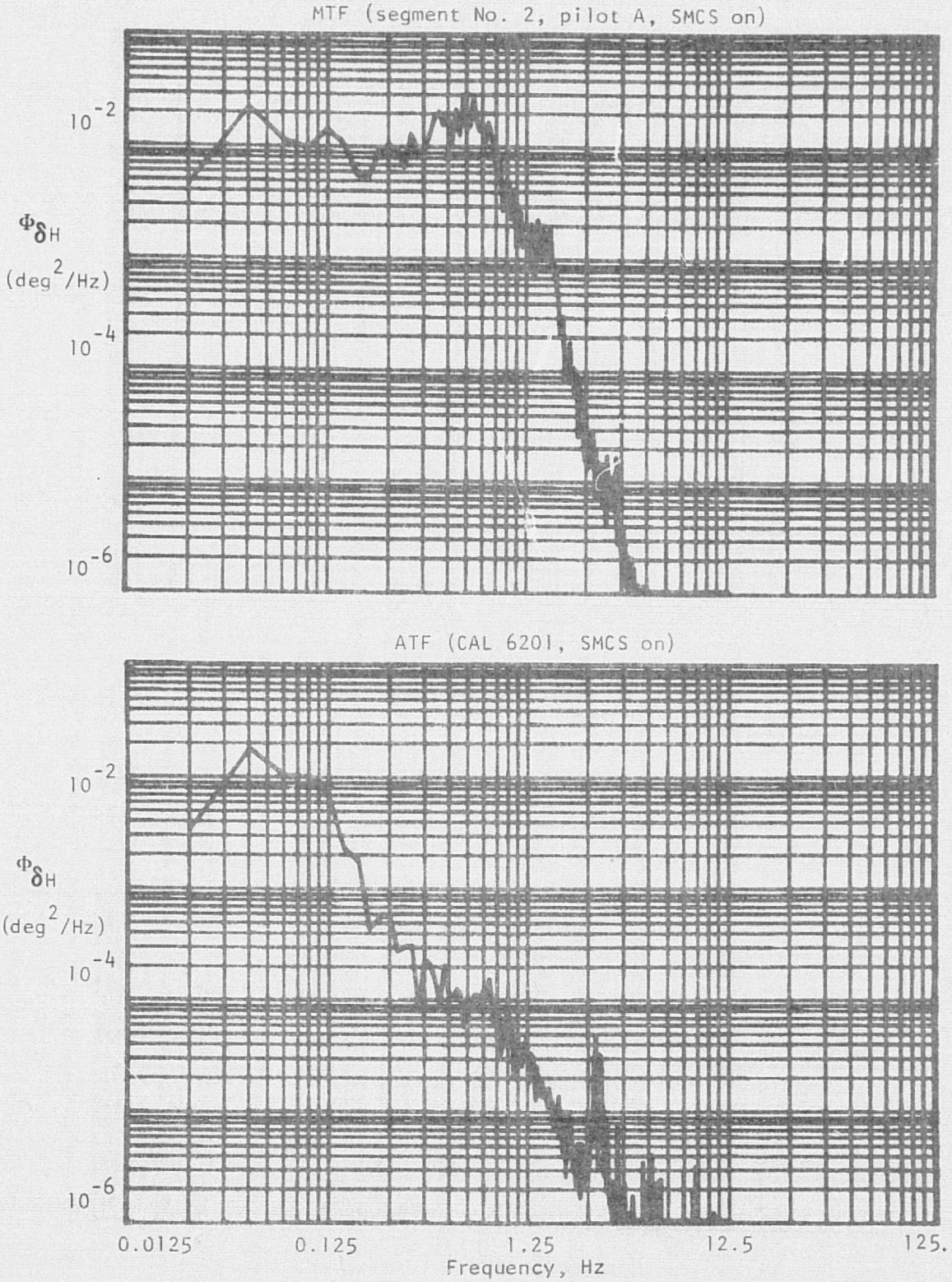

Figure 53.- Power spectral densities of pitch control surface (CAL 6201).

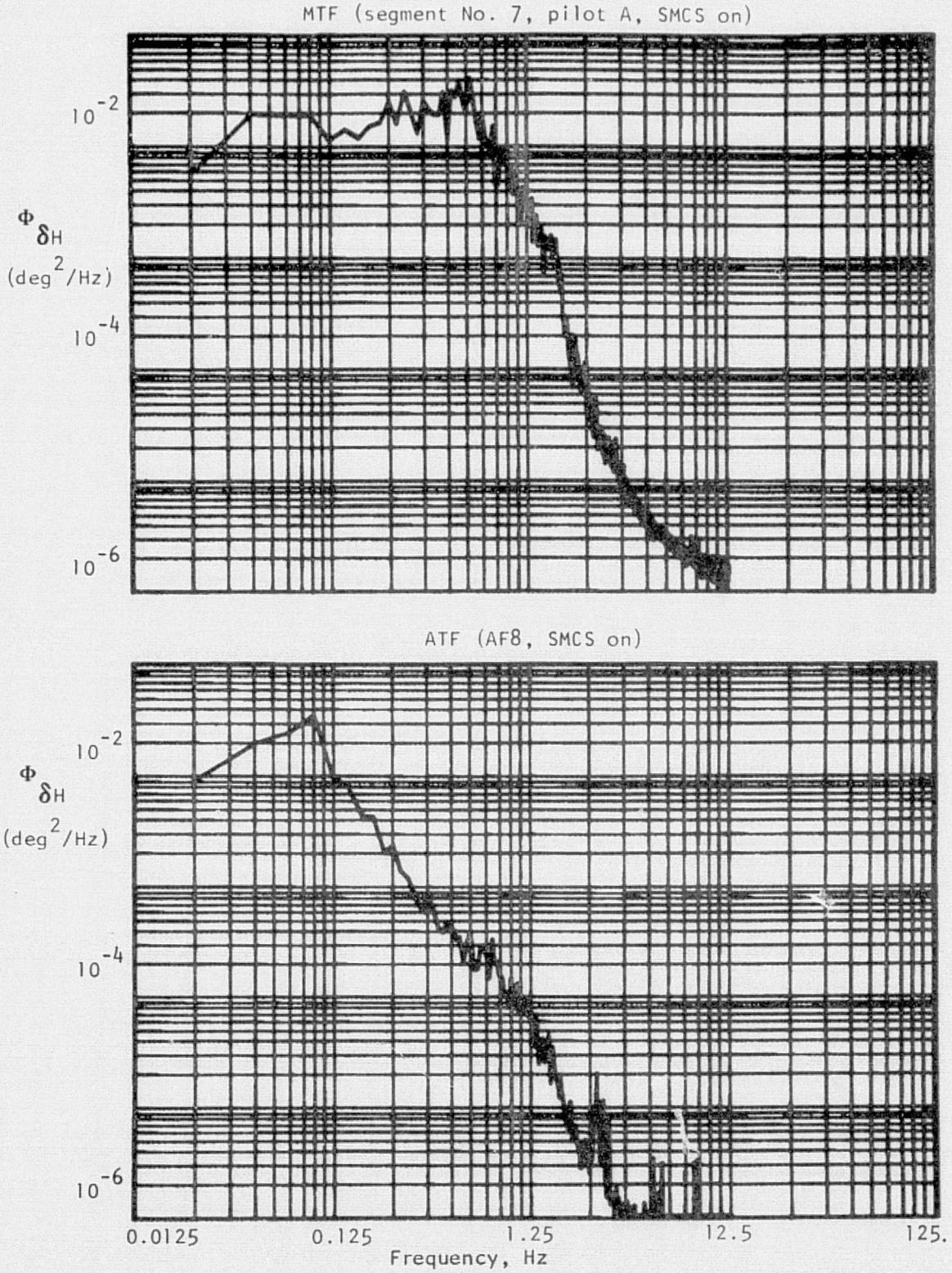

Figure 54.- Power spectral densities of pitch control surface (AF 8).

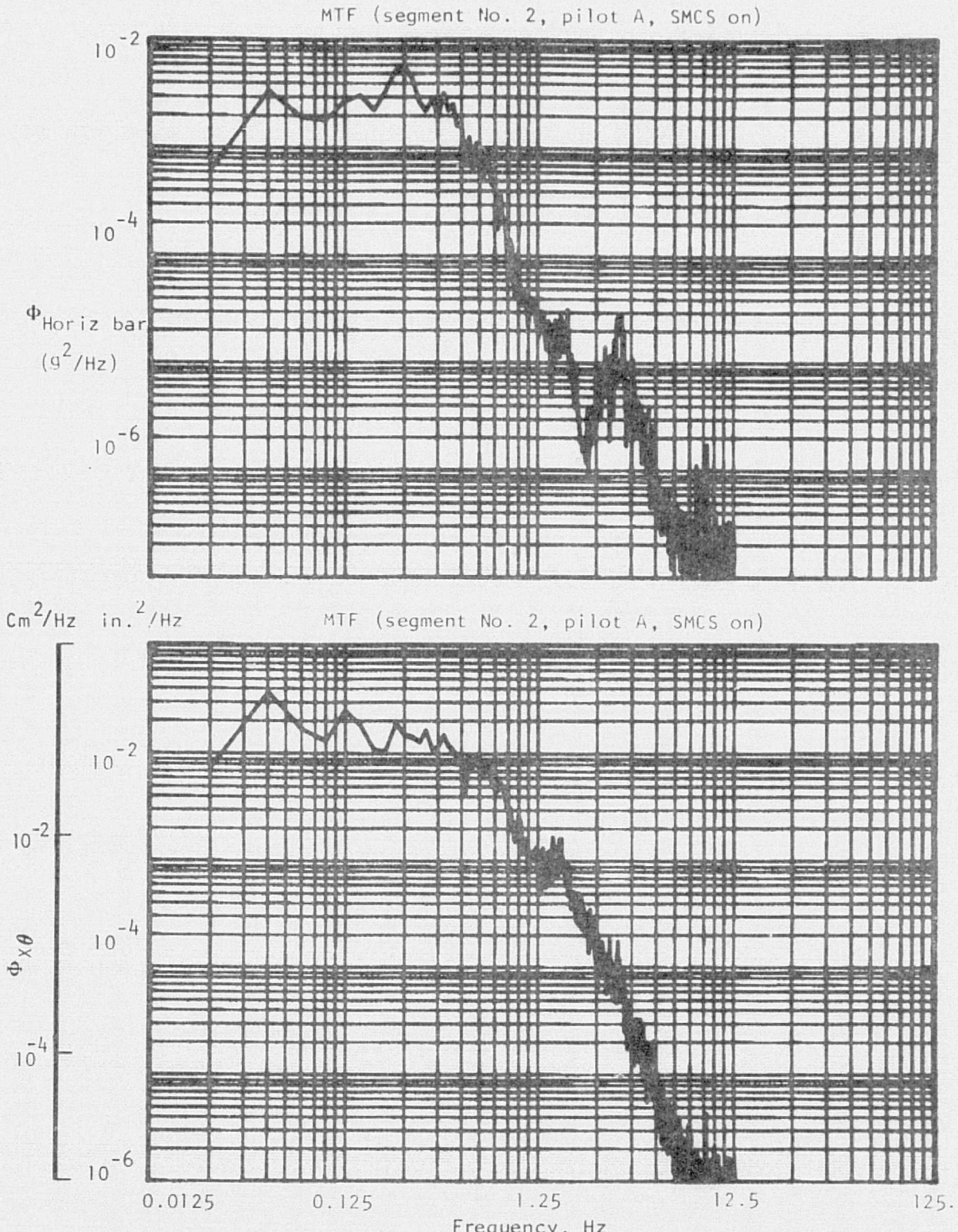

Figure 55.- Power spectral densities of pitch tracking error and pitch control stick.